nagra.

Arbeitsbericht NAB 22-03

TBO Rheinau-1-1: Data Report

Dossier VII Hydraulic Packer Testing

June 2023

R. Schwarz, M. Willmann, P. Schulte,
H. Fisch, S. Reinhardt, L. Schlickenrieder,
M. Voß & A. Pechstein

National Cooperative
for the Disposal of
Radioactive Waste

Hardstrasse 73
P.O. Box
5430 Wettingen
Switzerland
Tel. +41 56 437 11 11

nagra.ch

nagra.

Arbeitsbericht NAB 22-03

TBO Rheinau-1-1: Data Report

Dossier VII Hydraulic Packer Testing

June 2023

R. Schwarz[1], M. Willmann[2], P. Schulte[3], H. Fisch[3], S. Reinhardt[3], L. Schlickenrieder[1], M. Voß[1] & A. Pechstein[4]

[1] CSD Ingenieure AG
[2] Solexperts AG
[3] AFRY Switzerland Ltd
[4] Nagra

Keywords:
RHE1-1, Zürich Nordost, TBO, deep drilling campaign, hydrogeology, hydraulic packer tests, hydraulic conductivity, hydraulic head, gas threshold pressure test equipment

National Cooperative for the Disposal of Radioactive Waste

Hardstrasse 73
P.O. Box
5430 Wettingen
Switzerland
Tel. +41 56 437 11 11

nagra.ch

Nagra Arbeitsberichte ("Working Reports") present the results of work in progress that have not necessarily been subject to a comprehensive review. They are intended to provide rapid dissemination of current information.

This NAB aims at reporting drilling results at an early stage. Additional borehole-specific data will be published elsewhere.

In the event of inconsistencies between dossiers of this NAB, the dossier addressing the specific topic takes priority. In the event of discrepancies between Nagra reports, the chronologically later report is generally considered to be correct. Data sets and interpretations laid out in this NAB may be revised in subsequent reports. The reasoning leading to these revisions will be detailed there.

This Dossier was prepared by a project team consisting of:
R. Schwarz (QC of test analyses, QC of test reports, writing)
M. Willmann (performance/analysis of the hydraulic packer tests)
S. Reinhardt (analysis of the hydraulic packer tests)
H. Fisch (analysis of the hydraulic packer tests)
P. Schulte (analysis of the hydraulic packer tests)
L. Schlickenrieder (writing)
M. Voß (writing)
A. Pechstein (project management, conceptualisation, review)

The present report is based on the mobilisation report for the test equipment and on the reports for the performance and analysis of the hydraulic packer tests. These reports were written by the testing companies Solexperts AG (N. Dutler, U. Rösli, M. Willmann) and AFRY Switzerland Ltd (R. Brauchler, S. Reinhardt, H. Fisch, A. Maqueda, S. Reinhardt, P. Schulte).

Editorial work: P. Blaser and M. Unger

The Dossier has greatly benefitted from technical discussions with, and reviews by, external and internal experts. Their input and work are very much appreciated.

Table of Contents

Table of Contents I

List of Tables II

List of Figures V

1 Introduction 1
1.1 Context 1
1.2 Location and specifications of the borehole 6
1.3 Documentation structure for the RHE1-1 borehole 9
1.4 Scope and objectives of this dossier 10

2 Strategy for the hydrogeological investigations 11
2.1 Hydrogeological objectives of the TBO boreholes 11
2.2 Hydrogeological investigation concept for RHE1-1 11

3 Hydraulic packer tests 13
3.1 Test strategy 13
3.2 Test equipment 14
3.2.1 Downhole equipment 14
3.2.1.1 Heavy-duty double packer system 17
3.2.1.2 Packers 19
3.2.1.3 Downhole sensors in the quadruple sub-surface probe 20
3.2.1.4 Autonomous data logger in test interval 21
3.2.1.5 Zero-displacement shut-in tool 21
3.2.1.6 Test tubing 22
3.2.1.7 Slim tubing 23
3.2.1.8 Submersible pumps 24
3.2.2 Surface equipment 25
3.2.2.1 Flow board 25
3.2.2.2 Packer pressure control unit 26
3.2.2.3 Additionally recorded measurements at surface 27
3.2.2.4 Data acquisition system 28
3.2.3 Equipment for constant head injection tests with very low flow rates 29
3.2.4 Equipment for constant head injection step tests with low and high flow rates 30
3.2.5 Equipment for GTPT and interval fluid exchange 33
3.2.5.1 146 mm packers 36
3.2.5.2 127 mm packers 37
3.2.5.3 Stainless steel lines 38
3.2.5.4 Zero-displacement shut-in tool SIT1 38

3.2.5.5 Flow control board for GTPT 39
3.3 Test analyses 40
3.3.1 Workflow 40
3.3.2 Special effects 43
3.3.2.1 Borehole history 44
3.3.2.2 Interval temperature changes during testing 45
3.3.2.3 Mechanical effects 45
3.4 Test activities 46
3.5 Details of selected tests 53
3.5.1 Hydraulic packer test RHE1-1-LIA1 53
3.5.1.1 Interval characterisation 53
3.5.1.2 Test execution 54
3.5.1.3 Analysis 56
3.5.2 Hydraulic packer test RHE1-1-OPA2a 61
3.5.2.1 Interval characterisation 62
3.5.2.2 Test execution 62
3.5.2.3 Analysis 65
3.6 Summary of results and discussion of hydraulic tests 71
3.6.1 Investigation of the "pristine" / "undisturbed" formation 71
3.6.1.1 Summary tables and plots 71
3.6.1.2 Discussion of data and test results 81
3.6.2 Investigation of the artificially disturbed formation 81

4 Summary 85

5 References 87

Appendix A: Abbreviations, nomenclature and definitions A-1

Appendix B: Analysis plots of the hydraulic packer tests RHE1-1-LIA1 and RHE1-1-OPA2a B-1

List of Tables

Tab. 1-1: General information about the RHE1-1 borehole 6
Tab. 1-2: Core and log depth for the main lithostratigraphic boundaries in the RHE1-1 borehole 8
Tab. 1-3: List of dossiers included in NAB 22-03 9
Tab. 3-1: Preferred test sequence for formations with low to very low transmissivity 14
Tab. 3-2: Specifications for the HDDP 17

Tab. 3-3: Specifications for the HDDP components 18
Tab. 3-4: Specifications for the HDDP packers 19
Tab. 3-5: Specifications for the pressure transmitters mounted in the QSSP 20
Tab. 3-6: Specifications for the data logger 21
Tab. 3-7: Specifications for the zero-displacement shut-in tool 22
Tab. 3-8: Specifications for the test tubing 22
Tab. 3-9: Specifications for the slim tubing 23
Tab. 3-10: Specifications for the submersible pumps 24
Tab. 3-11: Specifications for the flowmeters 25
Tab. 3-12: Specifications for the pressure controller 27
Tab. 3-13: Specifications for the atmospheric pressure and air temperature sensors 28
Tab. 3-14: Specifications for the physico-chemical sensors 28
Tab. 3-15: Specifications for the equipment for constant head injection tests with very low flow rates 29
Tab. 3-16: Specifications for the equipment for constant head injection step tests with low flow rates 30
Tab. 3-17: Specifications for the equipment for constant head injection step tests with high flow rates 31
Tab. 3-18: Specifications for the 146 mm packers 36
Tab. 3-19: Specifications for the 127 mm packers 37
Tab. 3-20: Specifications for the zero-displacement shut-in tool (SIT1) 39
Tab. 3-21: Specifications for the gas flow controller / meters for the GTPT 39
Tab. 3-22: Summary of analytical analysis methods / techniques 41
Tab. 3-23: Specific periods of the borehole pressure history 45
Tab. 3-24: Hydraulic packer testing in borehole RHE1-1: Test interval and test specifications 48
Tab. 3-25: Hydraulic test RHE1-1-LIA1: Information on the test interval 54
Tab. 3-26: Hydraulic test RHE1-1-LIA1: Borehole pressure history 56
Tab. 3-27: Hydraulic test RHE1-1-LIA1: Formation parameter estimation based on the parameter optimisation of the SW-SWS sequence using a radial composite flow model considering both the borehole pressure history and temperature changes inside the test interval 58
Tab. 3-28: Hydraulic test RHE1-1-LIA1: 95% uncertainty range associated with the results of the parameter optimisation using a radial composite flow model for the SW-SWS sequence 58
Tab. 3-29: Hydraulic test RHE1-1-LIA1: Formation parameter estimation based on the parameter optimisation of the SW-SWS sequence using a radial homogeneous flow model considering both the borehole pressure history and temperature changes inside the test interval 59

Tab. 3-30: Hydraulic test RHE1-1-LIA1: Uncertainty ranges and best estimates for the formation parameters estimated by the perturbation analysis considering both the borehole pressure history and temperature changes inside the test interval 60

Tab. 3-31: Hydraulic test RHE1-1-LIA1: Uncertainty ranges and best estimates for the formation parameters as a result of the sampling analysis for the test zone compressibility considering both the borehole pressure history and temperature changes inside the test interval 60

Tab. 3-32: Hydraulic test RHE1-1-LIA1: Formation parameter estimation based on the parameter optimisation of the SWS-PW sequence using a radial composite flow model considering both the borehole pressure history and temperature changes inside the test interval 61

Tab. 3-33: Hydraulic test RHE1-1-LIA1: Best estimates for the formation parameters and associated uncertainty ranges 61

Tab. 3-34: Hydraulic test RHE1-1-OPA2a: Information on the test interval 62

Tab. 3-35: Hydraulic test RHE1-1-OPA2a: Borehole pressure history 66

Tab. 3-36: Hydraulic test RHE1-1-OPA2a: Formation parameter estimation based on the parameter optimisation of the SW-SWS-PW sequence using a radial composite flow model considering both the borehole pressure history and temperature changes inside the test interval. 68

Tab. 3-37: Hydraulic test RHE1-1-OPA2a: 95% uncertainty range associated with the results of the parameter optimisation using a radial composite flow model for the SW-SWS-PW sequence. 68

Tab. 3-38: Hydraulic test RHE1-1-OPA2a: Uncertainty ranges and best estimates for the formation parameters estimated by the perturbation analysis considering both the borehole pressure history and temperature changes inside the test interval 69

Tab. 3-39: Hydraulic test RHE1-1-OPA2a: Uncertainty ranges and best estimates for the formation parameters as a result of the sampling analysis for the test zone compressibility considering both the borehole pressure history and temperature changes inside the test interval 70

Tab. 3-40: Hydraulic test RHE1-1-OPA2a: Best estimates for the formation parameters and associated uncertainty ranges 70

Tab. 3-41: Summary of the hydraulic packer testing in borehole RHE1-1: Transmissivity and hydraulic conductivity 73

Tab. 3-42: Summary of the hydraulic packer testing in borehole RHE1-1: Hydraulic head estimates 74

Tab. 3-43: Summary of the hydraulic packer testing in borehole RHE1-1: Permeability 75

Tab. A-1: Lithostratigraphy abbreviations for test names in RHE1-1 ..... A-1

Tab. A-2: Test name definitions for hydraulic packer testing A-1

Tab. A-3: Test event abbreviations for hydraulic packer testing A-1

Tab. A-4: Parameter definitions A-2

Tab. A-5: Non-parameter abbreviations A-3

List of Figures

Fig. 1-1: Tectonic overview map with the three siting regions under investigation 1
Fig. 1-2: Overview map of the investigation area in the Zürich Nordost siting region with the location of the RHE1-1 borehole in relation to the boreholes Benken, TRU1-1 and MAR1-1 2
Fig. 1-3: Seismic amplitude cross-section and seismic attribute maps showing the Rheinau Fault 3
Fig. 1-4: Detailed seismic fault interpretation available for trajectory planning and discussed/executed well trajectories 4
Fig. 1-5: Conceptual structural model of the Rheinau Fault 5
Fig. 1-6: Lithostratigraphic profile and casing scheme for the RHE1-1 borehole 7
Fig. 3-1: General configuration and specifications of the HDDP in double packer configuration 16
Fig. 3-2: Schematic layout of the flow control unit 26
Fig. 3-3: Schematic layout of the packer control unit 27
Fig. 3-4: Schematic layout for injection with very low flow rates 29
Fig. 3-5: Schematic equipment layout for constant head injection step tests with low (top) and high (bottom) flow rates 32
Fig. 3-6: Schematic layout of the modified HDDP system with the four major phases of the GTPT 35
Fig. 3-7: Schematic layout of the flow control unit for the GTPT 40
Fig. 3-8: Flowcharts for the on-site hydraulic packer test analysis (left) and Quick Look Analysis (QLA) (right) 42
Fig. 3-9: Flowchart for the off-site Detailed Analysis (DA) of a hydraulic packer test 43
Fig. 3-10: Hydraulic packer test RHE1-1-OPA1a: Overview plot of pressure vs. time and date 49
Fig. 3-11: Hydraulic packer test RHE1-1-OPA1c: Overview plot of pressure vs. time and date 49
Fig. 3-12: Hydraulic packer test RHE1-1-OPA2a: Overview plot of pressure vs. time and date 50
Fig. 3-13: Hydraulic packer test RHE1-1-OPA2b: Overview plot of pressure vs. time and date 50
Fig. 3-14: Hydraulic packer test RHE1-1-OPA2c: Overview plot of pressure and flow rate vs. time and date 51
Fig. 3-15: Hydraulic packer test RHE1-1-OPA2d: Overview plot of pressure and flow rate vs. time and date 52
Fig. 3-16: Hydraulic packer test RHE1-1-LIA1: Overview plot of pressure vs. time and date 52
Fig. 3-17: Hydraulic test RHE1-1-LIA1: Downhole equipment installation record with system layout as used in the field test 55

Fig. 3-18: Hydraulic test RHE1-1-OPA2a: Downhole equipment installation record with system layout as used in the field test 64

Fig. 3-19: Summary of the hydraulic testing in borehole RHE1-1: Formation transmissivity profile 76

Fig. 3-20: Summary of the hydraulic testing in borehole RHE1-1: Formation hydraulic conductivity profile 77

Fig. 3-21: Summary of the hydraulic testing in borehole RHE1-1: Static formation pressure profile 78

Fig. 3-22: Summary of the hydraulic testing in borehole RHE1-1: Formation hydraulic head profile (m TVD) 79

Fig. 3-23: Summary of the hydraulic testing in borehole RHE1-1: Formation hydraulic head profile (m asl) 80

Fig. 3-24: Stabilised flow rates of each phase during RHE1-1-OPA2c (HI301 to 309) and OPA2d (HW) 82

Fig. 3-25: Summary of the development of the (disturbed) outer zone formation hydraulic transmissivity as a function of the interval pressure during hydraulic tests HE1-1-OPA2c and RHE1-1-OPA2d, including the uncertainty ranges of selected phases 83

Fig. B-1: Hydraulic test RHE1-1-LIA1: Entire record of the borehole pressure history used in the analysis B-1

Fig. B-2: Hydraulic test RHE1-1-LIA1: Log-log plots of PSR phase (no superposition, top left graph), SW phase (de-convoluted, top right graph), SWS phase (Agarwal time, bottom left graph) and PW phase (de-convoluted, bottom right graph) B-2

Fig. B-3: Hydraulic test RHE1-1-LIA1: Interval temperature ($T2^*$ memory gauge sensor), atmospheric pressure and downhole pressures of QSSP sensors (P1, P2, P3, P4) as well as temperature measurement at the QSSP (T2 sensor) B-2

Fig. B-4: Hydraulic test RHE1-1-LIA1: Cartesian pressure graph with the simulation result using the parameters resulting from a parameter optimisation using a radial-composite model (top: SW-SWS sequence with zoom on SW and late SWS phase; bottom: pressure residual plot) B-3

Fig. B-5: Hydraulic test RHE1-1-LIA1: Probability distribution function plot (left) and cumulative distribution function plot (right) of the simulation based on the optimised parameter set for the SW-SWS sequence B-3

Fig. B-6: Hydraulic test RHE1-1-LIA1: Sensitivities of the optimised parameters for the initial simulation B-4

Fig. B-7: Hydraulic test RHE1-1-LIA1: Cartesian pressure graph with simulation result using the parameters resulting from a parameter optimisation using a radial-homogeneous model (top: SW-SWS sequence with zoom on SW and late SWS phase; bottom: pressure residual plot) B-5

Fig. B-8: Hydraulic test RHE1-1-LIA1: Optimised parameters plotted against sorted SSE values of all perturbation runs and, in the lowest chart section, SSE value against the increasing run number B-6

Fig. B-9: Hydraulic test RHE1-1-LIA1: Cartesian pressure graph with simulations resulting from the use of the perturbation parameter sets associated with the lowest SSE (run #0) and the upper limit of the uncertainty range (run #394) as well as the initial simulation (top: SW-SWS sequence with zoom on SW and late SWS phase; bottom: pressure residual plot)..... B-7

Fig. B-10: Hydraulic test RHE1-1-LIA1: Scatter plots of the perturbation parameter sets and associated SSE values of the optimised parameters showing P_f versus K_{out} (top figure) and S_{Sout} versus K_{out} (bottom figure)..... B-8

Fig. B-11: Hydraulic test RHE1-1-LIA1: Parameter sets of the sampling analysis of the test zone compressibility (c_{tz}) B-9

Fig. B-12: Hydraulic test RHE1-1-LIA1: Cartesian pressure graph with simulation result using the parameters resulting from a parameter optimisation on the SWS-PW sequence with a radial-composite model (top: SW-SWS sequence with zoom on late SWS phase and early time PW; bottom: pressure residual plot) B-10

Fig. B-13: Hydraulic test RHE1-1-OPA2a: Entire record of the borehole pressure history used in the analysis..... B-11

Fig. B-14: Hydraulic test RHE1-1-OPA2a: Log-log plots of PSR phase (no superposition, top left graph), the SWS phase (without superposition, top right graph) and the same SWS phase with Agarwal time (bottom right graph)..... B-11

Fig. B-15: Hydraulic test RHE1-1-OPA2a: Deconvolved slug flow phase (SW, left graph) and deconvolved pulse phase (PW, right graph)..... B-12

Fig. B-16: Hydraulic test RHE1-1-OPA2a: Interval temperature ($T2^*$ memory gauge sensor), downhole pressures of QSSP sensors (P1, P2, P3, P4), atmospheric pressure and pressure of memory gauge (P2* sensor shown with an offset to ease comparison with P2)..... B-12

Fig. B-17: Hydraulic test RHE1-1-OPA2a: Cartesian pressure graph showing the numerical simulation based on the resulting parameter set of a parameter optimisation for the pressure sequence SW-SWS-PW, called reference case (RC) (top: SW-SWS-PW sequence with zoom on different sections; bottom: pressure residual plot) B-13

Fig. B-18: Hydraulic test RHE1-1-OPA2a: Probability distribution function plot (left) and cumulative distribution function plot (right) of the simulation based on the optimised parameter set for the SW-SWS-PW sequence B-13

Fig. B-19: Hydraulic test RHE1-1-OPA2a: Sensitivities of the optimised parameters for the initial simulation..... B-14

Fig. B-20: Hydraulic test RHE1-1-OPA2a: Optimised parameters plotted against sorted SSE values of all perturbation runs and, in the lowest chart section, SSE value against the increasing run number..... B-15

Fig. B-21: Hydraulic test RHE1-1-OPA2a: Comparison of the simulation based on the initial parameter set (reference case – RC) with the simulations associated with the parameter set of the lowest-SSE during the perturbation (run #0) and with the simulation run #06 (best estimate) derived from the perturbation analysis (top: SW-SWS-PW sequence with zoom on different sections; bottom: pressure residual plot)..... B-16

Fig. B-22: Hydraulic test RHE1-1-OPA2a: Scatter plots of formation parameters associated with their SSE values from perturbation analysis showing S_S versus K (top), P_f versus K (center) and P_f versus S_S (bottom figure) B-17

Fig. B-23: Hydraulic test RHE1-1-OPA2a: Sampling analysis of the test zone compressibility (c_{tz}) B-18

1 Introduction

1.1 Context

To provide input for site selection and the safety case for deep geological repositories for radioactive waste, Nagra has drilled a series of deep boreholes ("Tiefbohrungen", TBO) in Northern Switzerland. The aim of the drilling campaign is to characterise the deep underground of the three remaining siting regions located at the edge of the Northern Alpine Molasse Basin (Fig. 1-1).

In this report, we present the results from the Rheinau-1-1 borehole located in the siting region Zürich Nordost (Fig. 1-2). In the following, the main exploration objectives of this specific borehole are further outlined.

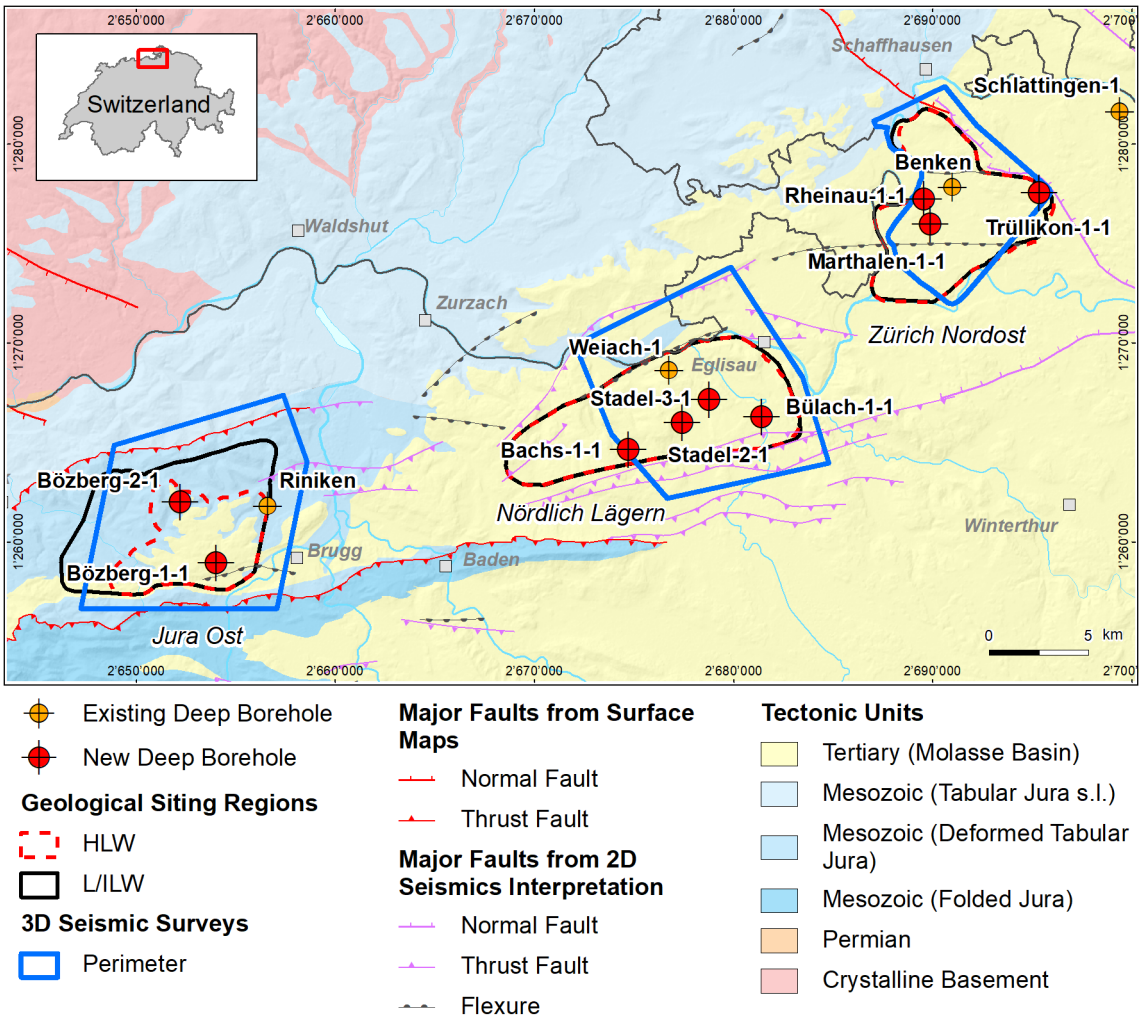

Fig. 1-1: Tectonic overview map with the three siting regions under investigation

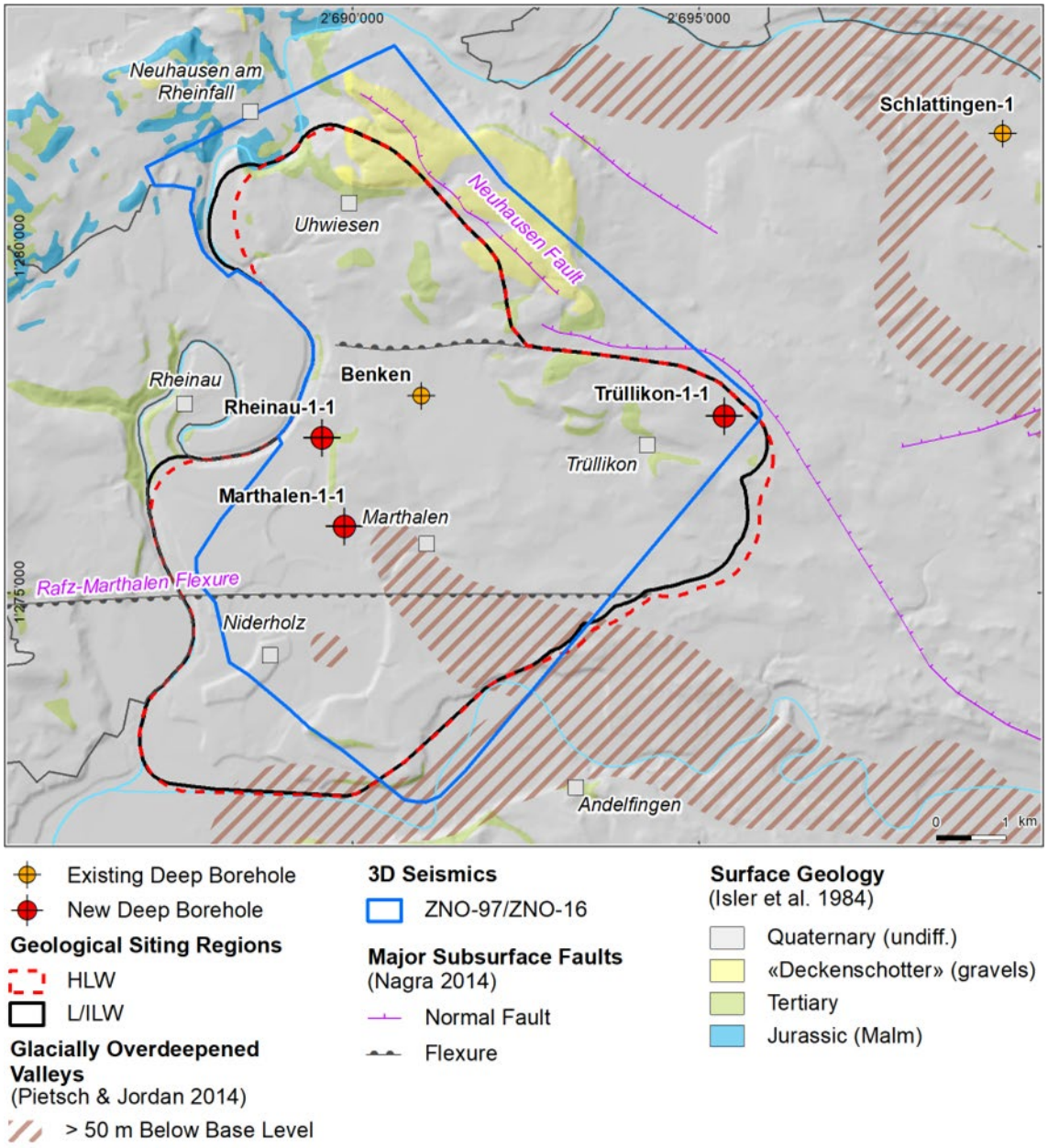

Fig. 1-2: Overview map of the investigation area in the Zürich Nordost siting region with the location of the RHE1-1 borehole in relation to the boreholes Benken, TRU1-1 and MAR1-1

Exploration objective of the Rheinau-1-1 borehole

In the context of Nagra's TBO project, the Rheinau-1-1 (RHE1-1) borehole is the only deviated borehole. It was planned as a case study with the primary objective of characterising the structural geology of the Opalinus Clay in the area of a steeply dipping fault. Furthermore, dedicated hydrological packer testing and investigations of natural tracers in porewater were conducted to investigate the self-sealing capacity of the Opalinus Clay. More specifically, a stepped constant head injection test was performed in addition to the standard hydraulic packer test to investigate the evolution of transmissivity as a function of effective stress in a fractured interval (*cf.* Dossier VII, Hydraulic Packer Testing for details).

To enable hydraulic testing in the Opalinus Clay with its relatively low strength and high swelling capacity, the maximum borehole deviation (with respect to vertical) was limited to approximately 35° (borehole plunge of 55°). Hence, for the absolute deviation, a trade-off had to be made between maximising the lateral coverage for fracture frequency statistics (large deviation desired) and robust in-situ testing (small deviation desired).

Given the above-outlined scientific goals and related technical requirements, the Rheinau Fault, located immediately east of the Rheinau-1 drill site, was selected for this case study. It is an NNE-SSW trending, steeply dipping fault showing only very minor indications of vertical offsets in seismic amplitude sections. Nevertheless, it was already identified in seismic attribute horizon slices during initial interpretation of Nagra's 3D seismic campaign in the Zürich Nordost siting region (Birkhäuser et al. 2001) and later confirmed during the analysis of follow-up seismic processing products (e.g. Nagra 2019). Fig. 1-3 shows that this fault has a clear seismic attribute expression along the boundaries of the formations below the Opalinus Clay and also along some of the more brittle units above (see horizon slices of the Top Bänkerjoch and Top Villigen Formations shown in Fig. 1-3). However, within the Opalinus Clay, no clear seismic expression is observed. Fig. 1-4 shows the 3D seismic interpretation considered for trajectory planning of the RHE1-1 borehole together with the discussed and executed borehole trajectories.

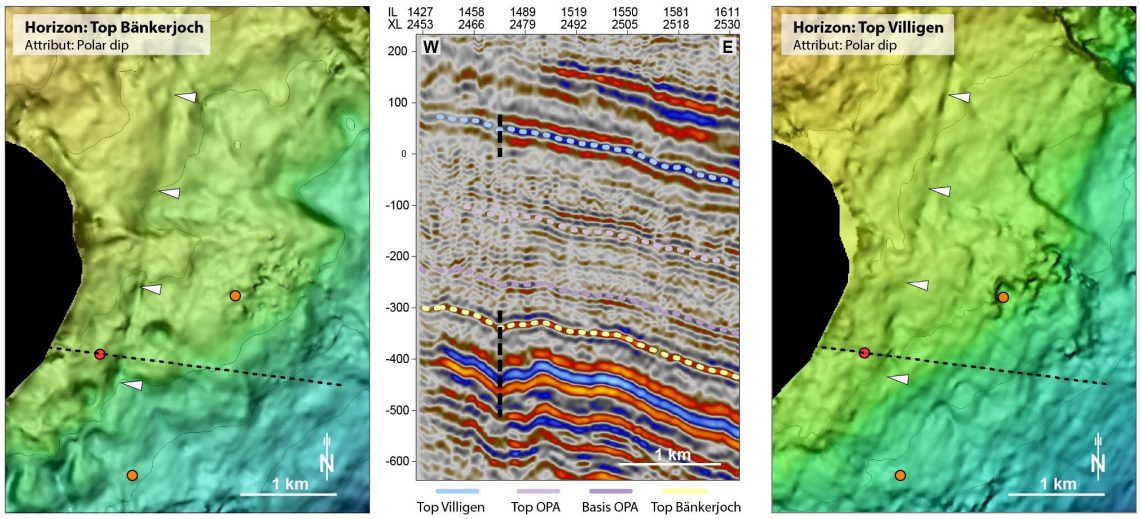

Fig. 1-3: Seismic amplitude cross-section and seismic attribute maps showing the Rheinau Fault

Left and right panels: Seismic attribute maps (polar dip) of a depth-migrated seismic cube (PSDM-A) overlain with depth values (yellowish and blueish colors indicate shallower and larger depths, respectively). The dashed black line indicates the position of the seismic section shown in the central panel. Red and orange dots show the position of the RHE1-1 borehole and neighouring boreholes, respectively. White trianlges mark the lineament representing the Rheinau Fault.

Central panel: Corresponding seismic amplitude section crossing the Rheinau Fault. The vertical axis indicates depth above sea level, and the horizontal axis shows the inline and crossline positions. The approximate trace of the Rheinau Fault above and below the Opalinus Clay is indicated by dashed black lines.

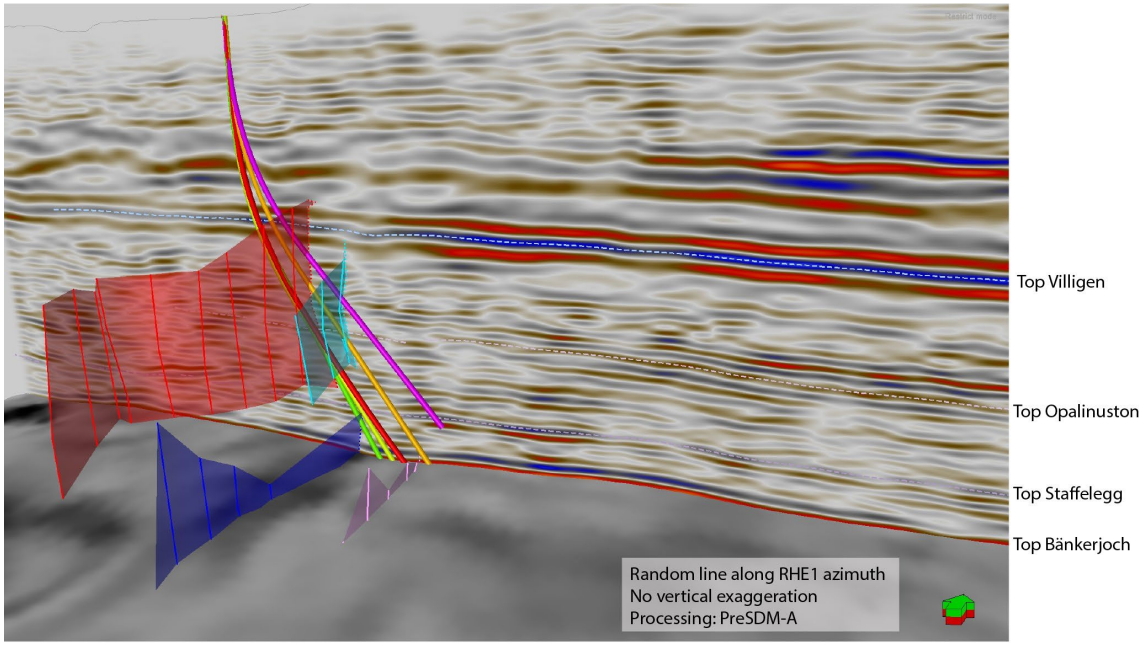

Fig. 1-4: Detailed seismic fault interpretation available for trajectory planning and discussed/ executed well trajectories

Cross-section shows seismic amplitude (seismic processing: pre-stack depth migration PDSM-A). The north direction is indicated by a green-and-red arrow. The vertical distance between the Top Opalinus Clay and Top Staffelegg is ~ 120 m and shows no vertical exaggeration. The horizon slice shows polar dip attribute. Semitransparent subvertical surfaces indicate intepreted faults. The final planned and the drilled trajectories are shown in light green and red, respectively. Other discussed trajectories are shown in yellow, orange and red.

Fig. 1-5 shows a conceptual structural model for the Rheinau Fault incorporating both 3D seismic interpretations and observations from other exploration boreholes as well as from outcrop studies. This conceptual model shows a pronounced mechanical stratigraphy of Northern Switzerland's Mesozoic sedimentary sequence with more focused deformation in the competent units, and distributed deformation in the incompetent units (Roche et al. 2020). Prior to drilling, three hypotheses were formulated on what the RHE1-1 borehole is likely to encounter in the Opalinus Clay. These hypotheses ranged from 1) absence of a distinct fault zone, likely due to a strong degree of strain partitioning within the rheologically weak Opalinus Clay, 2) one or several prominent fault zones, for example revealing cataclastic fault rock or scaly clay as it has been described to occur along larger faults within the Opalinus Clay (Jäggi et al. 2017) and 3) the former but including the occurrence of secondary mineralisations.

As this report represents a data documentation, it deliberately avoids engaging in a synthesis of the observations and test results. Nevertheless, the following results can already be highlighted:

- The drilled trajectory was within close limits compared to the planned well path (see Dossier I for a detailed comparison).
- The borehole did not yield any evidence of a larger-scale fault zone within the Opalinus Clay. However, a number of fault planes have been encountered (*cf.* Dossier V).
- In-situ hydraulic packer tests across these features (*cf.* Dossier VII) yielded hydraulic conductivities similar to undisturbed Opalinus Clay.

- The stepped constant head test demonstrated that a significant enhancement of the flow rate can only be achieved in existing fractures if the fluid pressure is raised considerably and the magnitude of elevated fluid pressure can be maintained (*cf.* Dossier VII).
- Excursions in the profiles of natural tracers can indicate past fluid flow. No such irregularities are seen for the RHE1-1 borehole in the Opalinus Clay (*cf.* Dossier VIII). The stable isotope porewater profiles show characteristics similar to the neighouring vertical boreholes MAR1-1 and Benken.

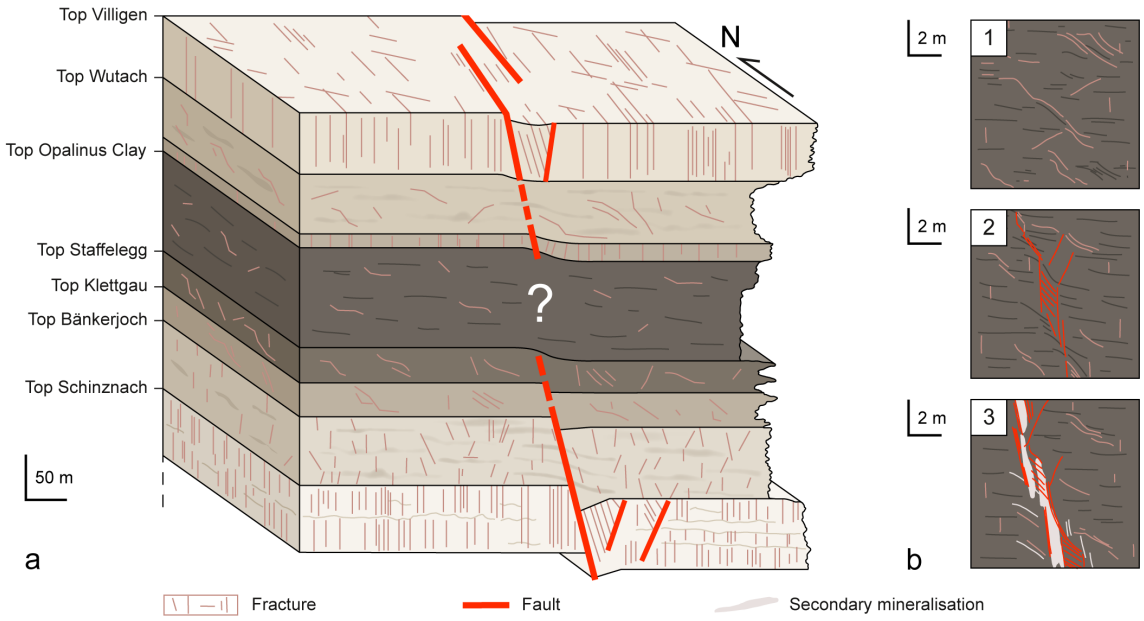

Fig. 1-5: Conceptual structural model of the Rheinau Fault

(a) Conceptual block model. The pronounced mechanical stratigraphy of the Mesozoic sequence in the area is stressed via a schematic weathering profile. The RHE1-1 borehole aimed at characterising the deformation style in the Opalinus Clay constituting a mechanically weak layer in between rheologically stiffer units (e.g. under- and overlying Schinznach/Bänkerjoch and Villigen/Wutach Formations). According to outcrop records and previous borehole results, these units show a significantly higher frequency of fault planes compared to the Opalinus Clay. In 3D seismics, the Rheinau Fault is also only clearly recognisable at the horizons related to stiffer formations.

(b) Hypothetic deformation characteristics of the Opalinus Clay to be encountered in the RHE1-1 borehole: 1) No exceptional deformation features besides small-scale fault planes as previously observed in vertical boreholes outside of seismically recognised faults. 2) One or several localised zones associated with cataclastic fault rock (e.g. scaly clay) as described for larger fault zones elsewhere (e.g. Jäggi et al. 2017). 3) The above, but also including secondary mineralisation (not to scale on picture).

1.2 Location and specifications of the borehole

The Rheinau-1-1 (RHE1-1) exploratory borehole is the eighth borehole drilled within the framework of the TBO project. The drill site is located in the western part of the Zürich Nordost siting region (Fig. 1-2). The deviated borehole reached a final depth of 827.99 m MD = 745.33 m TVD (true vertical depth)[1]. The borehole specifications are provided in Tab. 1-1.

Tab. 1-1: General information about the RHE1-1 borehole

Siting region	Zürich Nordost
Municipality	Rheinau (Canton Zürich / ZH), Switzerland
Drill site	Rheinau-1 (RHE1)
Borehole	Rheinau-1-1 (RHE1-1)
Coordinates	LV95: 2'689'563.92 / 1'277'235.06
Elevation	Ground level = top of rig cellar: 387.23 m above sea level (asl)
Borehole depth	827.99 m measured depth (MD) = 745.33 m true vertical depth (TVD) below ground level (bgl)
Borehole deviation at total depth (TD)	Inclination from vertical: 38.93° Azimuth from north: 76.25°
Drilling period	19th July – 10th October 2021 (spud date to end of rig release)
Drilling company	PR Marriott Drilling Ltd
Drilling rig	Rig-16 Drillmec HH102
Drilling fluid	Water-based mud with various amounts of different components such as[2]: …0 – 497 m: Polymers 497 – 828 m: Potassium silicate & polymers

The lithostratigraphic profile and the casing scheme are shown in Fig. 1-6. The comparison of the core versus log depth[3] of the main lithostratigraphic boundaries in the RHE1-1 borehole is shown in Tab. 1-2.

[1] Measured depth (MD) refers to the position along the borehole trajectory, starting at ground level, which for this borehole is the top of the rig cellar. For a perfectly vertical borehole, MD below ground level (bgl) and true vertical depth (TVD) are the same. In all Dossiers, depth refers to MD unless stated otherwise.

[2] For detailed information, see Dossier I.

[3] Core depth refers to the depth marked on the drill cores. Log depth results from the depth observed during geophysical wireline logging. Note that the petrophysical logs have not been shifted to core depth, hence log depth differs from core depth.

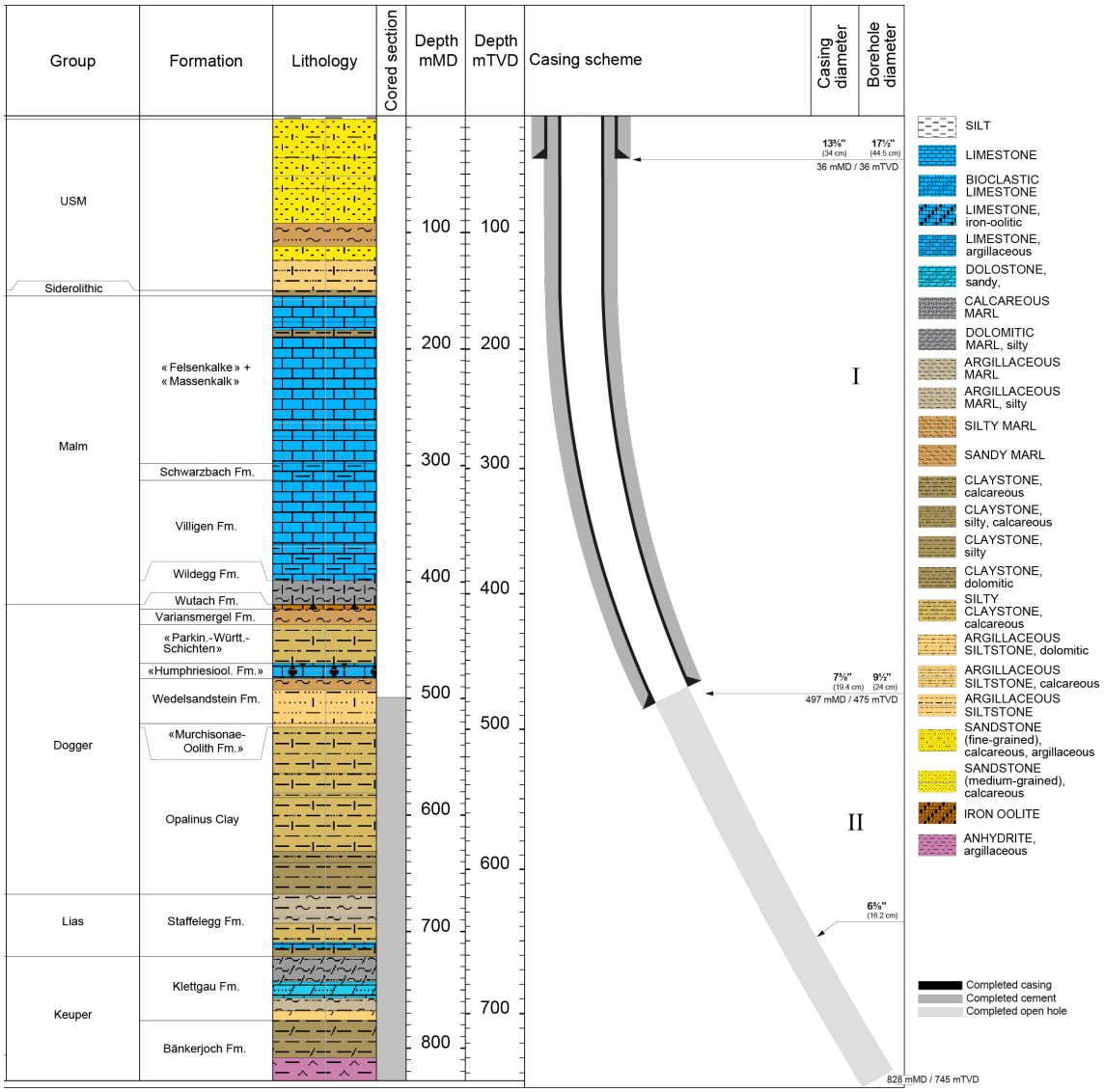

Fig. 1-6: Lithostratigraphic profile and casing scheme for the RHE1-1 borehole[4]

[4] For detailed information, see Dossiers I and III.

Tab. 1-2: Core and log depth for the main lithostratigraphic boundaries in the RHE1-1 borehole[5]

System / Period	Group	Formation		Core top depth in m (MD)	Log top depth in m (MD)		Core top depth in m (TVD)	Log top depth in m (TVD)	
Quaternary				**3**		—	**3**		–
Paleogene + Neogene	USM			149.90		—	149.88		–
	Siderolithic			**154.40**		—	**154.37**		–
Jurassic	Malm	«Felsenkalke» + «Massenkalk»		298.10		—	295.71		–
		Schwarzbach Formation		312.70		—	309.70		–
		Villigen Formation		398.80		—	389.75		–
		Wildegg Formation		419.20		—	408.04		–
	Dogger	Wutach Formation		423.40		—	411.78		–
		Variansmergel Formation		436.60		—	423.47		–
		«Parkinsoni-Württembergica-Sch.»		469.80		—	452.23		–
		«Humphriesioolith Formation»		482.80		—	463.20		–
		Wedelsandstein Formation		521.43	521.21	—	495.83	495.64	–
		«Murchisonae-Oolith Formation»		524.61	524.33	—	498.51	498.27	–
		Opalinus Clay		668.07	668.19	—	617.65	617.75	–
	Lias	Staffelegg Formation		**721.46**	**721.50**	—	**660.95**	**660.98**	–
Triassic	Keuper	Klettgau Formation		776.42	776.79	—	704.82	705.11	–
		Bänkerjoch Formation	final depth	827.99	828.24		745.33	745.52	

[5] For details regarding lithostratigraphic boundaries, see Dossiers III and IV; for details about depth shifts (core goniometry), see Dossier V.

1.3 Documentation structure for the RHE1-1 borehole

NAB 22-03 documents the majority of the investigations carried out in the RHE1-1 borehole, including laboratory investigations on core material. The NAB comprises a series of stand-alone dossiers addressing individual topics and a final dossier with a summary composite plot (Tab. 1-3).

This documentation aims at early publication of the data collected in the RHE1-1 borehole. It includes most of the data available approximately one year after completion of the borehole. Some analyses are still ongoing and results will be published in separate reports.

The current borehole report will provide an important basis for the integration of datasets from different boreholes. The integration and interpretation of the results in the wider geological context will be documented later in separate geoscientific reports.

Tab. 1-3: List of dossiers included in NAB 22-03

Black indicates the dossier at hand.

Dossier	Title	Authors
I	TBO Rheinau-1-1: Drilling	M. Ammen & P.-J. Palten
II	TBO Rheinau-1-1: Core Photography	D. Kaehr & M. Gysi
III	TBO Rheinau-1-1: Lithostratigraphy	M. Schwarz, P. Schürch, P. Jordan, H. Naef, R. Felber, T. Ibele & F. Casanova
IV	TBO Rheinau-1-1: Microfacies, Bio- and Chemostratigraphic Analysis	S. Wohlwend, H.R. Bläsi, S. Feist-Burkhardt, B. Hostettler, U. Menkveld-Gfeller, V. Dietze & G. Deplazes
V	TBO Rheinau-1-1: Structural Geology	A. Ebert, S. Cioldi, E. Hägerstedt, L. Gregorczyk & F. Casanova
VI	TBO Rheinau-1-1: Wireline Logging and Micro-hydraulic Fracturing	J. Gonus, E. Bailey, J. Desroches & R. Garrard
VII	TBO Rheinau-1-1: Hydraulic Packer Testing	R. Schwarz, M. Willmann, P. Schulte, H. Fisch, S. Reinhardt, L. Schlickenrieder, M. Voß & A. Pechstein
VIII	TBO Rheinau-1-1: Rock Properties and Natural Tracer Profiles	J. Iannotta, F. Eichinger, L. Aschwanden & D. Traber
IX		
X	TBO Rheinau-1-1: Petrophysical Log Analysis	S. Marnat & J.K. Becker
	TBO Rheinau-1-1: Summary Plot	Nagra

1.4 Scope and objectives of this dossier

The dossier at hand aims at providing a summary of the conducted hydrogeological investigations (excluding the detailed analysis of the gas threshold pressure test) and acquired hydrogeological data, including assessments of tests and results, but without interpretation.

Borehole RHE1-1 was drilled in the surrounding of a fault to exemplarily assess the actual structural and hydraulic impact of such structures on the Opalinus Clay. An important objective of the borehole was the hydrogeological characterisation of eventually encountered distinct fault zones and/or fractured sections within the Opalinus Clay. For this purpose, an injection test was designed to characterise the behaviour of encountered structures due to changes in the effective stress field around the borehole.

Borehole RHE1-1 was the 6th borehole in the TBO project in which a gas threshold pressure test (GTPT) was conducted. Because the downhole equipment for the GTPT is part of the packer system used for hydraulic packer testing, a description of the equipment is included in this report. The implementation, data collection and analysis of the GTPT will be reported separately.

This report focuses on hydraulic packer testing, and is organised as follows:

- Chapter 2 presents the general strategy for the hydrogeological investigations in the RHE1-1 borehole.
- Chapter 3 discusses all aspects of the hydraulic packer tests including planning of test strategies, test equipment used, general concerns for the analysis of tests, test activities and hydraulic packer test results in borehole RHE1-1. Selected tests and analyses are presented in detail. The results are summarised in tables and plots, and some assessments are made.
- Chapter 4 summarises and discusses the data and results, mainly for the hydraulic packer tests.

Finally, this report includes a set of appendices, which present relevant general project information and further investigation details.

2 Strategy for the hydrogeological investigations

2.1 Hydrogeological objectives of the TBO boreholes

The overall objectives of the hydrogeological investigations are the detailed determination of the hydraulic conductivity and hydraulic head in the aquifers, aquicludes and aquitards on the one hand, and the chemistry and isotopic composition of the deep groundwaters in the aquifers and the porewaters in the aquicludes and aquitards on the other. The results of the hydrogeological investigations in the TBO boreholes form an important dataset for site selection and the safety case. They are mainly needed for the characterisation of:

- Hydraulic and hydrochemical properties of the containment-providing rock zone, which consists of the host rock Opalinus Clay and the confining geological units above and below.
- Hydrogeological conditions in the aquifers providing the hydraulic and hydrochemical boundary conditions for the containment-providing rock zone and providing input for the identification of potential release paths as well as for the planning of the future access structures.

A description of the specific objectives of the RHE1-1 borehole is given in Section 1.1.

2.2 Hydrogeological investigation concept for RHE1-1

The hydrogeological investigations for borehole RHE1-1 comprised only hydraulic packer testing. The main objective was the hydrogeological characterisation of potentially occurring fault zones and/or fractured sections in the Opalinus Clay.

Due to the inclination of the borehole from the vertical and the test objectives of this borehole, no fluid logging and no hydraulic packer tests in the aquifers were carried out.

Hydraulic packer tests were performed in the Lias Group, Staffelegg Formation and in the Dogger Group, Opalinus Clay. They were used for the detailed hydraulic characterisation of selected borehole sections to determine transmissivity (T), hydraulic conductivity (K) and hydraulic head (h), and to identify the appropriate flow model. To characterise the behaviour of encountered structures due to changes in the effective stress field around the borehole, an injection test was designed consisting of multiple test parts. All RHE1-1 hydraulic tests were performed during a single scheduled phase of hydraulic packer testing. Depending on the transmissivity of the test interval and the test objectives, different test methods were applied in this borehole:

- Slug tests
- Pulse tests
- Constant head / constant pressure injection and withdrawal tests

These test methods usually were combined, i.e. executed one after the other as a test sequence in test-specific order.

A gas threshold pressure test (GTPT) was conducted in the Opalinus Clay of the RHE1-1 borehole. Groundwater samples were not collected since hydraulic packer tests in RHE1-1 focused on low transmissive borehole sections.

In the siting region Zürich Nordost, a long-term monitoring system was installed in borehole MAR1-1 and years before in the Benken borehole (Jäggi & Vogt 2020).

3 Hydraulic packer tests

3.1 Test strategy

The geological formations examined in the TBO boreholes exhibit a wide range of transmissivities. The host rock, Opalinus Clay, and its confining units are expected to have very low transmissivities, whilst the regional aquifers in the Malm and Muschelkalk Groups are expected to have relatively high transmissivities. In RHE1-1, only borehole sections with low to very low transmissivities were hydraulically tested. Therefore, only the preferred testing strategy for formations with low to very low transmissivity is presented in this report.

Nagra has long-established hydraulic testing strategies (e.g. Nagra 1997) to extract the maximum information in relation to the hydraulic characteristics of the various geological formations. The preferred testing strategy for low to very low transmissive formations is presented in Tab. 3-1. A typical test sequence is divided into different test phases: test preparation, diagnostic and main phase. The test sequence may be concluded with a pulse test (PW/PI) to check if the total test interval compressibility changed during the test. Modifications to the strategies are made according to the preliminarily available information, the specific test conditions encountered and results obtained while testing. This may lead to the omission of certain test phases, e.g. the diagnostic phase.

In the case of formations with low to very low transmissivity, as hydraulically tested in borehole RHE1-1, the test types and their duration need to consider pressure and temperature disturbances due to drilling which dissipate slowly. For the determination of hydraulic head, the borehole pressure history and test duration are important issues. Depending on the pressure difference between the static formation conditions and the pressure induced in the borehole during the pre-test pressure history, the estimates of hydraulic head can be strongly affected due to non-static pressure conditions in the surrounding borehole area.

A further aspect of the testing strategy is the use of drilling fluid (see Tab. 1-1) as a test fluid. In contrast to previous exploration boreholes drilled by Nagra (e.g. Benken), the exchange of drilling fluid in the test interval prior to hydraulic testing was generally not considered. The main reason was borehole stability. There were exceptions to this, however. The hydraulic test RHE1-1-OPA1 was conducted first with the drilling fluid of potassium silicate and polymers (*cf.* Dossier I). After the execution of the gas threshold pressure test (GTPT), the interval fluid was exchanged to synthetic porewater. The subsequent test sequence with synthetic porewater as test fluid was of short duration and strongly influenced by inherent pressure trends from the precedent GTPT.

Tab. 3-1: Preferred test sequence for formations with low to very low transmissivity

[1] For an explanation of the abbreviations, see Tab. A-3.

Test phase	**Phase** [1]	**Aims**
Test preparation phase	COM	Temperature and pressure equilibration in the test interval
	PSR	Pressure static recovery with closed shut-in tool; create pressure conditions for the initiation of the first test, first estimate of formation pressure; recognition of temperature and pressure trends
Diagnostic phase	PW	First estimates of hydraulic conductivity, which are used to plan the following test sequence
Main phase Version 1	SW	Estimation of hydraulic formation parameters during a flow phase
	SWS	Estimation of an accurate flow model and hydraulic parameters during shut-in conditions
	PW/PI (optional)	Estimation of the total test interval compressibility at the end of the test
Main phase Version 2	PW/PI	Estimation of hydraulic formation parameters (as an alternative to SW/SWS)

Hydraulic test RHE1-1-OPA2 was first conducted with drilling fluid (potassium silicate and polymers) before the interval fluid was replaced with synthetic porewater. The following test sequences were specifically designed to determine the hydraulic properties and flow behaviour due to changes in the effective stress field around the borehole. Based on the initial estimates of hydraulic transmissivity, a test phase intended to establish a flow period was designed as constant head/constant pressure injection and withdrawal test phases (HI, HW). A detailed description of the implementation of this test strategy (applied during RHE1-1-OPA2) is provided in Section 3.4.

Finally, the model implementation as a skin in the test analysis was assumed to adequately address any issues linked with drilling fluid properties at the borehole wall.

3.2 Test equipment

The most relevant components of the field test contractor's equipment have been drawn from the associated mobilisation report and are presented below.

3.2.1 Downhole equipment

The packer system referred to as the heavy-duty double packer system (HDDP) was used for all hydraulic packer tests in open borehole sections. Its top and bottom inflatable packers confine a test interval section of appropriate length for the intended test (Fig. 3-1). Packers with a non-inflated outer diameter of 114 mm (*cf.* Section 3.2.1.2) were used for hydraulic test RHE1-1-LIA1. All the other hydraulic tests were performed with the GTPT equipment with packers with a non-inflated outer diameter of 127 mm (*cf.* Section 3.2.5.2). Inflow and outflow occurred through a perforated filter segment covered by a filter screen mounted on a 2⅞" tubing above the bottom packer.

Four pressure transducers, mounted in a probe carrier shell above the top packer and referred to as the quadruple sub-surface probe or quadruple probe (QSSP), measured the pressures below (P1), within (interval pressure P2) and above the test interval (annulus pressure P3) as well as in the test tubing above the downhole shut-in tool (P4). In addition, the pressure in the test interval was recorded with an autonomous memory gauge at the bottom of the filter screen (P2*).

Temperatures were measured at the level of the QSSP by the temperature sensors associated with each pressure transducer (referred to as T1, T2, T3, T4, respectively) and additionally by the sensor associated with the memory gauge (named T2*).

A hydraulically controlled non-displacement downhole shut-in tool (SIT) placed above the probe carrier shell was used to isolate the test zone from the test tubing (2⅞" EUE API CT5 N80). A progressive cavity pump (PCP) or Moyno® type pump or a pump housing with a 4" submersible pump, integrated in the test tubing, can be used for production pumping tests. The PCP was not used in RHE1-1.

The quadruple flat-pack consisted of three hydraulic steel tubes of ¼" outer diameter (OD) and one electrical conductor coated in a thermoplastic protective cover. Two steel tubes were used for packer inflation and one for the control of the SIT and the pressure release valve (PRV), which was only used when the packers could not be sufficiently deflated by opening the packer lines at the surface.

Certain parts of the downhole equipment are described below in more detail.

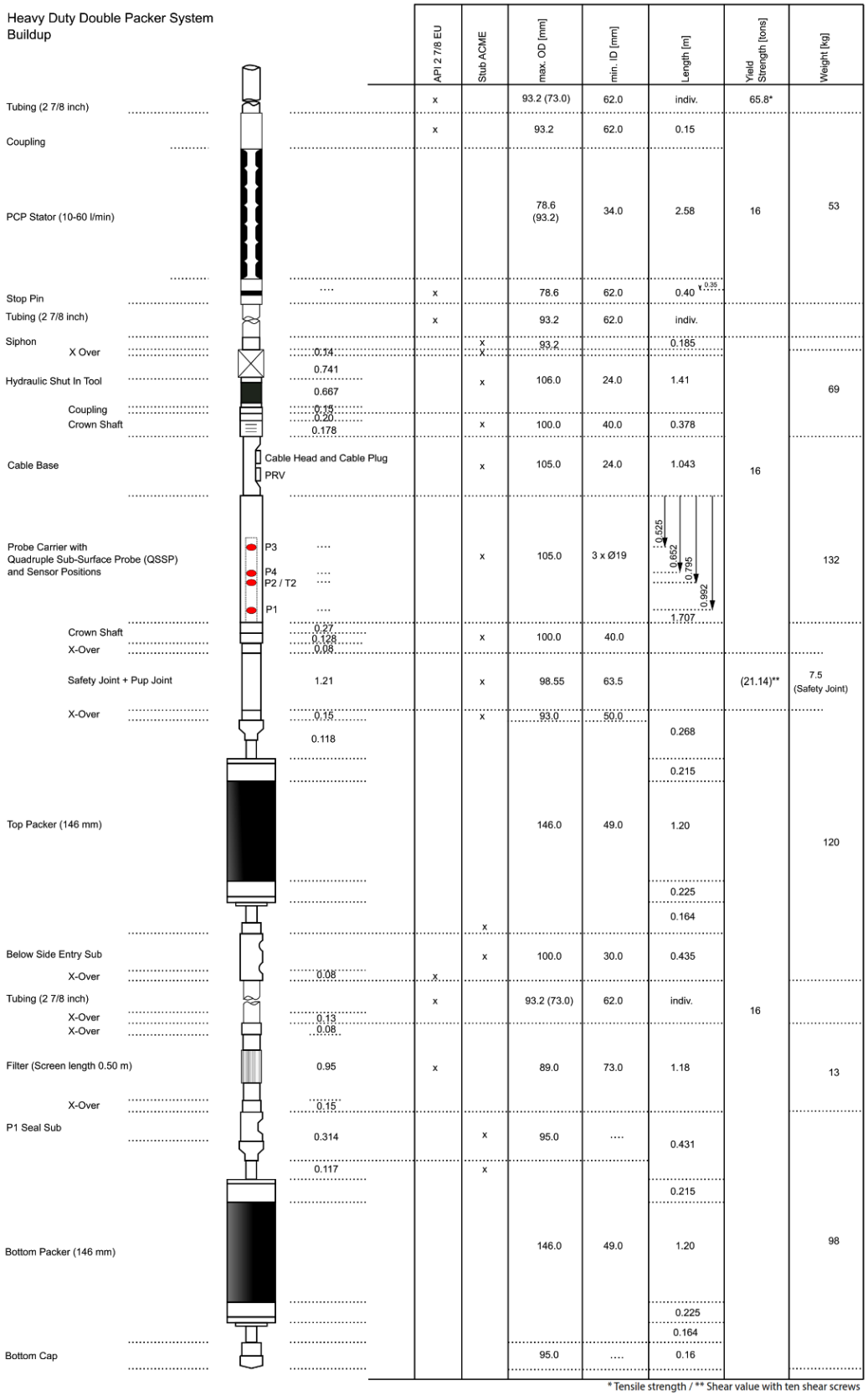

Fig. 3-1: General configuration and specifications of the HDDP in double packer configuration

3.2.1.1 Heavy-duty double packer system

The technical data of the heavy-duty double packer system (HDDP) are provided in Tab. 3-2. A summary of the downhole equipment with the most important component specifications is given in Tab. 3-3.

Tab. 3-2: Specifications for the HDDP

Tool Description	**HDDP**
Packer configuration	Double packer or single packer
Maximum installation depth	1'400 m (vertical); 1'500 m (inclined) along borehole axis
Maximum fluid pressure	20'000 kPa
Maximum differential pressure	114 mm packer system for 162 mm borehole: ~ 12'200 kPa 146 mm packer system for 216 mm borehole: ~ 8'000 kPa
Maximum downhole temperature	80 °C
Range of interval length	3 – 100 m
Probe	QSSP
Shut-in tool (SIT)	Zero-displacement valve
Control lines	4 core encapsulated flat-pack • Hydraulic line – bottom packer (PA1) • Hydraulic line – top packer (PA2) • Hydraulic line – shut-in tool (SIT) and packer pressure release valve (PRV) • ⅛" (3.175 mm) OD tubing encased single conductor cable

Tab. 3-3: Specifications for the HDDP components

Component	**Specifications**	**Minimum inner diameter (ID)** [mm]	**Weight**
Quadruple flat-pack	3 each ¼" OD × 0.049" WT316L stainless steel welded and cold drawn annealed tubes 25'500 kPa maximum test pressure Incorporating 1 each ⅛" OD × 0.022" WT316L stainless steel 16 AWG solid Cu conductor (P/N 024440) encapsulated to ¼" OD in TT200 thermoplastic Encapsulated as 33 mm × 11 mm in TT210 thermoplastic, suitable for maximum 98.9 °C brine service		0.637 kg/m
Tubing	2⅞" EU API CT5 N80	62	9.68 kg/m
Pup joints	2⅞" EU API CT5 L80/N80	62	9.68 kg/m
Shut-in tool (SIT)	Duplex 1.4462	24	69 kg
Pressure release valve (PRV)	Duplex 1.4462	24	132 kg
Cable base	Duplex 1.4462		
Quadruple sub-surface probe (QSSP)	Duplex 1.4462 4 combined pressure and temperature sensors P1/T1, P2/T2, P3/T3 and P4/T4	4 × Ø19	
Coarse thread safety joint	max OD: 3.88" (98.55 mm); min ID: 2.50" (63.50 mm) Thread connection: 2⅞" EUE 8RD with 2⅞" EUE Box x pin connections	63.5	11 kg
Packers for large borehole diameter	IPI 5¾" (146 mm), steel wire reinforced, duplex, natural rubber Packer 1 Packer 2	 49 49	 98 kg 106 kg
Packers for normal borehole diameter	IPI 4½" (114 mm), steel wire reinforced, duplex, Nitrile Butadiene Rubber (NBR) and natural rubber Packer 1 Packer 2	 49 49	 78 kg 67 kg
Filter	HP well screen: sand free filter screen mounted on 2⅞" tubing L80 Length: 0.50 m Length: 1.00 m	 73 73	 13 kg 19 kg
Total system weight	At 1'400 m depth including PCP, quadruple flat-pack cable and centralisers		approx. 15.2 t
Maximum applicable tensile force for entire system	Actual system weight at the corresponding depth, plus 16 tonnes (weakest point)		

3.2.1.2 Packers

Two types of packers were available for use for conventional hydraulic packer tests (without consideration of the additional equipment for a GTPT and/or an interval fluid exchange, *cf.* Section 3.2.5), a 114 mm packer for 162 mm diameter boreholes and a 146 mm packer for 216 mm diameter boreholes (Tab. 3-4). The packers were individually inflated with water through the packer inflation line. The inflation lines were integrated in the quadruple flat-pack and operated using a booster pump. Anti-freeze was added to the water if required. Both packer pressure lines were connected to the packer control board at the winch and equipped with pressure sensors (pressure range 0 – 30'000 kPa) for packer pressure monitoring. The packer pressure sensors were connected to the data acquisition system (DAS) for continuous recording. To keep packer pressures constant, the packers were connected to a pressure control unit (see Section 3.2.2.2).

Tab. 3-4: Specifications for the HDDP packers

Manufacturer	Inflatable Packers International, Perth, Australia	
Packer types	IPI 4½" (114 mm)	IPI 5¾" (146 mm)
Material and type	Duplex, NBR, sliding end (+ 4 natural rubber packer sleeves)	Duplex, natural rubber, sliding end
Reinforcement type	Steel wire reinforced	Steel wire reinforced
Borehole diameter	162 mm	216 mm
Packer diameters	125 – 230 mm (pressure dependent)	162 – 280 mm (pressure dependent)
Outer diameter, not inflated	114 mm max.	146 mm max.
Inner diameter	49 mm min.	49 mm min.
Overall length: Bottom packer Top packer	 1.93 m 2.08 m	 1.92 m 1.92 m
Rubber sleeve length	1.20 m	1.20 m
Thread connections	2⅞" EU pin × 2⅞" EU box	2⅞" EU pin × 2⅞" EU box
Max. working temperature for a period > 100 h	+80 °C	+80 °C
Packer inflation lines	Quadruple flat-pack, see Tab. 3-3	Quadruple flat-pack, see Tab. 3-3
Inflation method	Surface controlled	Surface controlled
Inflation fluid	Water and anti-freeze (if necessary)	Water and anti-freeze (if necessary)

3.2.1.3 Downhole sensors in the quadruple sub-surface probe

Four Keller PA-27XW transducers (for transducer type and specifications see Tab. 3-5) were used to monitor fluid pressures in the interval below the bottom packer (P1), within the testing interval (P2), in the annulus between the tubing and borehole wall above the top packer (P3) and in the test string (P4) above the downhole SIT. These four transducers were mounted in the QSSP probe, which was integrated in the probe carrier (see Fig. 3-1). The pressure sensors measured absolute pressure and corrected it to atmospheric pressure; the sensors generally showed ± 3 kPa at atmospheric pressure conditions.

Each pressure transducer had an associated temperature sensor (referred to as T1, T2, T3 and T4) for full thermal compensation of the pressure measurement (Tab. 3-5). The temperature sensor was mounted inside the pressure transducer housing. Because the temperature measurements were taken at the positions of the pressure transducers, they may not represent the effective temperature of the test interval fluid.

Tab. 3-5: Specifications for the pressure transmitters mounted in the QSSP

FS = full scale

Pressure transducer type	Keller PA-27XW, custom-made
Manufacturer	Keller, Winterthur, Switzerland
Year of commissioning	2018
Pressure range (full scale)	0 – 20'000 kPa (absolute)
Accuracy	-0.004…0.005% FS
Resolution	< 0.0007% FS
Minimum recording rate	1 Hz
Temperature range (FS)	-10 °C – 80 °C
Accuracy (temperature)	1 °C
Resolution (temperature)	0.01 °C
Output signal	RS485 (digital)

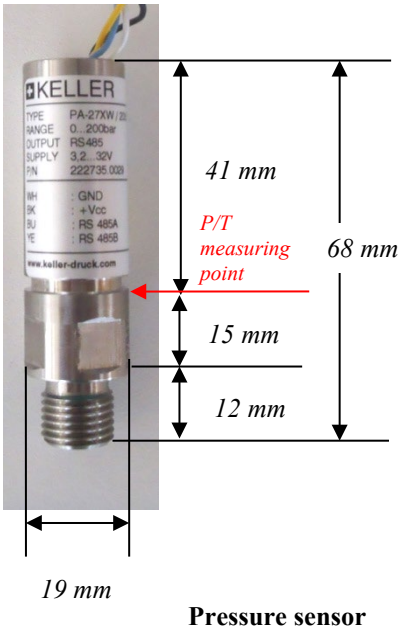

Pressure sensor

3.2.1.4 Autonomous data logger in test interval

Pressures and temperatures were recorded as redundant measurements in the interval at the lower end of the filter screen (referred to as P2* and T2*, respectively) with an autonomous data logger of the type DataCan Memory Pressure Gauge. The specifications are given in Tab. 3-6. The recorded pressure measurement is an absolute measurement.

Tab. 3-6: Specifications for the data logger

FS = full scale

Data logger type	DataCan Memory Pressure Gauge 1.25" Welded Piezo III
Manufacturer	DataCan, Red Deer, Canada
Pressure range (FS)	0 – 20'684 kPa (absolute)
Pressure accuracy	0.022% FS
Resolution	0.0003% FS
Temperature range	0 – 150 °C
Temperature accuracy	0.25 °C
Resolution	0.005 °C
Memory capacity	1'000'000 datasets
Minimum recording rate	10 Hz
Year of commissioning	2018

3.2.1.5 Zero-displacement shut-in tool

The downhole SIT controls the fluid connection between the interior of the test tubing and the test interval. The SIT is a zero-displacement valve that is hydraulically operated via a hydraulic line integrated in the quadruple flat-pack using a hand pump. An axially moveable valve piston opens and closes the valve. The valve piston is moved via the hydraulic (closure) line by applying pressure to close the valve. Releasing the pressure with a pre-stressed spring resets the valve piston and opens the valve (pressure-disturbance free opening).

With a pressure compensation element, the pressure at interval depth (annulus pressure) is used to support the spring and to keep the opening/closing pressure constant for the entire borehole depth. The spring force is high enough to ensure a proper functioning of the valve also at low groundwater levels. The specifications are given in Tab. 3-7.

Tab. 3-7: Specifications for the zero-displacement shut-in tool

Zero displacement shut-in tool (SIT)	Manufactured by Solexperts
Maximum water flow rate	Below 40 l/min without friction loss, max. 350 l/min
Pressure loss caused by SIT at a flow rate of 1 l/min and 10 l/min	± 0 kPa
Closing pressure	9'000 – 10'500 kPa

3.2.1.6 Test tubing

The test rods were made of API 5CT-05 2⅞" tubing. The detailed specifications of the test tubing are summarised in Tab. 3-8.

Tab. 3-8: Specifications for the test tubing

Test tubing type	Seamless steel tubing pipes: API 5CT-05 (PSL1), 8th edition Pup joints: EUE, Tubing & Coupling; API 5CT-05 (PSL1), 8th edition
Manufacturer	Interpipe Nikopolsky, Normec, Celle, Germany
Steel grade	N80/L80 (tubing), N80/L80 (pup joints)
Inner diameter	62.00 mm
Outer diameter	73.02 mm
Coupling outer diameter	93.20 mm
Thread	API 2⅞" EUE
Weight per metre	9.68 kg
Volume per metre	3.02 l
Individual tubing length	Range 2, approx. 9.5 m
Number of individual tubing lengths	111 (tested) + 35 (newly ordered)
Total length of test tubing	Approx. 1'500 m
Lengths of pup joints	Length, quantity 0.50 m, 2 1.00 m, 2 1.03 m, 1 1.50 m, 2 1.55 m, 1 1.83 m, 1 3.00 m, 3

3.2.1.7 Slim tubing

The rate of pressure increase during the flow phase of a slug test depends on the formation transmissivity and the diameter of the test tubing, which mainly defines the wellbore storage of the test system during the slug. To improve the resolution of the pressure change, a slim tubing was used to reduce the diameter of the test tubing for slug tests in formations with low transmissivity. However, the use of a slim tubing in formations with low transmissivity reduces the dominance of the wellbore storage term that is defined by the diameter. In this case, the wellbore storage term that is determined by the compressibility of the test fluid as well as the equipment (defined by determining the test zone compressibility during a shut-in phase) must be taken into account (Black et al. 1987).

The slim tubing consists of a stiff tube, which is installed into the test tubing. A packer at the bottom of the slim tubing with an outer diameter of 56 mm seals the annulus between the 2⅞" tubing and the slim tubing. The water level in the slim tubing was measured with the P4 sensor from the QSSP and additionally with a back-up pressure sensor installed at the bottom of the slim tubing packer, referred to as P4-slim. P4-slim has a smaller pressure range and thus a higher precision compared to P4. The technical specifications of the slim tubing are summarised in Tab. 3-9.

After lowering the water level in the 2⅞" test tubing for a slug withdrawal test to the specified depth, the slim tubing was installed in the tubing below the water level. Afterwards, the slim tubing packer was inflated, and the test was started by opening the SIT valve. The water level only increased in the slim tubing. The use of a stiff tube ensured a constant inner diameter independent of the pressure (fluid level). It should be noted, however, that in the numerical analysis an effective diameter of the slim tubing must be used when using a simulator based on Pickens et al. (1987).

Tab. 3-9: Specifications for the slim tubing

FS = full scale

Slim tubing	Manufactured by Solexperts	
Types	Polyethylene tube	Polyamide tube
Inner diameter	12 mm	6 mm
Outer diameter	16 mm	8 mm
Length	300 m	300 m
Packer specifications	Diameter 56 mm, sealing length 1'000 mm, working pressure 1 – 13.5 MPa	
Packer pressure line	Polyamide OD: 6 mm; ID: 3 mm	
Packer pressure sensor	Keller PAA-33X, 0 – 5'000 kPa, accuracy 0.1% FS	
Pressure sensor (P-slim)	Keller DCX-22, 0 – 5'000 kPa, accuracy 0.05% FS, resolution 0.0025% FS	
Installation procedure	Installation by fixing slim tubing to 1" stainless steel tubing to avoid rotations	

3.2.1.8 Submersible pumps

Frequency driven 3" and 4" Grundfos submersible pumps can be used for pumping tests and during open-hole pumping. The specifications are included in Tab. 3-10. The flow rate can be arbitrarily adjusted because of the frequency control of the pump.

Tab. 3-10: Specifications for the submersible pumps

Submersible pump types	4" down-hole pump	3" down-hole pump
Manufacturer	Grundfos, Fällanden, Switzerland	
Type	SP14-27E	SQE1-110
Regulation	Frequency-controlled	Frequency-controlled
Dimensions	101 × 3'040 mm	74 × 852 mm
Pumping rate at 150 m	100 l/min	10 l/min
Range of pumping rates	Max. 300 l/min	Max. 28 l/min
Maximum installation depth	160 m	160 m
Maximum temperature	40 °C	35 °C
Weight	57 kg (pump) 31 kg (motor)	6 kg
Pump housing	Yes	No
Specifications of pump housing	Length: 4.22 m OD max.: 180 mm Weight: 130.3 kg	
Purpose	Pumping tests	Pumping tests, (fluid logging)

3.2.2 Surface equipment

The surface equipment consisted of the following equipment:

- Winch for quadruple flat-pack cable
- Flow control system
- Pressure-maintenance system
- Data acquisition system

Most of the surface equipment parts were installed in a mobile measuring trailer.

3.2.2.1 Flow board

For the control and measuring of pump (and injection) rates, a flow board with three flowmeters of the type Yokogawa AXF/ADMAG was available. The flowmeters covered a flow rate range between 0.03 and 100 l/min (Tab. 3-11). The schematic layout of the flow control unit is displayed in Fig. 3-2.

Tab. 3-11: Specifications for the flowmeters

FS = full scale

	Measuring range and accuracy			
	Lower limit		**Upper limit**	
	[l/min]	[% FS]	[l/min]	[% FS]
AXF 002	0.03	1	2.945	0.35
AXF 005	0.1	1	11.78	0.35
ADMAG SE202	1.0	1	100	0.35

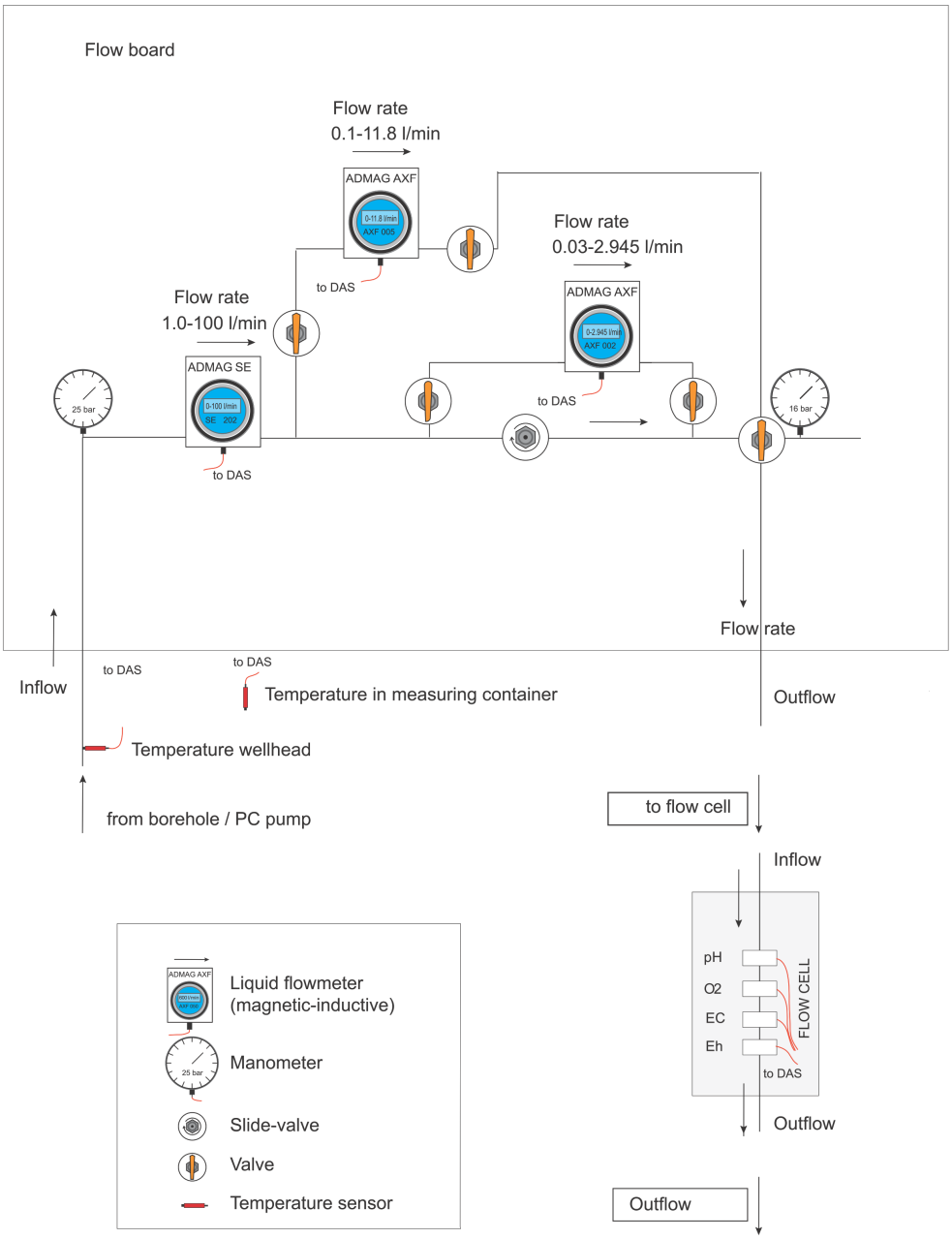

Fig. 3-2: Schematic layout of the flow control unit

3.2.2.2 Packer pressure control unit

Two transducers (type Keller PA-23SY, 30'000 kPa) mounted on the surface inflation control panel were used to monitor the packer inflation pressures (Fig. 3-3). The packer pressure lines are connected to a pressure vessel, which is pressurised by nitrogen. The pressure in the pressure vessel is controlled by a pressure controller for closed volumes. The specifications of the pressure controller are given in Tab. 3-12.

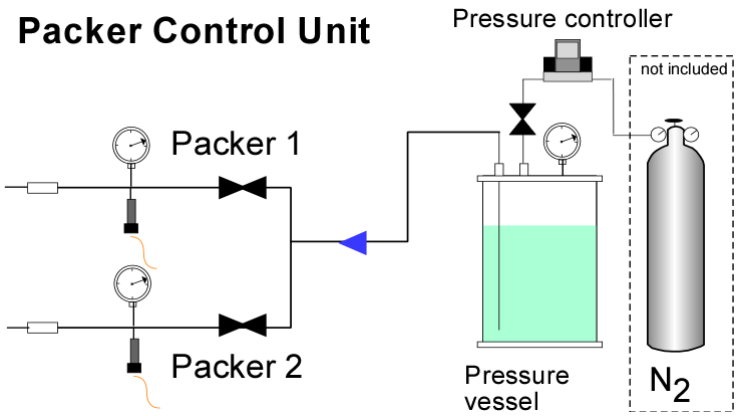

Fig. 3-3: Schematic layout of the packer control unit

Tab. 3-12: Specifications for the pressure controller

FS = full scale

Pressure controller type	Dual-valve pressure controller
Manufacturer	Alicat, USA
Pressure range	0 – 20'684 kPa
Accuracy	0.25% FS
Repeatability	0.08% FS

3.2.2.3 Additionally recorded measurements at surface

A single pressure transducer (type Keller PAA-33X, 80 – 120 kPa absolute) was mounted outside the monitoring trailer and used to monitor barometric pressure and air temperature (Tab. 3-13).

During pumping tests, the physico-chemical parameters (e.g. pH, EC, Eh, temperature and oxygen concentration) of the extracted fluid were recorded. The specifications of the physico-chemical sensors are given in Tab. 3-14. The sensors were calibrated on-site before and after each use.

Tab. 3-13: Specifications for the atmospheric pressure and air temperature sensors
FS = full scale

Pressure sensor type	Keller PAA-33X
Manufacturer	Keller, Winterthur, Switzerland
Pressure range	80 – 120 kPa
Accuracy	0.02% FS
Resolution	0.002% FS
Compensated temperature range	-10 – 80 °C
Accuracy temperature	≤ ± 2 °C
Resolution	≤ 0.01 °C

Tab. 3-14: Specifications for the physico-chemical sensors

Sensor type	**EC**	**pH**	**Eh**	**O_2**
Manufacturer	Xylem analytics, Weilheim, Germany			
Model	WTW TetraCon 325	WTW SensoLyt DW	WTW SensoLyt PtA/Pt	WTW FDO 700 IQ
Range	1 µS/cm – 2 S/cm	0 – 14	± 2'000 mV	0 – 20 mg/l
Accuracy	n/a	n/a	n/a	n/a
Resolution	n/a	n/a	n/a	0.01 mg/l (0.01 ppm)
Temperature range	0 – 100 °C	0 – 60 °C	0 – 60 °C	-5 – 50 °C

3.2.2.4 Data acquisition system

The data acquisition system (DAS) consisted of a Solexperts HDDP interphase for digital and analogue sensors, two industrial PCs, two screens and a keyboard. Data acquisition was performed through the Solexperts GeoMonitor II (GMII) software. The downhole pressures (P1, P2, P3, P4) and temperature measurements (T1, T2, T3, T4) were recorded in real-time through the quadruple flat-pack cable assembly. Surface measurements like flowmeter rates, packer pressures, atmospheric pressure and temperature, slim tubing packer pressure and the physico-chemical parameters were recorded either permanently or, if required, with the same scan rate as the downhole pressures from the QSSP.

The time intervals for scanning could be adjusted as required between 1 s (using a reduced number of sensors) and > 30 s.

The measurements were written to a data file on the PC hard drive in real-time with a continuous data collection and database model. From the PC hard drive, the data were transferred to another network PC continuously for 'online' analysis and data back-up. An uninterruptible power supply was utilised to protect the system from short power interruptions.

3.2.3 Equipment for constant head injection tests with very low flow rates

Very small flow rates for constant head injection tests (HI) can be measured with a pressure vessel on a scale. The equipment is presented in Tab. 3-15 and Fig. 3-4. Two pressure vessels were at hand to assure uninterrupted injection. The equipment was used for test RHE1-1-OPA1 with synthetic porewater as test fluid after the GTPT.

Tab. 3-15: Specifications for the equipment for constant head injection tests with very low flow rates

FS = full scale

Device	**Specifications**
Mettler scale	Range 35 kg, precision ± 1 g
Pressure vessel	Max. pressure 2'000 kPa, volume 20 l
Pressure sensor	Keller PAA-23SY, 0 – 3'000 kPa, absolute, accuracy 0.25% FS, resolution 0.001% FS [1]

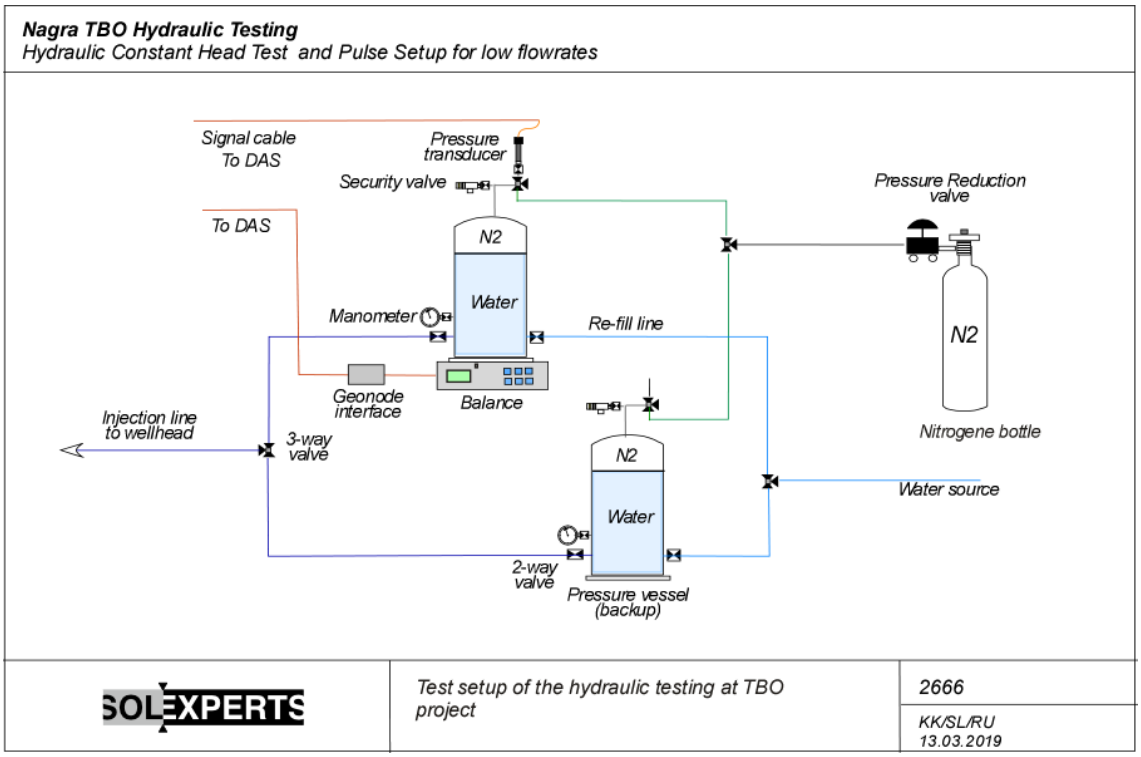

Fig. 3-4: Schematic layout for injection with very low flow rates

3.2.4 Equipment for constant head injection step tests with low and high flow rates

The test equipment described below was used for the constant head injection step test during RHE1-1-OPA2c. A constant head injection step test (series of HI tests) is used to evaluate the dependency of the transmissivity and the effective stress. Based on forward simulations, two different equipment layouts were feasible depending on the transmissivity. The equipment for low flow rates of up to 135 ml/min was to be used for transmissivities between 10^{-10} m^2/s and 10^{-13} m^2/s. The equipment for higher flow rates was to be used for transmissivities between 10^{-8} m^2/s and 10^{-10} m^2/s. The two equipment setups with specifications are presented in Tabs. 3-16, 3-17 and Fig. 3-5.

The equipment for low transmissivities (Tab. 3-16) consisted of a dual syringe pump system for flow rates between 0.001 and 135 ml/min at pressures up to 25'860 kPa. The pistons of the syringe pump allowed for automatic refill to assure continuous injection rates. They were connected to a pressurised tank on a balance to control the total injection volume.

The equipment for higher transmissivities (Tab. 3-17) consisted of the high-pressure pump suitable for flow rates between 1 and 5.1 l/min at pressures up to 40'000 kPa. The overflow valve was set to 20'000 kPa. The dome valve installed between overflow valve and the flowmeters controlled the pressure at constant level. The flow towards the wellhead was measured with two flowmeters, which could be switched depending on the measured flow rate during the constant head injection test.

Tab. 3-16: Specifications for the equipment for constant head injection step tests with low flow rates

FS = full scale

Device	**Specifications**
Mettler scale	Range 60 kg, precision ± 1 g
Pressure vessel	Max. pressure 1'500 kPa, volume 37 l
Pressure sensor	Keller PAA-23SY, 0 – 3'000 kPa, absolute, accuracy 0.25% FS, resolution 0.001% FS
Syringe pump	Teledyne 500 D continuous flow dual syringes pump system, flow range 0.001 – 135 ml/min, accuracy 0.5% of set point, pressure range 70 – 25'860 kPa, accuracy 0.5% FS, operating temperature 5 – 40 °C

Tab. 3-17: Specifications for the equipment for constant head injection step tests with high flow rates

FS = full scale

Device	**Specifications**
Flowmeter 30 – 800 ml/min	Küppers Elektromechanik GmbH, turbine flowmeter HM 9RP, suburban converter WT.02-K, ¼" line connections
Flowmeter 500 – 10'000 ml/min	GHM-GROUP – Honsberg, mechanical flow switch LABO-015GM010E-961821 with spring-supported piston and magnetic triggering of hall sensors with electronics LABO-HD1K-INS, ¼" line connections
Pressure sensor	Keller PAA-23SY, 0 – 3'000 kPa, absolute, accuracy 0.25 % FS, resolution 0.001% FS
Dome valve	Swagelok RDN2-02-VVK-L (RD2 Serie), max. pressure 40'000 kPa, ¼" line connections, flow coefficient c_v 0.05
Dome valve regulator	KPP1RWA421P20000 (KPP Serie), max. pressure 41'300 kPa, ¼" line connections, flow coefficient c_v 0.02
Overflow valve	Swagelok R3A proportional relief valve with ¼" line connections with spring opening at 20'000 kPa
Bypass valve	Swagelok SS-3HNRS4 high pressure union bonnet needle valve, max. pressure 51'200 kPa, ¼" line connections
High pressure pump	Speck Kolbenpumpe Type P21/7-400, max. pressure 40'000 kPa, max. flow 6.8 l/min, max. temperature 70 °C

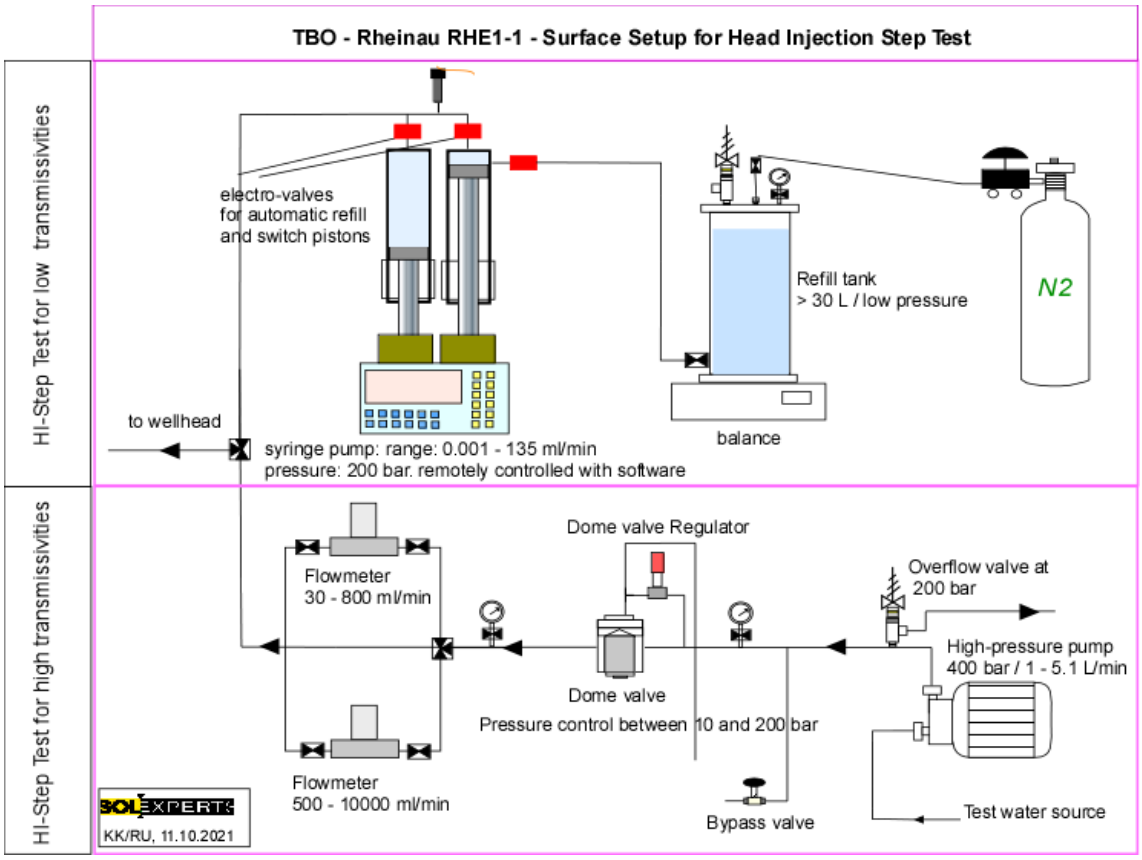

Fig. 3-5: Schematic equipment layout for constant head injection step tests with low (top) and high (bottom) flow rates

3.2.5 Equipment for GTPT and interval fluid exchange

The test equipment for the GTPT was designed in a modular way to be used together with the HDDP system. Additional equipment parts were provided by Nagra. The individual parts were assembled on-site, together with the HDDP system of the field test contractor.

The additional system parts for the downhole equipment were the following:

- X-over 2⅞" to 4½"
- Second shut-in tool (SIT1) with crown shaft below the bottom packer to control the displacement of the interval fluid to the exchange chamber
- 4½" exchange chamber of variable length (API 4½" tubing NU; N80, OD 114.3 mm, ID 100.5 mm, 18.75 kg/m; coupling OD 132 mm) below the HDDP system / lower SIT1 for the collection of exchanged interval fluid, e.g. drilling fluid, sodium hydroxide (NaOH) solution
- Bottom cap / bull nose 4½"
- Dip tube (OD 21.3 mm, wall thickness 2.6 mm) inside the exchange chamber, stainless steel with threads and couplings of variable length, with swivel connection and installation tools
- Four additional ¼" stainless steel lines (910 m, OD 6.35 mm, ID 4.55 mm) on separate coils (SIT1 line, backflow line from exchange chamber, injection line into the interval with a check valve, evacuation line from the interval with a check valve) besides the standard quadruple flat-pack
- Two pressure sensors Keller PA-23SY and one pressure sensor Keller PAA-33X to measure the pressure at the injection, evacuation and backflow lines
- Two inflatable packers with 139.7 mm top and end sub, 127 mm inflatable packer element including six through-going pieces of ¼" stainless steel lines and fittings; or alternatively as back-up solution, two 146 mm inflatable packers with a double mandrel including five through-going pieces of ¼" stainless steel lines and fittings

The additional surface equipment encompassed the following components:

- One gas flow controller 0.1 – 5 ln/min (injection line to interval) (ln = litre normal)
- Two gas flowmeters 3 – 150 ln/min (one connected to back flow line from exchange chamber and one to the injection line for NaOH to gas displacement)
- A flow control board for one gas flow controller and two gas flowmeters with valves and manometers
- Closed tanks for NaOH solution for injection via the (gas-) injection line
- An additional high-pressure injection pump instead of a booster to obtain a higher injection rate and to save time

The flow controller and flowmeters, as well as all other sensors of the GTPT system, were connected to the DAS.

The most relevant system parts are described in detail in the following sections.

A schematic overview of the GTPT system is shown in Fig. 3-6. The four diagrams show the planned test phases of the GTPT:

1. Repeatedly pressurising the exchange chamber with nitrogen (N_2) during the installation process to avoid any damage during installation
2. Injection of NaOH solution through the injection line to push the interval fluid to the exchange chamber and simultaneous extraction of N_2 from the exchange chamber to the surface via the extraction line, only SIT1 open
3. Injection of N_2 through the injection line to push the NaOH solution from the interval to the exchange chamber and extraction of N_2 from the exchange chamber to the surface via the extraction line, only SIT1 open
4. Start of GTPT: Relatively slow injection of N_2 at constant rate into the interval, SIT1 and SIT2[6] closed
5. After finishing the GTPT, preparation for the subsequent hydraulic test using synthetic pore water as interval fluid: Injection of synthetic porewater into the interval through the injection line and simultaneous extraction of N_2 through the evacuation line, SIT1 and SIT2 closed

The downhole GTPT equipment was used for the GTPT in the frame of test RHE1-1-OPA1 and for the fluid exchange during test RHE1-1-OPA2, where the interval fluid was also replaced by synthetic porewater by forcing the drilling fluid into the appendix in preparation of the constant head injection test sequence.

[6] In this section, the usual SIT from the HDDP, which controlled the fluid connection between the interior of the test rods and the test interval, is labelled SIT2; in the test string, it was positioned above SIT1, which controlled the fluid connection between the exchange chamber and the test interval during a GTPT.

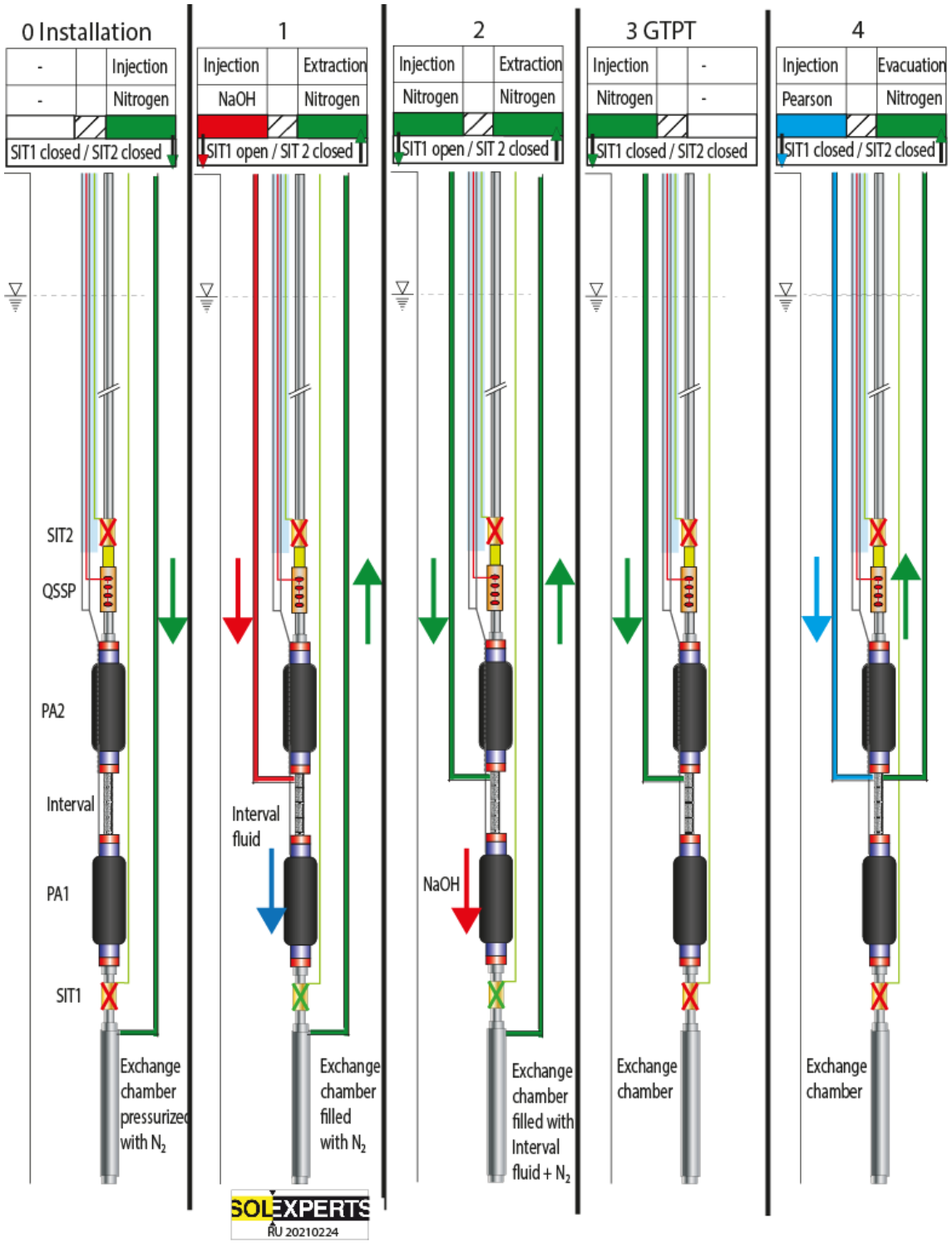

Fig. 3-6: Schematic layout of the modified HDDP system with the major phases of the GTPT

3.2.5.1 146 mm packers

The system comprised two packers with a diameter of 146 mm which had a double mandrel including five pieces of ¼" stainless steel lines and the corresponding fittings.

A detailed description of the packers and the use of the ¼" stainless steel lines is given in Tab. 3-18. Before installation, the packers with the corresponding lines were saturated with water and anti-freeze (if necessary). In RHE1-1 these packers were kept ready as back-up for the 127 mm packers.

Tab. 3-18: Specifications for the 146 mm packers

Manufacturer	Inflatable Packers International (IPI), Perth, Australia
Packer type	IPI 5¾" (146 mm)
Material and type	Duplex, 316 ss, Nitrile Butadiene Rubber (NBR), sliding end
Mandrel	Double mandrel with 5 through-going pieces of ¼" stainless steel lines
Use of ¼" stainless steel lines	Packer 1 (lower packer): 1. Not used 2. SIT1 line 3. Backflow line 4. Not used 5. Line to the QSSP sensor P1 Packer 2 (upper packer) 1. Injection line 2. SIT1 line 3. Backflow line 4. Evacuation line 5. Inflation line packer 1 Note: The final allocation of the line ports was defined on-site
Reinforcement type	Steel wire reinforced
Borehole diameter	162 / 216 mm
Packer diameters	162 – 280 mm (pressure dependent)
Outer diameter, not inflated	146 mm max.
Inner diameter	43.7 mm min.
Overall length: Bottom packer Top packer	 2.195 m 2.195 m
Weight	95 kg each
Rubber sleeve length	1.20 m
Thread connections	2⅞" EU pin × 2⅞" EU box
Packer inflation lines	Quadruple flat-pack
Inflation method	Surface controlled
Inflation fluid	Water and anti-freeze (if necessary)

3.2.5.2 127 mm packers

The system comprised two inflatable packers with 139.7 mm top and end sub, 127 mm inflatable packer element with six through-going pieces of ¼" stainless steel lines and fittings. Additionally, there were two X-overs, one at the bottom of PA1 and one at the bottom of PA2. They served for the P1 entry-sub, allowing to measure pressure below PA1 during testing and to connect the appendix for the interval fluid exchange.

A detailed description of the packers and the use of the ¼" stainless steel lines is given in Tab. 3-19. Before installation, the packers with the corresponding lines were saturated with water and anti-freeze.

Tab. 3-19: Specifications for the 127 mm packers

Manufacturer	Fangmann Downhole Tools, Cloppenburg, Germany
Packer type	Multichannel inflatable packer 5" (127 mm)
Mandrel	One mandrel with 6 through-going pieces of ¼" stainless steel lines
Use of ¼" stainless steel lines	Packer 1 (lower packer): 1. Not used 2. SIT1 line 3. Backflow line 4. Not used 5. Line to the QSSP sensor P1 6. Not used Packer 2 (upper packer) 1. Injection line 2. SIT1 line 3. Backflow line 4. Evacuation line 5. Inflation line packer 1 6. Not used Note: The final allocation of the line ports is defined on-site
Borehole diameter	162 mm
Outer diameter, not inflated	139.7 mm max.; inflatable element diameter 127 mm
Inner diameter	38.1 mm min.
Overall length: Bottom packer Top packer	 3.504 m 3.504 m
Weight	123.47 kg each
Rubber sleeve length	1.676 m
Thread connections	2⅞" EU pin × 2⅞" EU box
Packer inflation lines	Quadruple flat-pack
Inflation method	Surface controlled
Inflation fluid	Water and anti-freeze (if necessary)

3.2.5.3 Stainless steel lines

Four additional ¼" stainless steel lines (OD 6.35 mm, ID 4.55 mm), each with a length of 910 m, were installed together with the downhole equipment and used as follows:

- SIT1 line: activation and de-activation of the SIT1; marked with white tape
- Injection line: gas/fluid injection into the interval; marked with red tape
- Backflow line: backflow from the exchange chamber; marked with green tape
- Evacuation line: evacuation line from the interval; marked with brown tape

The lines were connected to the corresponding stainless steel feed-through, through the top and, if required, through the bottom packer double mandrel. At the surface, the lines were coiled up on the corresponding coils.

The outlet port for the injection line at the lower end of the top packer was equipped with a check valve which enabled flow into the test interval but no backflow from the test interval into the injection line. The check valve opened at a pre-set pressure difference. The outlet port of the evacuation line at the top of the interval was also equipped with a check valve which enabled flow from the test interval to the surface.

3.2.5.4 Zero-displacement shut-in tool SIT1

The new SIT1 was similar to the SIT2 (the HDDP SIT used for hydraulic packer testing) which controls the fluid connection between the interior of the test rods and the test interval. The SIT1 is a zero-displacement valve which controlled the fluid connection between the exchange chamber and the test interval. The SIT1 was hydraulically operated over a ¼" stainless steel line using the booster pump. The opening and closing were performed via an axially moveable valve piston. The valve piston was moved via the hydraulic (closure) line by application of pressure and the valve was closed. The valve piston was reset at pressure release through a pre-stressed spring, and the valve was opened (pressure-disturbance free opening).

With a pressure compensation element, the pressure at interval depth (annulus pressure) was used to support the spring and to keep the opening/closing pressure constant for the entire borehole depth. The spring force was high enough to ensure proper functioning of the valve, also at deep groundwater levels. The specifications are given in Tab. 3-20.

Tab. 3-20: Specifications for the zero-displacement shut-in tool (SIT1)

Manufacturer	Solexperts AG
Maximum water flow rate	Below 40 l/min without friction loss, max. 350 l/min
Pressure loss caused by SIT at a flow rate of 1 l/min and 10 l/min	± 0 kPa
Closing pressure	9'000 – 10'500 kPa

3.2.5.5 Flow control board for GTPT

For the control and measuring of gas injection and extraction rates, the high-pressure gas flow controller and flowmeters were mounted to a flow control board. The flow controller for the control of the injection flow rate had a measuring range of 0.1 – 5 ln/min. The two flowmeters for the flow rate measurements during the displacement of NaOH with gas and during backflow had a measuring range of 3 – 150 ln/min (Tab. 3-21). A schematic drawing of the flow board is included in Fig. 3-7.

In addition to the flow controller and flowmeters, the flow board was equipped with two manometers for 10'000 kPa, two for 16'000 kPa and one for 25'000 kPa maximum pressure. Two needle valves were used to control the flow rates at the injection side and at the backflow side.

Tab. 3-21: Specifications for the gas flow controller / meters for the GTPT

FS = full scale

	Gas flow controller (Flow_G_INJ)	Gas flowmeter (Flow_G_DIS)	Gas flowmeter (Flow_G_BCK)
Manufacturer	Bronkhorst	Bronkhorst	Bronkhorst
Type	IN-FLOW	IN-FLOW	IN-FLOW
Measuring range	0.1 – 5 ln/min	3 – 150 ln/min	3 – 150 ln/min
Accuracy (incl. linearity)	± 0.5% Rd (reading), ± 0.1% FS	± 0.5% Rd (reading), ± 0.1% FS	± 0.5% Rd (reading), ± 0.1% FS
Inlet pressure	5'000 – 20'000 kPa (calibrated for 12'500 kPa)	7'000 – 20'000 kPa (calibrated for 13'500 kPa)	5'000 – 10'000 kPa (calibrated for 7'500 kPa)
Output pressure	100 – 15'000 kPa	–	–
Minimum ΔP	200 kPa	–	–
Medium	N_2	N_2	N_2

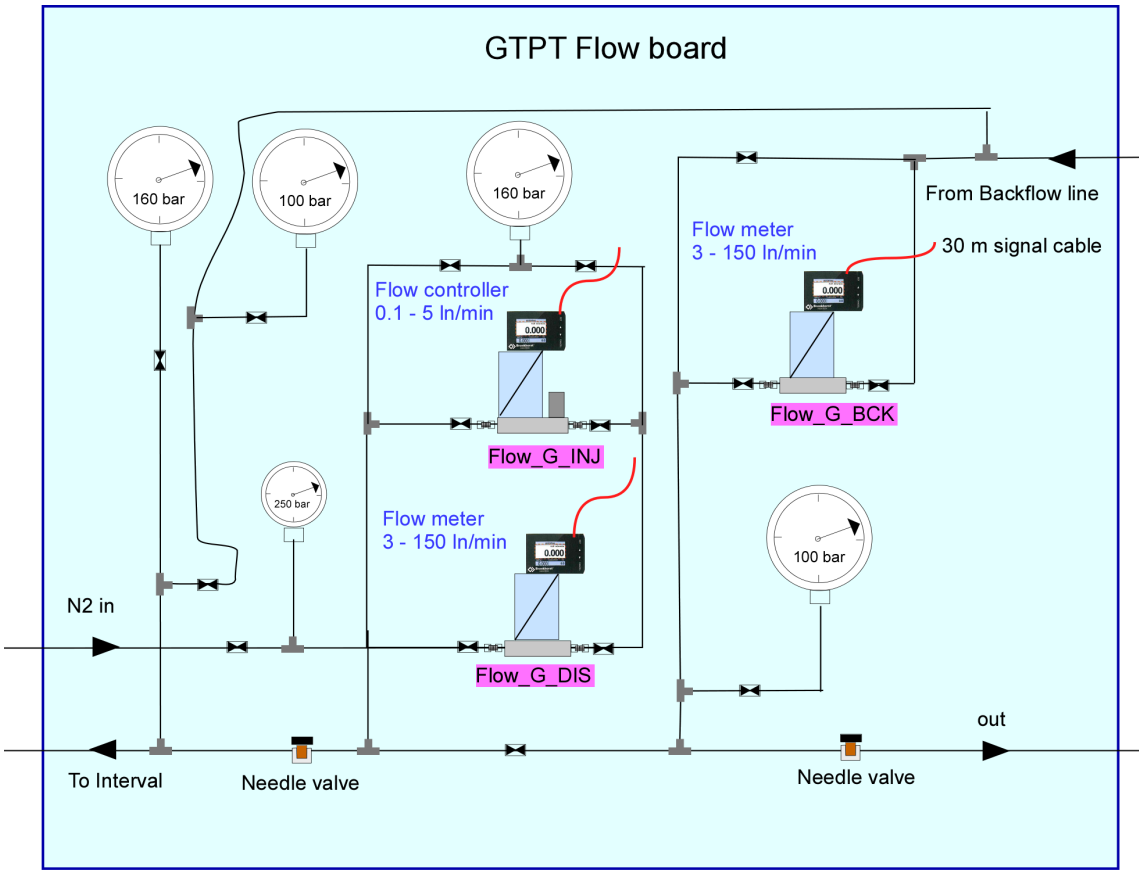

Fig. 3-7: Schematic layout of the flow control unit for the GTPT

3.3 Test analyses

3.3.1 Workflow

For borehole RHE1-1, the general on-site analysis approach involved mainly numerical techniques considering the entire borehole pressure history. Analytical solutions and graphical diagnostic representations were used to analyse the flow model selected, to present the results and to conduct more detailed consistency checks between measurements and simulations. This ensured a comprehensive evaluation of the recorded data. The numerical solutions were assessed further with a perturbation analysis. Prior to commencement of the hydraulic tests, the starting input parameters and in particular, the representation of the borehole history period, were defined.

The analysis workflow supported the test design to achieve the quality objectives defined by Nagra:

- Identification of the most appropriate flow model, e.g. by log-log diagnostic plots (Agarwal 1980)
- Numerical simulation of individual test sequences in cartesian coordinates
- The suitability of the applied flow model was checked with diagnostic representations of the recorded and simulated pressure data, and a limited perturbation analysis was used to assess the credibility of the numerical solution

- Assessment of the credibility of the numerical solution and associated uncertainties through perturbation and sampling analysis
- Numerical simulation of the entire test sequence in cartesian coordinates using the optimised parameter set obtained from individual phase analysis

  This final step was used to check the consistency of the model with the entire dataset
- Consistency check of the test analysis and the estimated parameters by the technical supervisor

The results were used to continually optimise the test design to achieve the quality objectives within the dedicated time of testing. A general flowchart of the analysis work is provided in Fig. 3-8.

Three programmes were used for the analytical and numerical interpretation: Hugo TM (Solexperts AG), Multisim (AFRY Switzerland Ltd.) and nSIGHTS software (Geofirma Engineering Ltd. & INTERA Inc. 2011). The Cooper-Bredehoeft-Papadopulos type-curves were used to analyse both slug and pulse tests (Cooper et al. 1967, Bredehoeft & Papadopulos 1980). Recovery tests were analysed according to Agarwal (1980). A summary of the applied test analysis methods is presented in Tab. 3-22.

Tab. 3-22: Summary of analytical analysis methods / techniques

Test phase	**Analysis method**	**Reference**
Pulse test	Type-curve matching	Bredehoeft & Papadopulos (1980)
	Diagnostics: log-log plot showing dimensionless ΔP and derivative using the deconvolution approach of Peres et al.	Peres et al. (1989)
Slug test (flow phase SW)	Type-curve matching	Cooper et al. (1967) Ramey & Agarwal (1972)
	Diagnostics: log-log plot showing dimensionless ΔP and derivative using the deconvolution approach of Peres et al.	Peres et al. (1989)
Slug test recovery (pressure recovery after slug flow phase, SWS)	Diagnostics: log-log plot showing ΔP and derivative versus "equivalent time" (Agarwal)	Agarwal (1980)
	Straight-line analysis on transient pressure data	Agarwal (1980)
Constant head / constant pressure test	Straight-line analysis on transient pressure data	Jacob & Lohman (1952)
Pressure recovery after constant head / constant pressure tests	Diagnostics: log-log plot showing ΔP and derivative versus "superposition time" (Agarwal)	Agarwal (1980)
	Straight-line analysis on transient pressure data	Agarwal (1980) Jacob & Lohman (1952)

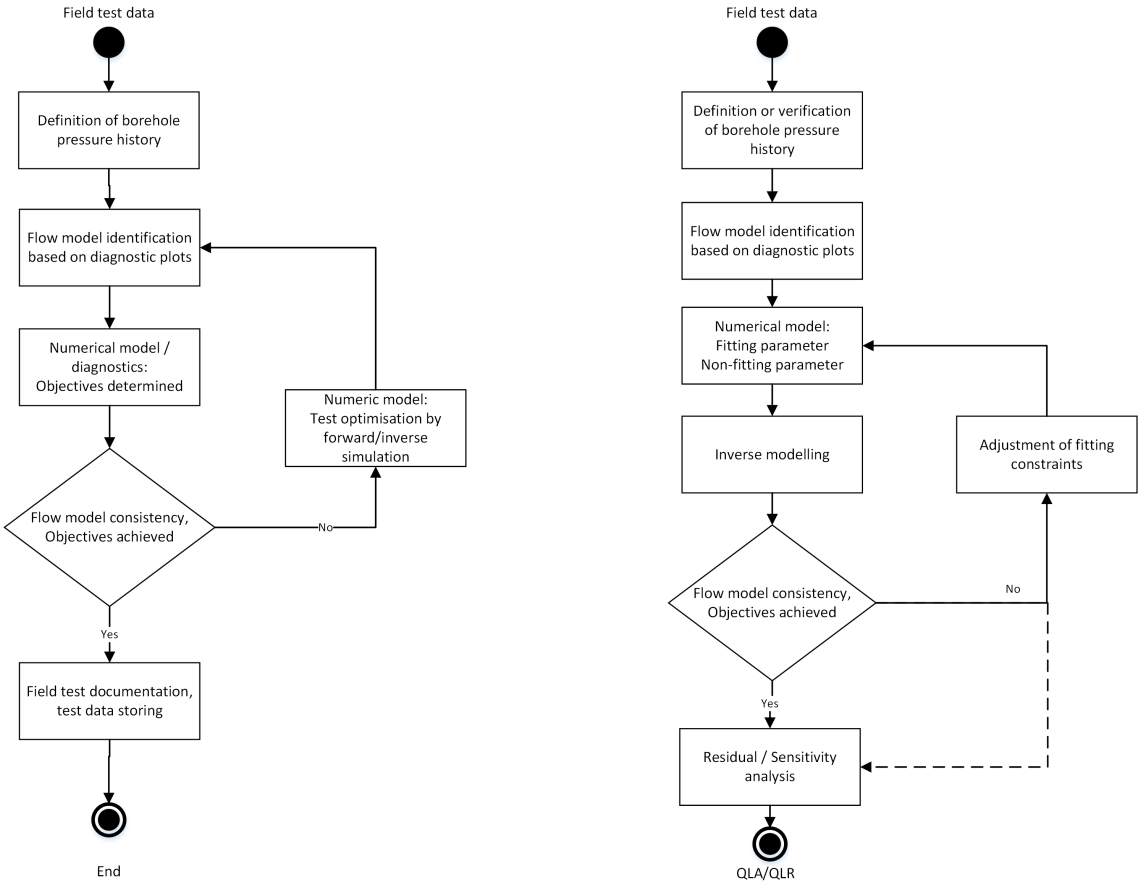

Fig. 3-8: Flowcharts for the on-site hydraulic packer test analysis (left) and Quick Look Analysis (QLA) (right)

The Detailed Analysis (DA) was performed off-site after the test had been completed and was based on the Quick Look Analysis (QLA) reported in the Quick Look Report (QLR). The QLR was reviewed as part of the Quality Control (QC) programme. During this task, open questions and potential ambiguities of the analysis were defined. Based on the outcome of the QC review, further specifications and, if necessary, further analyses were implemented. Fig. 3-9 provides the general flowchart of the DA, which includes perturbation and non-fitting parameter analysis (of the sampling analysis), to obtain the most reasonable parameter results and ranges of uncertainty. The work is summarised in a Detailed Report (DR), with the QLR included as an Appendix.

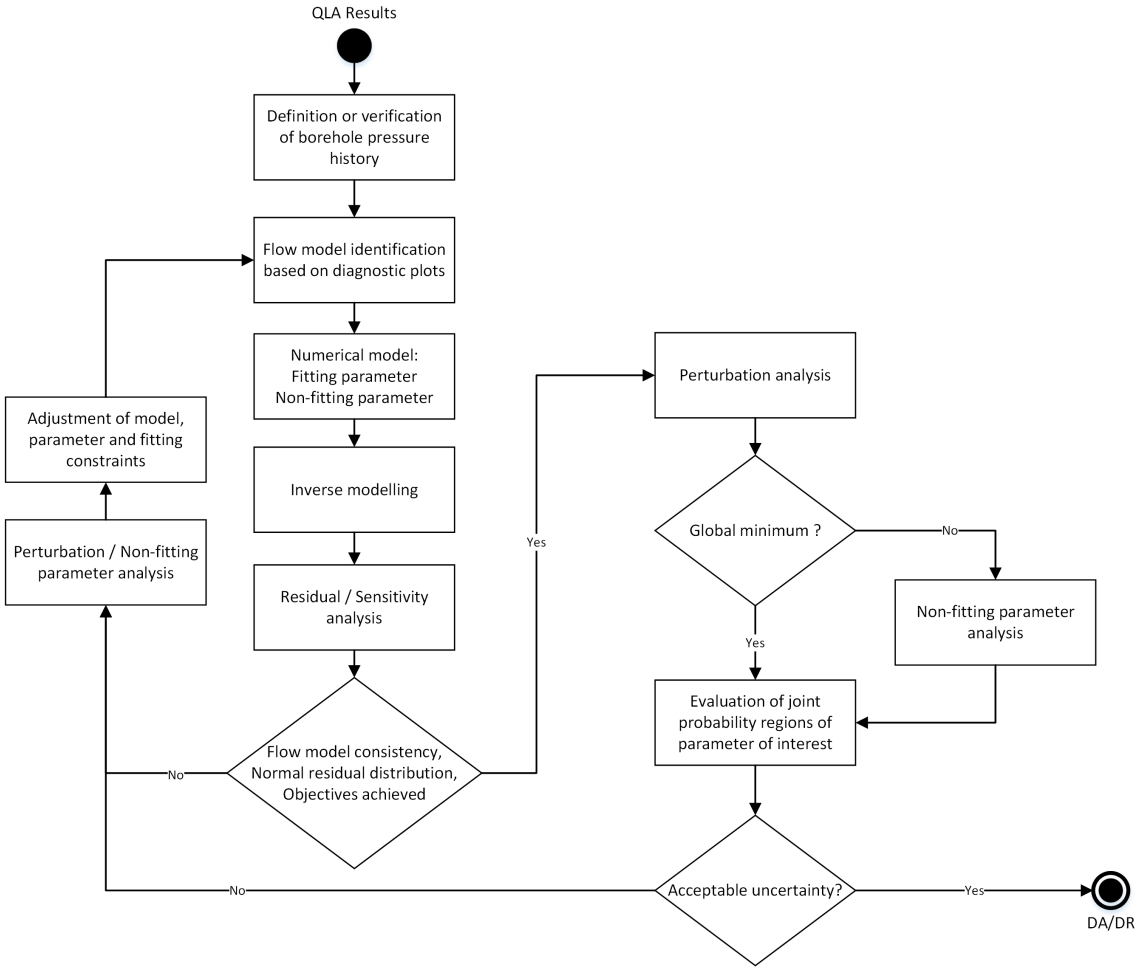

Fig. 3-9: Flowchart for the off-site Detailed Analysis (DA) of a hydraulic packer test

3.3.2 Special effects

The time series measured during hydraulic packer tests are the pressure and temperature inside the test interval. Their development over time was analysed to estimate the hydraulic properties of the formation surrounding the test interval. Various factors affected the recorded time series. All hydraulic tests are affected by factors beyond the test execution and the model used for their analysis (analytical solutions based on assumptions to derive them, numerical models based on the physical processes included in their base equation system). These are referred to as disturbances because they are not considered in the analysis. However, it is possible to describe the development of temperature and pressure signals using the diffusion equation. Disturbances are of short duration in formations with medium to high transmissivity. In formations with low transmissivity, disturbances in the pressure or temperature field can have a significant influence on the pressure signal measured during the test in the test interval (e.g. Nagra 1997, Grauls 1999, Nagra 2001).

Any disturbances of the pressure field during the time before the hydraulic test is started are summarised under the name 'borehole pressure history'. Disturbances in the pressure and temperature fields can be caused by drilling and other activities before testing. In addition, disturbances can occur even during testing, e.g. mechanical effects (including poroelastic effects)

due to changes in the stress field surrounding the interval, or osmosis due to the chemical interaction of the formation and the drilling fluid. However, results from the experiment 'Deep Borehole Hydraulic Testing Experiment' in the Mont Terri Rock Laboratory show that osmotic effects have no significant impact on the determination of transmissivity and hydraulic head (Marschall et al. 2003).

As the TBO boreholes are multi-purpose boreholes with many other objectives besides hydraulic packer testing, there is always a trade-off between disciplines regarding optimal test conditions. Most hydraulic packer tests were performed without exchange of drilling fluid with testing fluid in order to maintain borehole stability. In addition to this preventative measure, the numerical analysis tool can estimate the effect of these influences, so that plausibility ranges for the parameter estimations can be defined. In the following, possible individual special effects that have previously been identified, e.g. for the Benken borehole (Nagra 2001), are discussed in more detail.

3.3.2.1 Borehole history

All numerical analyses took into account the borehole pressure history. The borehole pressure history was constructed based on activities that took place prior to hydraulic testing. Drilling through the centre of the test interval was used as the starting point of the pressure history. The borehole pressure history data were incorporated into the numerical analyses. The following information was used:

- Date and time of drilling through the interval centre, from drilling logs
- Drilling fluid density
- Drilling fluid level in the borehole prior to testing
- Pressure records of preceding hydraulic testing

The drilling fluid densities were measured four times per day and documented in the drilling mud report by the drilling mud engineer from SIRIUS-ES GmbH. In addition, continuous recordings were available from the mud logging company GEODATA during periods of coring and mud circulation, and mud level measurements in the borehole were performed from time to time.

Most affected by the borehole pressure history is the determination of the static formation pressure or the hydraulic head / hydraulic potential (which are derived from the static formation pressure), which in turn depends on the transmissivity of the formation. In formations with low transmissivity, like the Opalinus Clay, the determination of the static formation pressure can be impossible to carry out in a reasonable time due to the long duration of the pressure history. This was proven by measurements carried out using the Benken long-term monitoring system, which demonstrated that the static formation pressures of the Opalinus Clay determined by hydraulic tests were much higher than those subsequently determined by long-term measurements (e.g. Jäggi & Vogt 2020).

The specific periods of the borehole pressure history taken into account for the analysis of the hydraulic packer tests in borehole RHE1-1 are provided in Tab. 3-23.

Tab. 3-23: Specific periods of the borehole pressure history

History refers to the period prior to the separation of the test interval from the rest of the borehole through the inflation of the last packer, which marks the beginning of hydraulic testing.

Test name	**Drilling through interval centre:** date and time	**Start hydraulic testing:** date and time	**Borehole history duration** [h]
RHE1-1-LIA1	11.08.2021 16:22	27.08.2021 12:47	380.40
RHE1-1-OPA1	02.08.2021 14:02	02.09.2021 09:33	739.52
RHE1-1-OPA2	06.08.2021 05:12	13.09.2021 17:43	924.52

3.3.2.2 Interval temperature changes during testing

All activities inside the open borehole also affect the temperature field in and around the borehole. In formations with low transmissivity, this temperature disturbance affects the pressure field surrounding the borehole due to coupled thermo-hydraulic processes. The analysis of hydraulic tests using the numerical software packages nSIGHTS, Multisim and WellSi can incorporate temperature changes during the hydraulic test that lead to a change in fluid volume and thus pressure within a confined test interval volume. The fluid volume change in the test interval was calculated using the volumetric thermal expansion coefficient of the interval fluid (water), which itself is temperature-dependent. The pressure change is linearly dependent on the interval fluid volume change using a proportionality factor, the compressibility of the interval.

3.3.2.3 Mechanical effects

The mechanical deformations caused by drilling- and testing-related stress redistribution in the formation can also influence the pressure response during a hydraulic test. Normally, the conceptual model for the description of the storage coefficient used in the underlying hydraulic models assumes a compressible pore volume and an incompressible grain structure. In this model, changes in pore pressure are considered as movement of the fluid into and out of the pore volume. The coupling between fluid volume change and mechanical deformations results in a time-dependent deformation for an elastic medium (Detournay & Cheng 1988). The Opalinus Clay has shown a time-dependent deformation during tunnel excavation in the Mont Terri Rock Laboratory (see Lisjak et al. 2015 for a summary of the observations and for a numerical interpretation of the data). Opalinus Clay time-dependent behaviour is most likely due to the undrained and drained excavation response, rather than mechanical creep phenomena. In formations with low transmissivity, time-dependent deformations can have an influence on the pressure signal observed in the test interval.

However, there are no data on mechanical deformations available for the tests in borehole RHE1-1 that would allow the characterisation of mechanical effects on the tests in formations with low transmissivity. Deformations of the borehole wall can be included in the analysis by all the numerical software packages used by the means of an appropriate parameterisation during the analysis in the same way as for temperature changes inside the interval. The resulting pressure change is caused by volume changes, which can be either linear or quadratic. The proportionality factor between the volume change and the pressure change is the interval compressibility.

3.4 Test activities

The main exploration objective of the deviated borehole RHE1-1 (*cf.* Section 1.1) resulted in a unique hydraulic testing campaign. Only three hydraulic tests were performed although two of these were multi-part tests. The most important test specifications are summarised in Tab. 3-24.

The borehole RHE1-1 was drilled to the depth of 828 m MD (745.34 m TVD) before hydraulic testing started. A petrophysical logging campaign was performed between the end of drilling and the hydraulic testing phase. The measured pressures (measured by the downhole QSSP sensors) for all tests conducted in RHE1-1 are provided in Figs. 3-10 to 3-16. The figures were taken directly from the corresponding analysis reports of the field test contractor.

The 127 mm packers of the GTPT equipment (*cf.* Section 3.2.5.2) were used for hydraulic tests in the Opalinus Clay. The 114 mm packers were used for hydraulic test RHE1-1-LIA1 (*cf.* Section 3.2.1.2).

The geological formations (*cf.* Dossier III) encompassed by the hydraulic tests are as follows:

- Dogger Group with a focus on Opalinus Clay (RHE1-1-OPA1 and RHE1-1-OPA2)
- Lias Group with a focus on the Staffelegg Formation with the Frick, Beggingen and Schambelen Members (RHE1-1-LIA1)

The hydraulic test RHE1-1-OPA1 was conducted in three parts (including a GTPT), each with specific conditions and objectives:

- RHE1-1-OPA1a (Fig. 3-10): a hydraulic test conducted with drilling fluid of potassium silicate and polymers (*cf.* Dossier I) as test interval fluid; to determine the hydraulic conductivity and static pore pressure before the GTPT sequence
- RHE1-1-OPA1b: the actual GTPT with preceding interval fluid exchange; to determine the gas entry pressure
- RHE1-1-OPA1c (Fig. 3-11): a hydraulic test conducted with synthetic porewater as test interval fluid; to determine any changes in hydraulic conductivity or mobility caused by the precedent gas injection and after pressure reduction in the test interval.

Only the hydraulic test RHE1-1-OPA1a is of concern for estimating representative hydraulic parameters of the formation. The analysis of the actual GTPT is not part of this report. The hydraulic test RHE1-1-OPA1c was of short duration and strongly influenced by inherent pressure trends from the precedent GTPT which impeded the estimation of hydraulic formation parameters after the GTPT.

The hydraulic test RHE1-1-OPA2 had the general objective to determine the hydraulic transmissivity with respect to changing effective stress conditions by changing the interval pressure. Hence, the hydraulic test was performed in several phases. The first phases focused on the estimation of the formation hydraulic properties. Then, a series of constant head injection (HI) phases with a stepwise increase of the interval pressure was conducted to investigate the hydraulic transmissivity with respect to changing effective stress conditions. These were followed by a recovery phase and eventually by test phases to determine the hydraulic conductivity and flow model after the series of HI phases. The entire hydraulic test RHE1-1-OPA2 was divided into four parts with the following conditions and objectives:

- RHE1-1-OPA2a (Fig. 3-12): hydraulic test sequence with the drilling fluid of potassium silicate and polymers (*cf.* Dossier I) as test interval fluid; to determine the formation hydraulic properties, especially the hydraulic conductivity and flow model

- RHE1-1-OPA2b (Fig. 3-13): hydraulic test sequence after the replacement of the drilling fluid with synthetic porewater inside the test interval; to determine the formation hydraulic properties and conditions after the fluid exchange for the subsequent injection tests
- RHE1-1-OPA2c (Fig. 3-14): hydraulic test sequence of constant head / constant pressure injection steps (series of HI phases) with synthetic porewater as test interval fluid; to determine the injection flow rate and the hydraulic transmissivity as function of increasing interval pressure
- RHE1-1-OPA2d (Fig. 3-15): hydraulic test sequence with synthetic porewater as test interval fluid; to determine the hydraulic transmissivity and flow model after the series of HI phases and a subsequent recovery phase with decreasing interval pressure.

The hydraulic test RHE1-1-LIA1 (Fig. 3-16) was performed conventionally, i.e. not as a multi-part test, using the HDDP system with 114 mm packers. It followed petrophysical logging. The drilling fluid was used as the interval test fluid for the test RHE1-1-LIA1, i.e. the test was performed without any prior fluid exchange.

All hydraulic tests were performed in an inclined cored borehole section with a borehole diameter of 6⅜".

The density and viscosity of the drilling fluid were recorded by the mud engineer in daily mud reports. No considerable mud losses were reported while drilling borehole RHE1-1. Sodium-fluorescein at a concentration of approximately 1 ppm was used to trace the drilling mud, while 1.5-naphthalene disulfonate acid – NDSA was used as tracer for the water in the test tubing at concentrations of approximately 10 ppm.

The SIT was closed during the entire time the HDDP was lowered to the test depth and also during installation. Therefore, in test intervals with low transmissivity, the interval fluid density was not affected by traced water in the test tubing during the performance of initial withdrawal tests. If a pressure increase of more than 100 kPa was observed in the test interval during inflation of the top packer, the SIT was opened and the COM phase started. Due to the higher density of the mud in the test interval, for formations with low transmissivity, it was assumed that no flow occurred from the test tubing into the test interval during the COM phase. Flow from the formation into the borehole by means of a longer test phase at reduced interval pressure (i.e. a slug or pumping test phase) was created during all tests.

A swabbing tool was used to create the pressure difference between the test tubing and the test interval.

The interval temperature change was included in the analysis of the hydraulic packer tests. The temperature increase in the test interval, from the start of the initial pressure recovery (PSR) after closing the shut-in valve until the end of the test, ranged from 0.15 K to 1.63 K for all tests.

Tab. 3-24: Hydraulic packer testing in borehole RHE1-1: Test interval and test specifications

[1] For an explanation of the test names and test phases see Tabs. A-2 and A-3, respectively.

[2] Time between inflation of the last packer and deflation of the first packer.

[3] FM = flow model, T = transmissivity, h_s = static hydraulic head.

Test name [1]	**Interval depth** [m MD] ([mTVD])	**Interval centre** [m MD] ([mTVD])	**Packer configuration**	**Test phases** [1]	**Testing period** [2] (duration)	**Geological information** [depth and length values are rounded; groups and formations are usually named from top down; for details see Dossier III]	**Objectives** [3] [secondary aims in brackets ()]
RHE1-1-OPA1a	548.00 – 554.32 (518.18 – 523.48)	551.16 (520.83)	Double	PSR, SW, SWS, PI	02.09. – 05.09.2021 (72.7 h)	Dogger Group («Brauner Dogger»): test interval entirely within the 'Sub-unit with silty calcareous beds' of the Opalinus Clay. The test interval was defined in order to target a faulted interval between approximately 550.0 and 552.0 m MD (519.86 – 521.54 m TVD).	T, (h_s), FM Followed by GTPT to estimate gas entry pressure
RHE1-1-OPA1c			Double	PSR2, PW, HI1, HI2, HIS, PW2	09.09. – 11.09.2021 (31.2 h)		(T), (h_s), FM Investigate self-sealing behaviour after GTPT
RHE1-1-OPA2a	612.18 – 621.50 (571.68 – 579.39)	616.84 (575.54)	Double	PSR, SW, SWS, PW, (DISP1)	13.09. – 16.09.2021 (62.7 h)	Dogger Group («Brauner Dogger»): test interval entirely within the 'Mixed clay-silt-carbonate sub-unit' of the Opalinus Clay. The test interval aimed to target a faulted interval between approximately 616.0 and 618.5 m MD (574.84 –576.91 m TVD).	T, (h_s), FM
RHE1-1-OPA2b			Double	PSR2, SW2, SWS2, PI, (DEGA1), PSR3, PW2, (DEGA2), PSR4, PW3	16.09. – 18.09.2021 (61.2 h)		T, (hs), FM
RHE1-1-OPA2c			Double	HI1, HI2, PW4, (DEGA3), PSR5, PW5, HI3 (HI301 – HI309), MRS	18.09. – 23.09.2021 (108.5 h)		T, (hs), FM T as a function of effective stress
RHE1-1-OPA2d			Double	PW6, PW7, HW, HWS, PW8	23.09. – 30.09.2021 (153.7 h)		T, (hs), FM T after/ during interval pressure bleed off
RHE1-1-LIA1	707.00 – 720.35 (649.29 – 660.06)	713.68 (654.68)	Double	PSR, SW, SWS, PW	27.08. – 30.08.2021 (77.3 h)	Lias Group: The test interval is entirely within the heterogeneous succession of mostly marl and claystone of the Staffelegg Formation consisting of the Frick (2.21 m), Beggingen (4.94 m) and Schambelen (6.20 m) Members.	T, (hs), FM Explore faults in the Beggingen and Schambelen Members

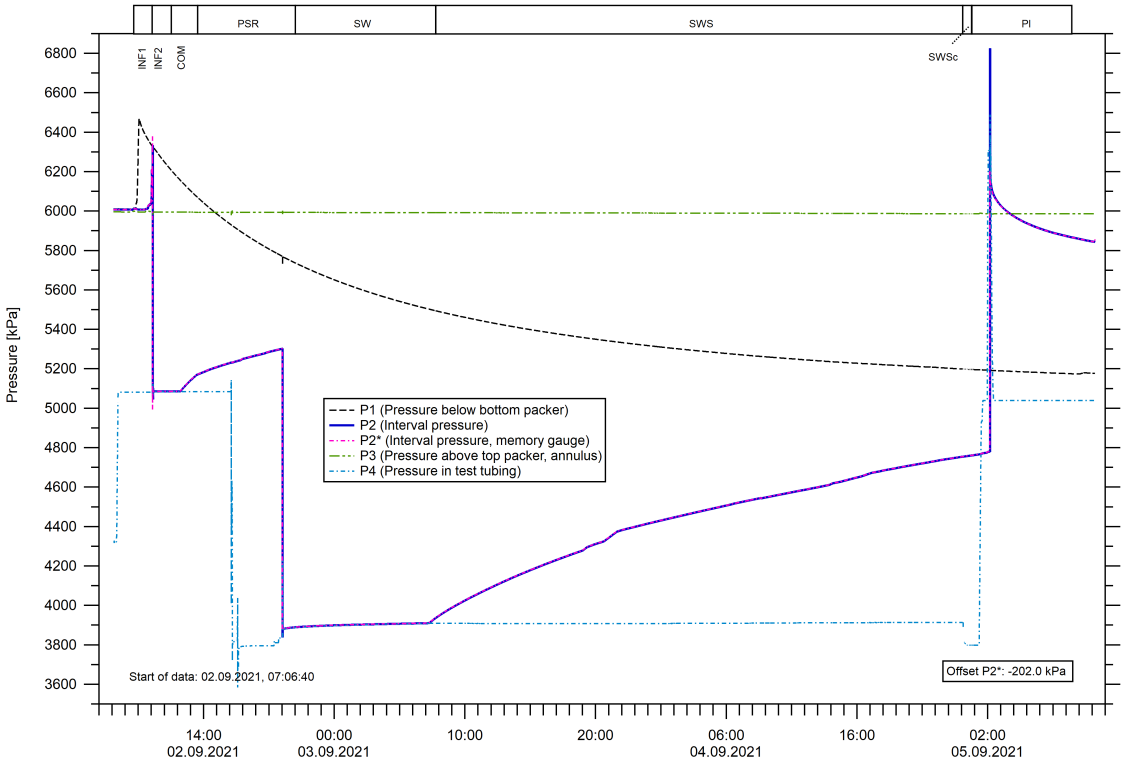

Fig. 3-10: Hydraulic packer test RHE1-1-OPA1a: Overview plot of pressure vs. time and date

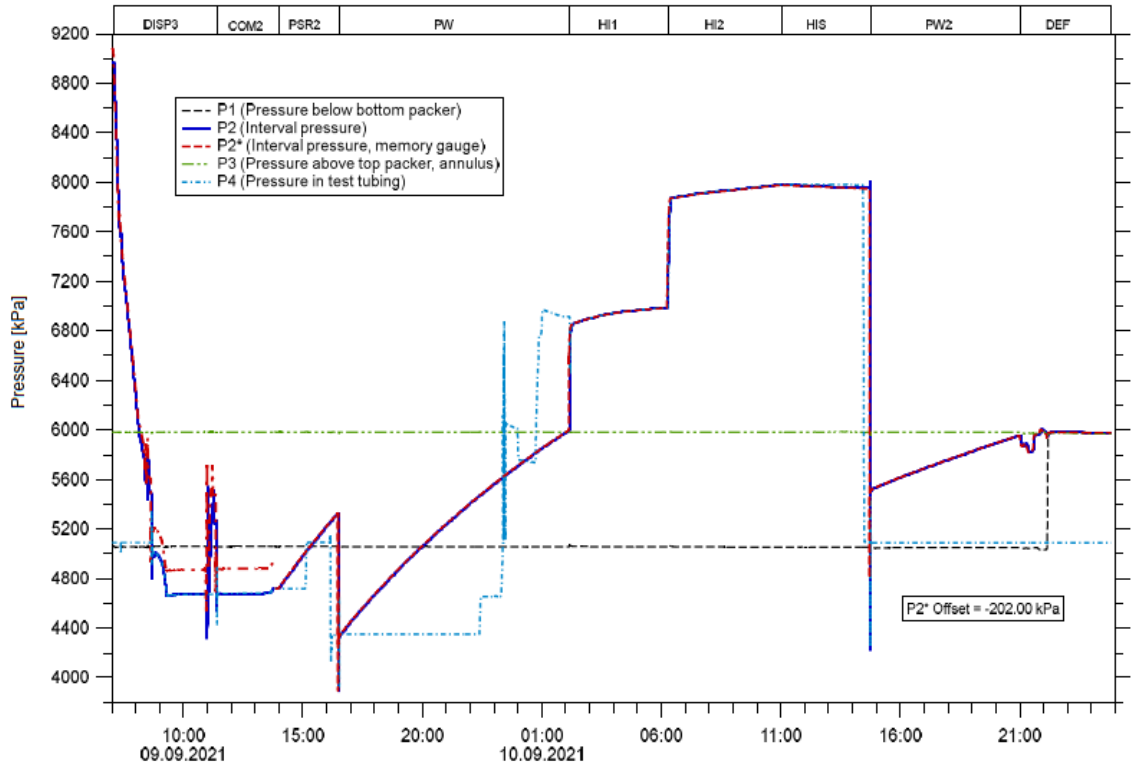

Fig. 3-11: Hydraulic packer test RHE1-1-OPA1c: Overview plot of pressure vs. time and date

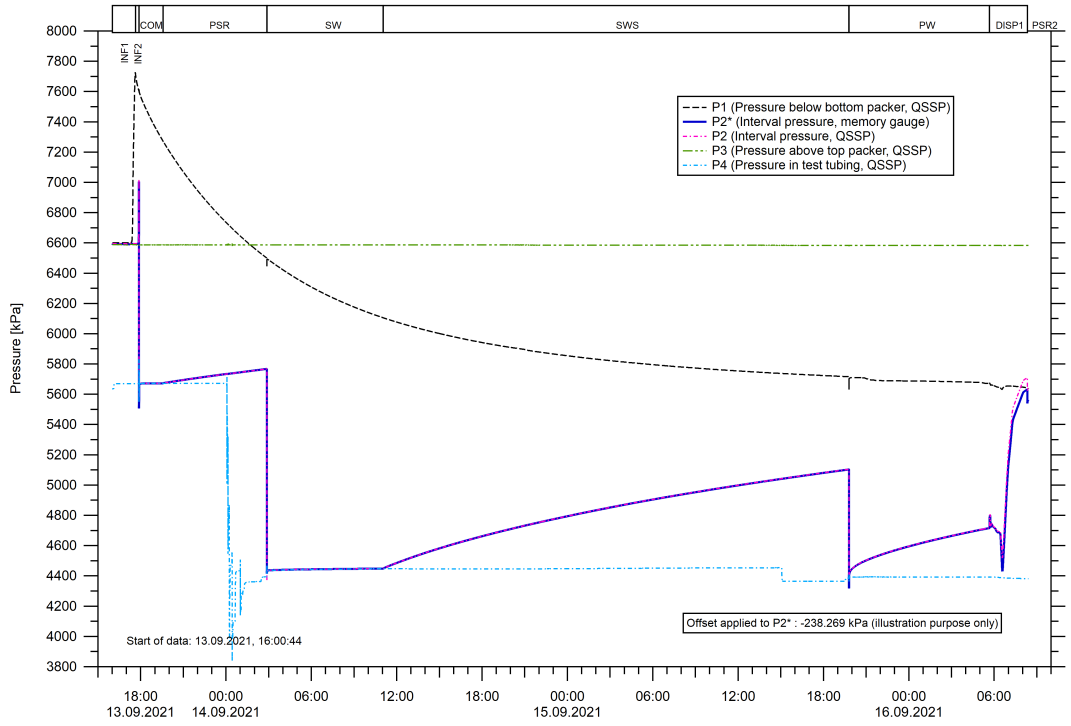

Fig. 3-12: Hydraulic packer test RHE1-1-OPA2a: Overview plot of pressure vs. time and date

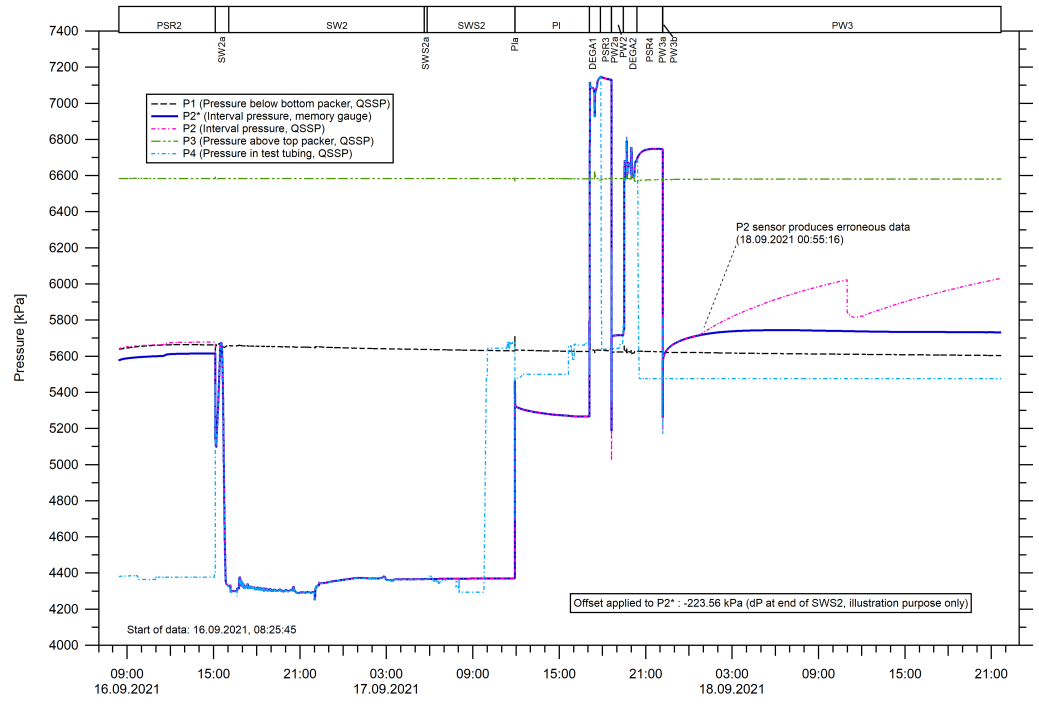

Fig. 3-13: Hydraulic packer test RHE1-1-OPA2b: Overview plot of pressure vs. time and date

Note the erratic behaviour of the QSSP sensor P2 during PW3 indicating a malfunction. The DataCan memory pressure gauge P2* shows reliable measurements used for data analysis.

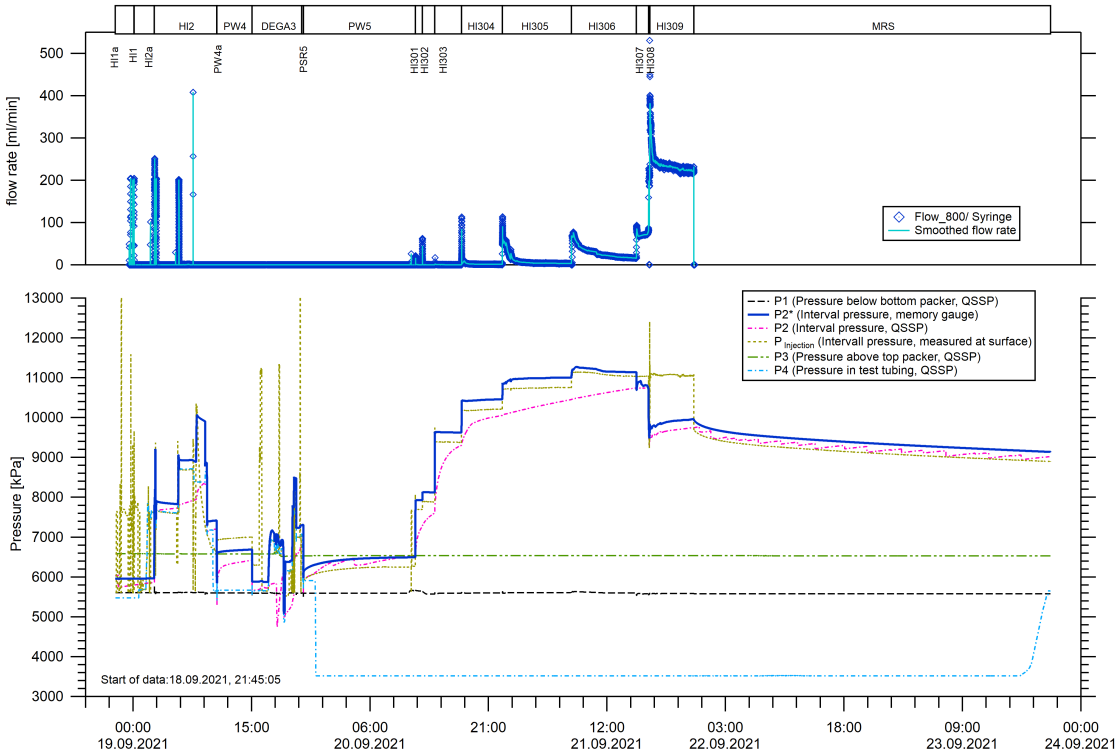

Fig. 3-14: Hydraulic packer test RHE1-1-OPA2c: Overview plot of pressure and flow rate vs. time and date

Note the erratic behaviour of the QSSP sensor P2 indicating a malfunction. The DataCan memory pressure gauge P2* provides reliable measurements (in agreement with measurements in the injection line by a pressure gauge at the surface $P_{Injection}$) used for data analysis.

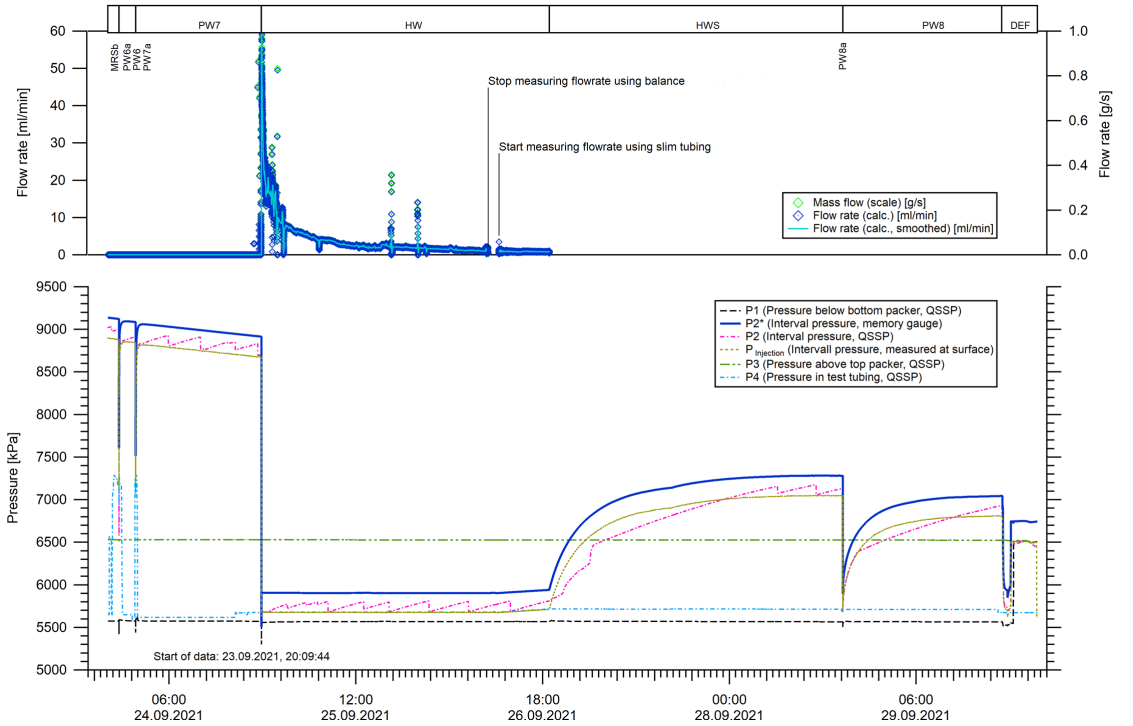

Fig. 3-15: Hydraulic packer test RHE1-1-OPA2d: Overview plot of pressure and flow rate vs. time and date

Note the erratic behaviour of the QSSP P2 gauge indicating a malfunction. The DataCan memory pressure gauge P2* provides reliable measurements (in agreement with measurements in the injection line by a pressure gauge at the surface $P_{Injection}$) used for data analysis.

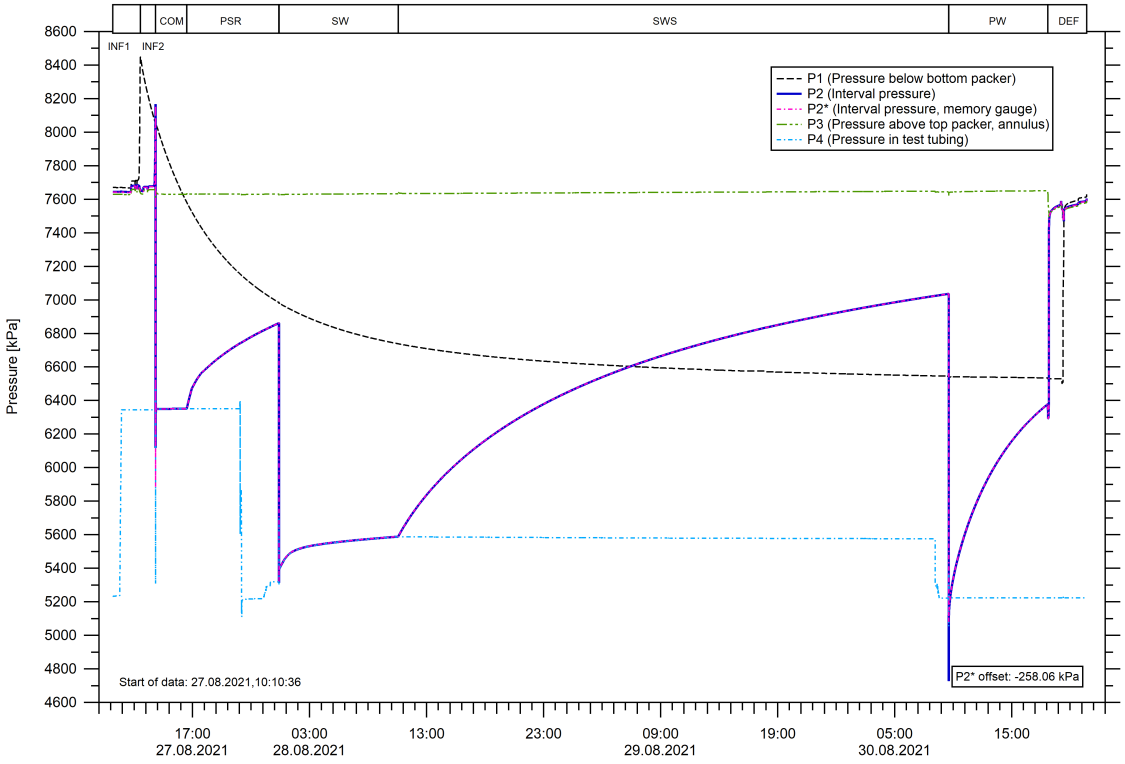

Fig. 3-16: Hydraulic packer test RHE1-1-LIA1: Overview plot of pressure vs. time and date

3.5 Details of selected tests

Two of the hydraulic packer tests are presented below in more detail: RHE1-1-LIA1 and RHE1-1-OPA2a. Both hydraulic tests were performed in a double packer configuration in a sequence of a slug withdrawal, slug recovery and pulse withdrawal phase. The chosen test procedure mainly corresponds to the preferred test strategy for formations with very low to low transmissivity (*cf.* Tab. 3-1 in Section 3.1). Based on the findings from previous hydraulic tests of the TBO campaign, an initial diagnostic phase was abandoned in favour of an extension of the duration of the main test phase.

The following two test examples demonstrate the application of the main approach used to provide estimates of the formation parameters including the associated ranges of uncertainty. The results of the two test analyses are provided in Section 3.6 along with the results of all tests performed.

3.5.1 Hydraulic packer test RHE1-1-LIA1

The hydraulic packer test RHE1-1-LIA1 represents an example of testing in a formation with low hydraulic transmissivity. It was the first hydraulic test interval after the borehole had been cored to a depth of 828 m MD. The test has a medium duration of the borehole pressure history with 380.40 hours (*cf.* Tab. 3-23) and a test duration of 77.3 hours (83.2 hours of measurement) focused on determining the hydraulic properties of the formation, especially the hydraulic conductivity. The hydraulic test RHE1-1-LIA1 was performed without any prior fluid exchange, i.e. using the drilling fluid of potassium silicate and polymers (*cf.* Dossier I) as test interval fluid. The entire analysis is based on the measurements of the QSSP sensor P2 at 702.08 m MD (645.31 m TVD).

3.5.1.1 Interval characterisation

The hydraulic test interval RHE1-1-LIA1 was separated from the entire borehole using a double packer configuration. The hydraulic test RHE1-1-LIA1 was performed between 27 and 30 August 2021. The entire interval (707.00 – 720.35 m MD) was located in a cored borehole section of the Staffelegg Formation of the Lias Group (668.07 – 721.46 m MD) including the Frick (692.89 – 709.21 m MD), Beggingen (709.21 – 714.15 m MD) and Schambelen Members (714.15 – 721.46 m MD). No fluid losses were observed during drilling.

The HDDP was described in Section 3.2. The hydraulic test was conducted with the drilling fluid (potassium silicate and polymers) as test interval fluid. The primary test objectives were to obtain reliable estimates of the formation hydraulic conductivity and the flow model. The estimation of the freshwater hydraulic head was defined as an objective of second priority due to the duration of the pressure history, the relatively short testing duration, and uncertain influence of possible mechanical coupled processes. Details of the tested interval and test duration are provided in Tab. 3-25. The borehole pressure history is presented at the beginning of Section 3.5.1.3 in detail.

Tab. 3-25: Hydraulic test RHE1-1-LIA1: Information on the test interval

[1] Time between last packer inflation and first packer deflation.

Test	**Depth**		**Length**	**Packer configuration**	**Hydraulic testing**		
	from [m MD] [m TVD]	to [m MD] [m TVD]	[m]		Start date	End date	Duration [1] [h]
RHE1-1-LIA1	707.00 649.29	720.35 660.06	13.35	Double	27.08.2021	30.08.2021	77.28

3.5.1.2 Test execution

Fig. 3-17 shows the system installation record as provided by the field test contractor. The stator of the progressive cavity pump (PCP) was not installed in the test string. The hydraulic test in interval RHE1-1-LIA1 was performed after completion of the coring to a depth of 828 m MD, a petrophysical logging and several installations of the GTPT test equipment and abandoned hydraulic tests before (see description of the borehole pressure history at the beginning of Section 3.5.1.3).

The HDDP was installed in borehole RHE1-1 at the interval position RHE1-1-LIA1 on 27.08.2021. After the installation of the first two test tubing rods, the tubing was filled with traced tap water (1.5-NDSA of a concentration of approx. 10 ppm) and the system was pulled back approximately 9 m from rig floor. The shut-in tool (SIT) was opened to release the air. The SIT was then closed during the following run-in hole (RIH) of the HDDP. During installation of the test tubing, the test tubing was regularly filled up to the top with traced tap water and the QSSP pressure sensors were checked (after every 10th rod). Inflation of upper packer to approximately 64.5 bar after the inflation of the lower packer to approximately 67 bar at the position of test interval RHE1-1-LIA1 started 380.40 hours after drilling through interval centre. Due to the squeeze effect that occurred in the interval during inflation of the upper packer, the SIT was opened to initiate a compliance phase (COM) that lasted 2.7 hours. Next, the SIT was closed, and the initial pressure recovery phase (PSR) commenced, lasting around 7.9 hours. In preparation of the next test phase, the fluid level in the test tubing was lowered and the slim tubing with an inner diameter of 6 mm was installed. A slug withdrawal test (SW) was performed that lasted for 10.2 hours. The SW test was terminated with the closure of the SIT valve. The subsequent pressure recovery (SWS) was recorded for 47.0 hours. Finally, a pulse withdrawal test (PW) was performed over the course of 8.5 hours after the deinstallation of the 6 mm slim tubing that started about 1.1 hour before the pulse. After the subsequent deflation (DEF) of the packer the packer system was removed from the borehole.

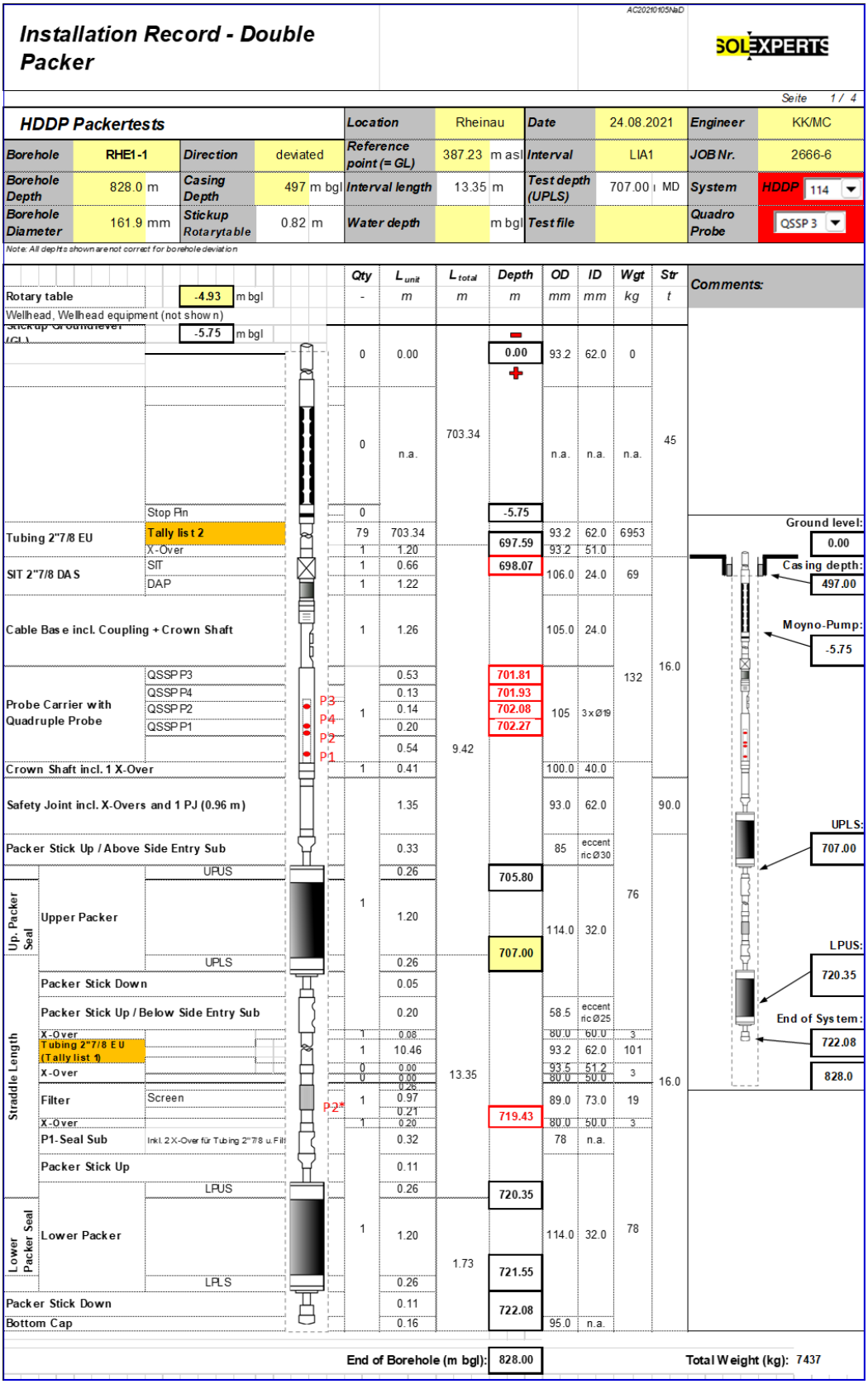

Fig. 3-17: Hydraulic test RHE1-1-LIA1: Downhole equipment installation record with system layout as used in the field test

3.5.1.3 Analysis

Borehole pressure history

The borehole pressure history was calculated for the depth of the P2 sensor that is used for the analysis of the hydraulic test RHE1-1-LIA1. It is shown in Fig. B-1 (see Appendix B) and summarised in Tab. 3-26. Calculation of the mean interval fluid density (prior to packer inflation) using the P2 (QSSP sensor) pressure measurements gave a density value of 1'200.43 kg m^{-3}. This value corresponds well with the documented density for the drilling mud in the daily report by the mud engineers (1'200 kg m^{-3}). Measurements of the mud level were taken several times during the work at RHE1-1 and used for the construction of the borehole pressure history. For periods without a mud level measurement, the mud level was assumed to be at the level of the drain pipe at -3.95 m MD, because during these periods, the drillers generally kept the borehole filled with mud up to the level of the drain pipe.

Tab. 3-26: Hydraulic test RHE1-1-LIA1: Borehole pressure history

[1] Interval pressure at the level of the P2 sensor (645.31 m TVD) with a pressure offset of 7.76 kPa as calculated from the history information, i.e. fluid level and density.

[2] Drilling through the interval centre (654.68 m TVD).

[3] P1 sensor measurement during testing corrected to the P2 sensor level (645.31 m TVD).

[4] Start of the inflation of the last/upper packer (PA2). The DAS had been started earlier (27.08.2021 10:10).

Description	**Start date and time**	**Duration** [h] **Total: 380.40**	**Pressure** [1] [kPa]
Drilling [2]	11.08.2021 16:23	164.12	7'655
POOH of the core string	18.08.2021 12:30	9.00	7'655
BOP	18.08.2021 21:30	1.50	7'655
Petrophysical logging	18.08.2021 23:00	88.75	7'655
RIH HDDP	22.08.2021 15:45	15.08	7'655
RHE1-1-OPA1-A [3]	23.08.2021 06:50	13.87	7'655
RHE1-1-OPA1-B [3]	23.08.2021 20:42	2.27	7'656
POOH HDDP	23.08.2021 22:58	28.03	7'626
RIH HDDP	25.08.2021 03:00	8.52	7'666
RHE1-1-LIA1-A	25.08.2021 11:31	6.48	7'666
POOH HDDP	25.08.2021 18:00	25.33	7'628
RIH HDDP	26.08.2021 19:20	17.45	7'644
RHE1-1-LIA1	27.08.2021 12:47 [4]		7'645

After drilling and petrophysical logging, a few attempts were made to install the GTPT test equipment (Section 3.2.5) to perform the hydraulic packer test RHE1-1-OPA1. This first trial of the hydraulic test was named to RHE1-1-OPA1-A. The second trial, referred to as RHE1-1-OPA1-B, was abandoned because the lower packer did not inflate. The system was then removed

from the borehole. After a rearrangement of the HDDP, the test equipment (Section 3.2.1) was installed in the interval position of RHE1-1-LIA1. However, due to damages on the pressure lines of the upper packer during the installation procedure, the packer did not inflate, and the system was deinstalled. This trial is referred to as RHE1-1-LIA1-A.

Throughout this period of trials since the end of the petrophysical logging, the pressure was measured whenever it was possible and extrapolated to the depth of the P2 transducer at RHE1-1-LIA1. During the hydraulic tests RHE1-1-OPA1-A and RHE1-1-OPA1-B the pressure was measured by the P1 QSSP sensor and during RHE-1-1-LIA1-A by the P2 QSSP sensor and included in the evaluation of the borehole pressure history. Once the HDDP was at test depth, the P2 QSSP sensor measured the pressure directly (Fig. B-1).

Flow model evaluation

The log-log representations of the PSR phase and the SWS phase show a sustained period dominated by wellbore storage (Fig. B-2). After this period the log-log plot of the PSR phase shows an unusually sharp "kink" in the pressure curve, that is reflected in the sudden flattening of the pressure derivative (Fig. B-2, top left). No conclusions can be drawn from this behaviour for the hydraulic flow model as it could also be caused by system compliance effects. Pressure and derivative curves of the SWS phase start to separate slightly approximately one log cycle before the phase was terminated (Fig. B-2, bottom left), indicating the faint beginning of a transition phase possibly to an infinite acting radial flow (IARF) phase. The deconvolved SW pressure measurement (Fig. B-2, top right) also shows an early, two log cycle lasting horizontal trend of the derivative and an increase towards late-middle and late time. Unfortunately, a possible flattening indicating a later IARF phase was not achieved during the SW phase. The deconvolved pressure measurement of the PW phase (Fig. B-2, bottom right), however, shows an initial phase with half unit slope of pressure and derivative, indicating an early-time period dominated by fracture flow. However, given that previous phases of the borehole history are not considered, this interpretation is not robust. Finally, it must be concluded that no clear formation behaviour indicating IARF conditions became visible in any test phase. The existence of a slightly disturbed near borehole zone (skin zone) cannot be excluded either. Therefore, a radial composite model with infinite lateral extent as outer boundary condition is preferred as conceptual flow model in the analysis where the inner zone could be used to represent a possible skin zone.

Analysis of the slug and slug recovery withdrawal (SW-SWS) sequence

Temperature changes occurring during the test within the closed test interval were considered in the analysis. Fig. B-3 shows the development of the interval temperature measured by the memory gauge (T2*) and pressure as measured by the QSSP. The test sequence of SW-SWS was selected for the optimisation of the hydraulic parameters. The slug phase was performed using a 6 mm diameter slim tubing with a small packer at the bottom end which was lowered into the 2⅞" tubing. Once in position, the packer of the slim tubing was expanded to provide a seal against the 2⅞" tubing. For the simulation, a corrected slim tubing radius was used considering the physical slim tubing and the contribution of the system compliance (i.e. the compressibility of the test zone of 5.62×10^{-10} Pa^{-1} and the compressibility of the water column between the SIT and the slim tubing packer) according to Black et al. (1987).

The results, derived from the parameter optimisation based on the measured pressure of the SW-SWS sequence, are shown in Tab. 3-27. The cartesian match for the entire sequence's pressure measurements is displayed in Fig. B-4. The fit quality was judged as poor for the SW phase (the simulated pressure data deviate significantly from the measurements) and very good for the SWS phase (the simulated pressure data closely trace the measurements).

Tab. 3-27: Hydraulic test RHE1-1-LIA1: Formation parameter estimation based on the parameter optimisation of the SW-SWS sequence using a radial composite flow model considering both the borehole pressure history and temperature changes inside the test interval

[1] Static formation pressure at the depth of the P2 sensor (645.31 m TVD).

SW-SWS results (radial composite flow model)	**K** [m s^{-1}]	**Ss** [m^{-1}]	**P_f** [1] [kPa]
Best estimate	6.60×10^{-13}	1.27×10^{-6}	7'744.2

The pressure residuals (Fig. B-4 bottom graph) of the simulation remain small during the SWS phase. The residuals were analysed further to check the suitability of the used flow model. In Fig. B-5, a normal distribution of the pressure residuals indicates clearly that the chosen conceptual flow model is applicable. Over the entire analysed test sequence, a very good sensitivity on the formation hydraulic conductivity exists as well as a sensitivity on the static formation pressure, even if this sensitivity is significantly lower (see Fig. B-6).

Joint parameter regions of the SW-SWS sequence

Based on the results of the parameter optimisation using a radial composite flow model, it is possible to estimate the joint parameter regions. Tab. 3-28 provides the 95% uncertainty ranges for the results of the parameter optimisation. The calculated ranges seem to be unrealistically small due to the well-defined and well-constrained minimum of the objective function / sum of squared error (SSE) values. Therefore, further investigations were performed to estimate the uncertainty ranges of the formation parameters.

Tab. 3-28: Hydraulic test RHE1-1-LIA1: 95% uncertainty range associated with the results of the parameter optimisation using a radial composite flow model for the SW-SWS sequence

[1] Static formation pressure at the depth of the P2 sensor (645.31 m TVD).

SW-SWS results (joint parameter region)	**K** [m s^{-1}]	**Ss** [m^{-1}]	**P_f** [1] [kPa]
95% uncertainty range	$6.58 – 6.62 \times 10^{-13}$	$1.26 – 1.28 \times 10^{-6}$	7'742 – 7'746

Estimates of the formation parameter values and uncertainty ranges

A parameter analysis to assess the uncertainty of the results for the formation parameter estimation was considered necessary. However, further analyses to assess the effect of the slight changes of the borehole pressure history on the uncertainty of the results were not considered due to prior analysis results from other TBO boreholes. The influence of the borehole pressure history is always included in the analysis as described above using pressure records from measurements taken during coring and hydraulic testing (see Tab. 3-26). Previous analysis results (from the MAR1-1 and BOZ2-1 boreholes) showed no significant influence of small changes in drilling fluid density. The analysis of the uncertainty in the results is thus reduced to a consideration of the uncertainty associated with the choice of the flow model, parameter optimisation procedure

and any inaccuracies in the determination of the wellbore storage. The former can be estimated using an alternative flow model. A perturbation analysis can estimate the influence of the current procedure. In this analysis, the bandwidth of the parameters is determined based on several individual optimisations, which can, for instance, identify whether the result corresponds to a global or local minimum in the parameter space. The possible influence of uncertainties in the determination of the wellbore storage is assessed by means of a sampling analysis, in which the parameters are optimised in multiple runs depending on a representative bandwidth for the wellbore storage.

Considering the small amount of information that can be used to identify the flow model (see above), the only alternative to the chosen flow model is to use a radial homogeneous flow model with a reduction in model parameters and associated uncertainties. The results, derived from the parameter optimisation based on the measured pressure of the SW-SWS sequence, are shown in Tab. 3-29. The cartesian match for the entire sequence's pressure measurement is displayed in Fig. B-7. The fit quality is generally poor and the difference between the simulated and measured pressure curves is significantly larger than when the simulated pressure is based on a radial composite flow model (Fig. B-4).

Tab. 3-29: Hydraulic test RHE1-1-LIA1: Formation parameter estimation based on the parameter optimisation of the SW-SWS sequence using a radial homogeneous flow model considering both the borehole pressure history and temperature changes inside the test interval

[1] Static formation pressure at the depth of the P2 sensor (645.31 m TVD).

[2] Parameter reached the upper optimisation limit.

SW-SWS results (radial homogeneous flow model)	**K** [m s^{-1}]	**S_S** [m^{-1}]	**P_f** [1] [kPa]
Best estimate	1.40×10^{-12}	3.80×10^{-6} [2]	7'306.7

A perturbation analysis with 500 runs was conducted to investigate if the objective function forms either a global minimum or multiple local minima in the parameter space of the radial composite flow model. Furthermore, a perturbation analysis allows to identify a possible non-uniqueness of the solution and/or to estimate the uncertainty of the optimised formation parameters. The parameter results of each single parameter optimisation of the perturbation runs are shown against increasing values of the objective function/SSE in Fig. B-8. The first 395 runs (run #0 to run #394) cover an SSE range between 4.286×10^7 and 4.461×10^7 (Fig. B-8). Within this range the matches of the SW-SWS sequence were accepted to be used for the estimation of the parameter uncertainty ranges. Tab. 3-30 shows the resulting best estimates of the formation parameters and the associated uncertainty ranges for the simulation with the lowest SSE. Fig. B-9 shows the simulation using the parameter set associated with the lowest SSE, the parameter set of the chosen upper SSE limit (run #394) and the initial parameter set (analysis of the slug and slug recovery withdrawal (SW-SWS) sequence). Focusing on the bottom graph of Fig. B-9 with the pressure residuals of all three simulations, it can be concluded that no strong differences exist between the resulting simulated pressure curves. However, a clear mismatch during the slug phase (SW) using the radial composite flow model is still obvious. Fig. B-10 indicates that there are clear correlations between all formation parameters. It is also visible in Fig. B-10 that from run #395 onwards, the maximum value of the formation specific storage (upper limit of the plausibility range of S_S) affects the correlations to an unknown extent, which disqualifies these runs for the estimation of the uncertainty range.

Tab. 3-30: Hydraulic test RHE1-1-LIA1: Uncertainty ranges and best estimates for the formation parameters estimated by the perturbation analysis considering both the borehole pressure history and temperature changes inside the test interval

[1] Static formation pressure at the depth of the P2 sensor (645.31 m TVD).

Perturbation analysis results (SW-SWS)	**K** [m s^{-1}]	**S_S** [m^{-1}]	**P_f** [1] [kPa]
Best estimate	6.60×10^{-13}	1.27×10^{-6}	7'744.2
Uncertainty range	$6.19 – 6.60 \times 10^{-13}$	$1.27 – 1.46 \times 10^{-6}$	7'743.8 – 7’776.7

The sampling analysis for the test zone compressibility was performed for a maximum suitable range of values between 4.0×10^{-10} Pa^{-1} and 9.0×10^{-10} Pa^{-1}. The resulting parameter sets in combination with the resulting objective function value/SSE value as a function of the value of the test zone compressibility are represented in Fig. B-11. Tab. 3-31 lists the resulting best estimates for the formation parameters and the associated uncertainty ranges. Considering Fig. B-11, a clear minimum of the resulting objective function value/SSE distribution cannot be identified. Correspondingly, the simulation with a test zone compressibility (c_{tz}) value of 4.25×10^{-10} Pa^{-1}, which is in line with the estimated interval fluid compressibility, was chosen as lower limit of the uncertainty range. The upper limit of the uncertainty range was derived from the upper limit of the field measurements (dip meter measurement starting PW), stated with a value of 6.74×10^{-10} Pa^{-1}.

Tab. 3-31: Hydraulic test RHE1-1-LIA1: Uncertainty ranges and best estimates for the formation parameters as a result of the sampling analysis for the test zone compressibility considering both the borehole pressure history and temperature changes inside the test interval

[1] Static formation pressure at the depth of the P2 sensor (645.31 m TVD).

Sampling analysis results (SW-SWS)	**K** [m s^{-1}]	**S_S** [m^{-1}]	**P_f** [1] [kPa]
Best estimate	5.99×10^{-13}	1.18×10^{-6}	7'756
Uncertainty range	$5.99 – 7.08 \times 10^{-13}$	$1.18 – 1.37 \times 10^{-6}$	7'737 – 7'756

In a last step, a parameter optimisation based on the pressure measurement of the SWS-PW sequence was performed. Fig. B-12 shows the resulting simulation. The pressure residuals of the SWS phase are slightly larger than for the initial simulation while the pressure residuals of the PW sequence are generally high. The measured pressure is significantly overestimated at early times and underestimated at late times by the simulation. However, the result demonstrates that the conceptual model of a radial composite model can also be successfully applied to the entire test sequence. Tab. 3-32 presents the results for the formation parameters.

Tab. 3-32: Hydraulic test RHE1-1-LIA1: Formation parameter estimation based on the parameter optimisation of the SWS-PW sequence using a radial composite flow model considering both the borehole pressure history and temperature changes inside the test interval

[1] Static formation pressure at the depth of the P2 sensor (645.31 m TVD).

SWS-PW results (radial composite flow model)	**K** [m s^{-1}]	**S_S** [m^{-1}]	**P_f** [1] [kPa]
Best estimate	3.52×10^{-13}	2.62×10^{-6}	7'713.7

Summary of the analysis

Tab. 3-33 presents the results of the analysis of the formation parameters of interval RHE1-1-LIA1. The best estimates for the formation parameters were derived from the sampling analysis of the test zone compressibility using the parameter set that respects the interval fluid compressibility as lower limit of the test zone compressibility (4.25×10^{-10} Pa^{-1}) and also represents the simulation with the lowest SSE value (*cf.* Fig. B-10). The uncertainty ranges of the formation parameters were taken from the perturbation and sampling analysis taking into account the result of the parameter optimisation on the SWS-PW sequence.

Tab. 3-33: Hydraulic test RHE1-1-LIA1: Best estimates for the formation parameters and associated uncertainty ranges

[1] Static formation pressure at the centre of the test interval (654.68 m TVD) considering the sensor offset of 7.76 kPa and an interval fluid density of 1'218.48 kg m^{-3} [7].

RHE1-1-LIA1	**K** [m s^{-1}]	**S_S** [m^{-1}]	**P_S** [1] [kPa]
Best estimate	5.99×10^{-13}	1.18×10^{-6}	7'860
Uncertainty range	$3.52 – 7.08 \times 10^{-13}$	$1.18 – 2.62 \times 10^{-6}$	7'817 – 7'881

3.5.2 Hydraulic packer test RHE1-1-OPA2a

The hydraulic packer test RHE1-1-OPA2a represents an example of testing in a formation with very low hydraulic transmissivity. The test was the first part of hydraulic testing in the test interval RHE1-1-OPA2. As it was the last hydraulic test interval investigated after the borehole had been cored to a depth of 828 m MD, the test has a long duration of the borehole pressure history of 924.52 hours (*cf.* Tab. 3-23). The first part (RHE1-1-OPA2a) has a duration of 62.71 hours and focused on determining the hydraulic properties of the formation under unchanged interval conditions compared to the time of drilling. This means especially, it was performed using the

[7] The interval fluid density was calculated as a mean value using the corresponding measurements of the P2 QSSP sensor and P2* memory gauge sensor at various points of time between the end of the PSR phase and the end of the PW phase.

drilling fluid of potassium silicate and polymers (*cf.* Dossier I) as test interval fluid. The total duration of hydraulic testing in the interval RHE1-1-OPA2, including test parts a to d, adds up to 386 hours. The RHE1-1-OPA2a test analysis is based on the measurements of the P2* sensor of the memory gauge positioned inside the test interval at 620.33 m MD (578.42 m TVD).

3.5.2.1 Interval characterisation

The test interval RHE1-1-OPA2 was separated from the remaining borehole using a double packer configuration. The hydraulic test RHE1-1-OPA2a was performed between 13th and 16th September 2021. The entire interval (612.18 – 621.50 m MD) was located in a cored borehole section of the Opalinus Clay of the Dogger Group (524.61 – 668.07 m MD).

The HDDP was described in Section 3.2. The hydraulic test was conducted with the drilling fluid (potassium silicate and polymers) as test interval fluid. The primary test objectives were to obtain reliable estimates of the hydraulic transmissivity (conductivity), and to determine the most appropriate flow model. The estimation of the freshwater hydraulic head was defined as an objective of second priority due to the long borehole pressure history and short hydraulic test duration, and uncertain influence of possible mechanical coupled processes. Details of the tested interval and test duration are provided in Tab. 3-34. The borehole pressure history is presented at the beginning of Section 3.5.2.3.

Tab. 3-34: Hydraulic test RHE1-1-OPA2a: Information on the test interval

[1] Time between last packer inflation and the end of the first test phase (begin of the interval fluid displacement).

Test	**Depth**		**Length**	**Packer configuration**	**Hydraulic testing**		
	from [m MD] [m TVD]	to [m MD] [m TVD]	[m]		Start date	End date	Duration [1] [h]
RHE1-1-OPA2	612.18 571.68	621.50 579.39	9.32	Double	13.09.2021	16.09.2021	62.71

3.5.2.2 Test execution

Fig. 3-18 shows the system installation record as provided by the field test contractor. The stator of the progressive cavity pump (PCP) was not installed in the test string, but an appendix was added at the lower end of the HDDP allowing to capture fluid during the interval fluid displacement procedure in preparation test sequences following test RHE1-1-OPA2a. The hydraulic test in interval RHE1-1-OPA2 was performed after completion of the coring to a depth of 828 m MD, petrophysical logging and hydraulic testing in other intervals. No fluid losses were observed during drilling.

The HDDP was installed in borehole RHE1-1 at the interval position RHE1-1-OPA2 on 13.09.2021. After the installation of the first two test tubing rods, the tubing was filled with traced synthetic porewater (1.5-NDSA of a concentration of approx. 10 ppm) and the system was pulled back approximately 9 m from rig floor. The upper shut-in tool (SIT2) was opened to release the air. The SIT2 was then closed during the following run-in hole (RIH) of the HDDP. During installation of the test tubing, the test tubing was regularly filled up to the top with traced synthetic porewater and the QSSP pressure sensors were checked. The inflation of the upper packer to

approximately 68.5 bar after the inflation of the lower packer to approximately 71 bar at the position of test interval RHE1-1-OPA2 started 924.52 hours after drilling through the interval centre. Due to the squeeze effect that occurred in the interval during the inflation of the upper packer, the SIT2 was opened to initiate a compliance phase (COM) that lasted 1.7 hours. Next, the SIT2 was closed and the initial pressure recovery phase (PSR) commenced, lasting around 7.3 hours. In preparation of the next test phase, the fluid level in the test tubing was lowered and the slim tubing with an inner diameter of 6 mm was installed. A slug withdrawal test (SW) was performed that lasted for 8.2 hours. The SW test was terminated with the closure of the SIT2 valve. The subsequent pressure recovery (SWS) was recorded for 32.7 hours. Finally, a pulse withdrawal test (PW) was performed over the course of 9.9 hours after the deinstallation of the 6 mm slim tubing and the installation of a slim tubing with an inner diameter of 12 mm. After this phase, the first hydraulic test part was terminated by starting the interval fluid displacement before the second part (RHE1-1-OPA2b) was started.

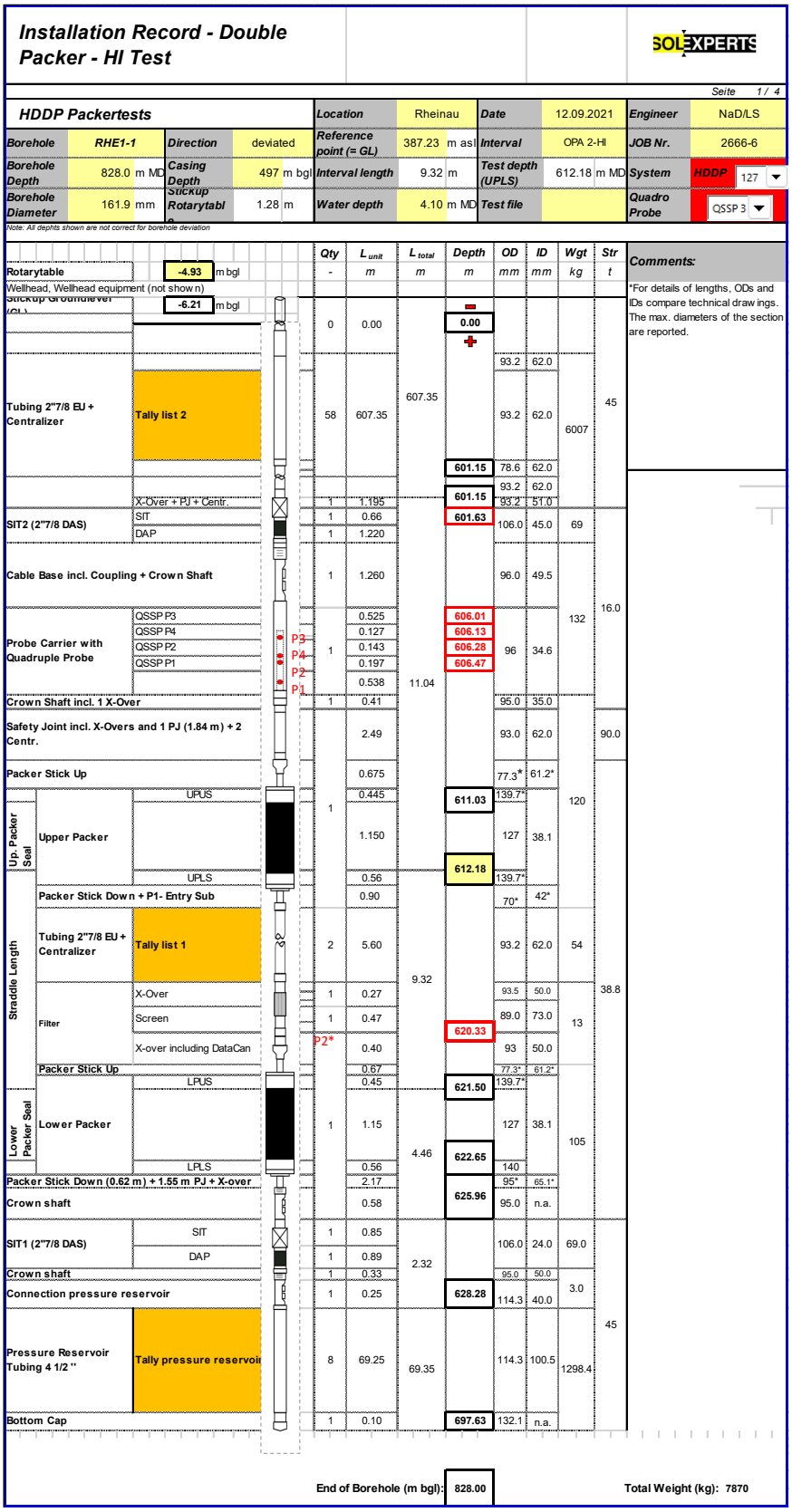

Fig. 3-18: Hydraulic test RHE1-1-OPA2a: Downhole equipment installation record with system layout as used in the field test

3.5.2.3 Analysis

Borehole pressure history

The borehole pressure history was determined for the depth of the P2* sensor which was used for the analysis of the RHE1-1-OPA2a test. It is shown in Fig. B-13 and summarised in Tab. 3-35. Calculation of the mean interval fluid density (prior to packer inflation) based on the P2 (QSSP sensor) and P2* (memory gauge) pressure measurements gave a density value of 1'205.2 kg m^{-3}. This value corresponds well with the documented density for the drilling mud in the daily report by the mud engineers (1'200 kg m^{-3}). Measurements of the mud level were taken several times during the work at RHE1-1 and used for the construction of the borehole pressure history. For periods without a mud level measurement, the mud level was assumed to be at the level of the drain pipe at -3.95 m MD, because during these periods, the drillers generally kept the borehole filled with mud up to the level of the drain pipe.

The borehole history period between the end of drilling and the beginning of the test RHE1-1-LIA1 is described in Section 3.5.1.3. For the duration of the test RHE1-1-LIA1 in the test interval below the RHE1-1-OPA2 test interval, the pressure measured by the P3 QSSP sensor was extrapolated to the depth of the P2* transducer at RHE1-1-OPA2. Then followed by the test RHE1-1-OPA1 in the test interval above the RHE1-1-OPA2 test interval, for which the pressure measured by the P1 QSSP sensor was extrapolated to the depth of the P2* transducer at RHE1-1-OPA2. Once the HDDP was at test depth, the P2* memory gauge sensor measured pressure directly (Fig. B-13).

Tab. 3-35: Hydraulic test RHE1-1-OPA2a: Borehole pressure history

[1] Interval pressure at the level of the P2* sensor (578.42 m TVD) with a pressure offset of 105.07 kPa as calculated from the history information, i.e. fluid level and density.

[2] Drilling through the interval centre (616.84 m MD).

[3] P1 sensor measurement during testing corrected to the P2* sensor level (578.42 m TVD).

[4] P3 sensor measurement during testing corrected to the P2* sensor level (578.42 m TVD).

[5] Start of the inflation of the last/upper packer (PA2). The DAS had been started earlier (13.09.2021 16:00).

[6] Measured with the P2* sensor (578.42 m TVD) at the water level measurement of -3.93 m MD prior to packer inflation.

Description	**Start date and time**	**Duration** [h] **Total: 924.52**	**Pressure** [1] [kPa]
Drilling [2]	06.08.2021 05:12	295.30	6'967
POOH of the core string	18.08.2021 12:30	9.00	6'967
BOP	18.08.2021 21:30	1.50	6'967
Petrophysical logging	18.08.2021 23:00	88.75	6'967
RIH HDDP	22.08.2021 15:45	15.08	6'907
RHE1-1-OPA1-A [3]	23.08.2021 06:50	13.87	6'967
RHE1-1-OPA1-B [3]	23.08.2021 20:42	2.27	6'968
POOH HDDP	23.08.2021 22:58	28.03	6'968
RIH HDDP	25.08.2021 03:00	8.52	6'936
RHE1-1-LIA1-A [4]	25.08.2021 11:31	6.48	6'977
POOH HDDP	25.08.2021 18:00	25.33	6'940
RIH HDDP	26.08.2021 19:20	14.83	6'958
RHE1-1-LIA1 [4]	27.08.2021 10:10	79.90	6'957
POOH HDDP	30.08.2021 18:04	12.93	6'920
Check-trip	31.08.2021 07:00	19.80	6'958
RIH HDDP	01.09.2021 02:48	28.30	6'856
RHE1-1-OPA1 [3]	02.09.2021 07:06	209.73	6'856
POOH HDDP	11.09.2021 00:50	17.17	6'828
BOP	11.09.2021 18:00	4.50	6'857
Check-trip	11.09.2021 22:30	29.88	6'857
RIH HDDP	13.09.2021 04:23	13.33	6'817
RHE1-1-OPA2	13.09.2021 17:43 [5]	-	6'829 [6]

Flow model evaluation

The hydraulic test sequence was analysed using a 2-zone radial composite flow model. This flow model approach was based on the analysis of the shut-in phase (PSR) using a log-log presentation of the pressure difference over time and the slug recovery phase (SWS) using Agarwal superposition time as well as the de-convolved pressure of the slug phase (SW) and pulse phase (PW).

Figs. B-14 and B-15 show the diagnostic plots for the PSR and SWS, SW and PW phases, respectively. The diagnostic plot for the PSR phase shows a long-lasting period dominated by wellbore storage and the log-log plot for the SWS phase shows a similar picture. Towards the end of the PSR, the pressure and derivative curve show a faint beginning of a transition phase to a possible infinite acting radial flow (IARF) phase. Using uncorrected SWS elapsed time (Fig. B-14 top right graph), the beginning of a potential transition towards a radial flow regime could be presumed. This feature disappears when using Agarwal superposition time (Fig. B-14 bottom right graph). Instead, a late time increase of pressure and derivative curve appears. This is most probably related to uncertainties in the production time because the production history was limited to the slug flow phase (SW), as the previous test phases and the borehole pressure history were not considered. The derivative in the de-convolution plot of the slug phase (Fig. B-15 left graph) and de-convolved pulse test pressure data (PW, Fig. B-15 right graph) show nearly parallel behaviour along an imperfect half-unit slope. The half-unit slope feature can indicate an infinite conductivity fracture. However, given that previous phases of the borehole history are not considered, this interpretation is not robust. Hence, a clear formation response confirming IARF conditions cannot be seen in either of these figures. A 2-zone radial composite flow model (with the inner zone representing a thin skin zone around the borehole) with infinite lateral extent as outer boundary condition is favoured as a conceptual model in the analysis.

Analysis of the slug, slug recovery and pulse withdrawal (SW-SWS-PW) sequence

Temperature changes during the test within the closed test interval were considered in the analysis. Fig. B-16 shows the development of the interval temperature measured by the memory gauge (T2*) and pressure, as measured by the memory gauge and the QSSP, respectively. The entire test sequence of SW-SWS-PW was selected for the optimisation of the hydraulic parameters. The slug phase was performed using a 6 mm diameter slim tubing with a small packer at the bottom end which was lowered into the 2⅞" tubing. Once in position, the packer of the slim tubing was expanded to provide a seal against the 2⅞" tubing. For the simulation, a corrected slim tubing radius was used considering the physical slim tubing and the contribution of the system compliance (i.e. the compressibility of the test zone of 5.68×10^{-10} Pa^{-1} and the compressibility of the water column between the SIT2 and the slim tubing packer) according to Black et al. (1987).

The results, derived from the parameter optimisation based on the measured pressure of the SW-SWS-PW sequence, are shown in Tab. 3-36. The cartesian match for the entire sequence pressure measurement is displayed in Fig. B-17. The fit quality was judged as moderate for the SW phase (the pressure data are slightly overestimated at late time), very good for the SWS phase and equally good for the PW phase (the pressure data are slightly underestimated at late time).

Tab. 3-36: Hydraulic test RHE1-1-OPA2a: Formation parameter estimation based on the parameter optimisation of the SW-SWS-PW sequence using a radial composite flow model considering both the borehole pressure history and temperature changes inside the test interval.

[1] Static formation pressure at the depth of the P2* sensor (578.42 m TVD).

SW-SWS-PW results (radial composite flow model)	**K** [m s^{-1}]	**Ss** [m^{-1}]	**P_f** [1] [kPa]
Best estimate	3.67×10^{-14}	2.39×10^{-6}	7'451.6

The pressure residuals (Fig. B-17 bottom graph) of the simulation remain under 2 kPa. Further analysis of the residuals was carried out to check the suitability of the used flow model. Fig. B-18 shows that a normal distribution of the pressure residuals indicates clearly that the chosen conceptual flow model is applicable. Over the entire analysed test sequence, a very good sensitivity on the formation hydraulic conductivity exists as well as a sensitivity on the static formation pressure, even if this sensitivity is significantly lower (see Fig. B-19).

Joint parameter regions of the SW-SWS-PW sequence

Based on the results of the parameter optimisation using a radial composite flow model, it is possible to estimate the joint parameter regions. Tab. 3-37 provides the 95% uncertainty ranges for the results of the parameter optimisation. The calculated ranges seem to be unrealistically small due to the well-defined and well-constrained minima of the objective function/SSE values. Therefore, further investigations were performed to estimate the uncertainty ranges of the formation parameters.

Tab. 3-37: Hydraulic test RHE1-1-OPA2a: 95% uncertainty range associated with the results of the parameter optimisation using a radial composite flow model for the SW-SWS-PW sequence.

[1] Static formation pressure at the depth of the P2* sensor (578.42 m TVD).

SW-SWS-PW results (joint parameter region)	**K** [m s^{-1}]	**Ss** [m^{-1}]	**P_f** [1] [kPa]
95% uncertainty range	$3.66 – 3.67 \times 10^{-14}$	$2.38 – 2.39 \times 10^{-6}$	7'450 – 7'453

Estimates of the formation parameter values and uncertainty ranges

A parameter analysis to assess the uncertainty of the results was considered necessary. However, further analyses to assess the effect of a slight change of the borehole pressure history on the uncertainty of the results were not considered due to prior analysis results from other TBO boreholes. The influence of the borehole pressure history is always included in the analysis as described above using pressure records from measurements taken during coring and hydraulic testing (see Tab. 3-35). Previous analysis results (from the MAR1-1 and BOZ2-1 boreholes) showed no significant influence of small changes in drilling fluid density. The analysis of the uncertainty in the results is thus reduced to a consideration of the uncertainty associated with the parameter optimisation procedure and any inaccuracies in the determination of the wellbore

storage. The former can be estimated using a perturbation analysis. In this analysis, the bandwidth of the parameters is determined based on several individual optimisations, which can, for instance, identify whether the result corresponds to a global or local minimum in the parameter space. The possible influence of uncertainties in the determination of the wellbore storage is assessed by means of a sampling analysis, in which the parameters are optimised in multiple runs depending on a representative bandwidth for the wellbore storage.

A perturbation analysis with 250 runs was conducted to investigate if the objective function is forming either a global minimum or multiple local minima in the parameter space and to identify a possible non-uniqueness of the solution and/or to estimate, if possible, the uncertainty of the optimised formation parameter. The parameter results of each single parameter optimisation of the perturbation runs are shown against increasing values of the objective function/sum of squared errors (SSE) in Fig. B-20. The first 90 runs (run #0 to run #89) cover an SSE range between 135'102 and 1'646'390 (Fig. B-20). Within this range the matches of the SW-SWS-PW sequence were accepted to be used for the estimation of the parameter uncertainty ranges. Tab. 3-38 shows the resulting best estimates of the formation parameters and the associated uncertainty ranges for the simulation with the lowest SSE. The best estimate was chosen from run #6 by expert opinion because the parameter estimates derived from the run associated with the lowest SSE (run #0) shows a formation specific storage value above the defined plausibility range and seems to be significantly affected by an overestimation of the static formation pressures (difference of 885 kPa between run#0 and run #6). The plausibility range of the formation specific storage was derived from the mechanical parameters of the Opalinus Clay to be between $0.53 – 3.78 \times 10^{-6}$ m^{-1}. Additionally, Fig. B-21 shows the simulation using the parameter set associated with the lowest SSE, the best parameter estimated based on expert opination (run #6) and the initial parameter set (analysis of the slug, slug recovery and pulse withdrawal (SW-SWS-PW) sequence). Focusing on the bottom graph of Fig. B-21 that presents the pressure residuals of all three simulations, it can be concluded that the lower SSE value is based on a slightly better representation during slug-recovery phase (SWS), however, also a clear overestimation during the slug phase (SW) and an incorrect slope during the pulse phase (PW) is resulting. Because run #6 balances the residuals among all three phases and respects the plausibility range of the formation specific storage, this run was chosen to describe the best estimate. Fig. B-22 indicates that there are clear correlations between all formation parameters.

Tab. 3-38: Hydraulic test RHE1-1-OPA2a: Uncertainty ranges and best estimates for the formation parameters estimated by the perturbation analysis considering both the borehole pressure history and temperature changes inside the test interval

[1] Static formation pressure at the depth of the P2* sensor (578.42 m TVD).

[2] Reached the lower limit of the investigation range and upper value lies above the upper limit of the plausibility range.

Perturbation analysis results	**K** [m s^{-1}]	**Ss** [m^{-1}]	**P_f** [1] [kPa]
Best estimate	3.43×10^{-14}	2.59×10^{-6}	7'530
Uncertainty range	$1.68 – 12.7 \times 10^{-14}$	$0.50 – 5.91 \times 10^{-6}$ [2]	6'176 – 8'415

The sampling analysis for the test zone compressibility was performed for a maximum suitable range of values between 4.0×10^{-10} Pa^{-1} and 1.5×10^{-9} Pa^{-1}. The resulting parameter sets in combination with the resulting objective function value/SSE value as a function of the value of the test zone compressibility are represented in Fig. B-23. Tab. 3-39 lists the resulting best estimates

for the formation parameters and the associated uncertainty ranges for the simulation with the lowest SSE (test zone compressibility of 6.89×10^{-10} Pa^{-1}). The uncertainty range for the test zone compressibility was defined between 4.33×10^{-10} Pa^{-1} as the lower limit, which corresponds approximately to the fluid compressibility, and an upper limit of 1.2×10^{-9} Pa^{-1}. The upper limit was chosen by expert opinion due to the relatively short test interval (small interval volume of 0.192 m^3) of less than 10 m where the compressibility of the packers could contribute in a larger portion to the test-zone compressibility.

Tab. 3-39: Hydraulic test RHE1-1-OPA2a: Uncertainty ranges and best estimates for the formation parameters as a result of the sampling analysis for the test zone compressibility considering both the borehole pressure history and temperature changes inside the test interval

[1] Static formation pressure at the depth of the P2* sensor (578.42 m TVD).

Sampling analysis results	**K** [m s^{-1}]	**S_S** [m^{-1}]	**P_f** [1] [kPa]
Best estimate	3.55×10^{-14}	2.38×10^{-6}	7'464
Uncertainty range	$2.42 – 9.20 \times 10^{-14}$	$1.73 – 2.39 \times 10^{-6}$	6'944 – 7'521

Summary of the analysis

Tab. 3-40 presents the results of the analysis of the formation parameters of interval RHE1-1-OPA2a. The best estimates for the formation parameters were derived from the best estimate of the perturbation analysis due to a slightly better value of the objective function and the use of the measured test zone compressibility of 5.68×10^{-10} Pa^{-1}. The uncertainty ranges of the formation parameters from the sampling analysis were smaller than the uncertainty ranges derived from the perturbation analysis. Therefore, the uncertainty ranges for the formation parameters were defined by the results of the perturbation analysis, except for the range of the formation specific storage. This range was derived directly from the plausibility ranges associated with the mechanical parameters of the Opalinus Clay.

Nevertheless, the best estimate and the wide uncertainty range of the static formation pressure significantly exceed the expected formation pressure. The derived freshwater heads, based on the estimated formation pressures, are therefore judged as unrealistic and considered to represent "apparent" heads.

Tab. 3-40: Hydraulic test RHE1-1-OPA2a: Best estimates for the formation parameters and associated uncertainty ranges

[1] Static formation pressure at the centre of the test interval (575.54 m TVD) considering the sensor offset of 105.07 kPa and an interval fluid density of 1'205.2 kg m^{-3}.

[2] Defined through the plausibility limits derived from the mechanical parameters of the Opalinus Clay.

RHE1-1-OPA2a	**K** [m s^{-1}]	**S_S** [m^{-1}]	**P_S** [1] [kPa]
Best estimate	3.43×10^{-14}	2.59×10^{-6}	7'390
Uncertainty range	$1.68 – 12.7 \times 10^{-14}$	$0.53 – 3.78 \times 10^{-6}$ [2]	6'038 – 8'276

3.6 Summary of results and discussion of hydraulic tests

The Opalinus Clay was investigated in the RHE1-1 borehole using two hydraulic tests. Tests RHE1-1-OPA1 and RHE1-1-OPA2 were conducted sequentially in test intervals of 6.32 m and 9.32 m length, respectively. Both tests were performed as multi-part tests with different objectives (*cf.* Section 3.4).

RHE1-1-OPA1 was the first hydraulic test in the Opalinus Clay after drilling to a depth of 828 m MD and consisted of three parts. The first part (RHE1-1-OPA1a, Fig. 3-10) preceded the performance of a GTPT (RHE1-1-OPA1b), followed by a second hydraulic test sequence (RHE1-1-OPA1c, Fig. 3-11). The two hydraulic test parts, with drilling fluid and synthetic pore water as test interval fluid, respectively, were carried out to determine the hydraulic properties or the changes in these through the implementation of the GTPT.

The RHE1-1-OPA2 hydraulic test was performed in four parts: a, b, c and d. The first part RHE1-1-OPA2a (Fig. 3-12), where the drilling fluid was used as interval test fluid, followed the test strategy for low-permeability formations (*cf.* Section 3.1). Before the following parts, the interval fluid was replaced with synthetic porewater. The second test part RHE1-1-OPA2b (Fig. 3-13) was also carried out according to the test strategy (*cf.* Section 3.1) to determine the formation hydraulic properties and conditions after the fluid exchange for the subsequent test parts. The third part RHE1-1-OPA2c (Fig. 3-14) consists of a series of constant head / constant pressure (HI) test phases designed to characterise the behaviour of encountered structures due to changes in the effective stress field around the borehole. Finally, the fourth hydraulic test part RHE1-1-OPA2d (Fig. 3-15) was conducted with a constant head / constant pressure withdrawal phase and a subsequent pressure recovery phase followed by a pulse withdrawal phase to determine the hydraulic conductivity and flow model after the series of HI phases (RHE1-1-OPA2c).

The Staffelegg Formation of the Lias Group was examined with one hydraulic packer test. Test RHE1-1-LIA1 was performed with a double packer configuration and is discussed in detail in Section 3.5.1.

3.6.1 Investigation of the "pristine" / "undisturbed" formation

3.6.1.1 Summary tables and plots

The results of the transmissivity and hydraulic conductivity estimates for all tested intervals are summarised in Tab. 3-41, and the estimated freshwater hydraulic heads and static formation pressures are documented in Tab. 3-42. Both tables present the best estimates along with confidence ranges as determined by the field test contractor in the corresponding analysis reports. They present the results from hydraulically testing the "pristine" / "undisturbed" formation using the test strategy described in Section 3.1 with the drilling fluid (potassium silicate and polymers) as test interval fluid (tests RHE1-1-OPA1a, RHE1-1-OPA2a and RHE1-1-LIA1). The permeabilities for all tested intervals are summarised in Tab. 3-43 and were calculated based on the hydraulic conductivities provided in Tab. 3-41. An assumed density of 1'000 kg m^{-3} and a dynamic viscosity of 1×10^{-3} Pa s were used for the calculation of the hydraulic permeabilities.

The hydraulic parameters T, K, P_S and h_S (in terms of m TVD and m asl) are illustrated with respect to both the borehole depth (in m MD and TVD) and the geological profile in Figs. 3-19 to 3-23. The best estimates for these parameters are indicated by vertical lines in the cor-

responding interval position. The associated confidence ranges are shown as dashed rectangles, delimited vertically by the corresponding interval extent and laterally by the minimum and maximum values.

The hydraulic tests which aimed to characterise the behaviour of encountered structures after gas injection during the GTPT (test RHE1-1-OPA1c), and, due to changes in the effective stress field around the borehole (tests RHE1-1-OPA2b to OPA2d) are discussed in Section 3.6.2 along with a summary of the test results.

Tab. 3-41: Summary of the hydraulic packer testing in borehole RHE1-1: Transmissivity and hydraulic conductivity

[1] Interval length according to m MD.

[2] Based on the results presented by the field test contractor. Values are rounded.

[3] Based on results of RHE1-1-OPA1a and RHE1-1-OPA2a, respectively.

Test interval details and hydraulic model							**Transmissivity and hydraulic conductivity**					
Test name	**Interval depth**				**Interval length** [1]	**Hydraulic model**	**Best estimate** [2]		**Lowest estimate** [2]		**Highest estimate** [2]	
	From [m MD m TVD]	**To** [m MD m TVD]	**From** [m asl]	**To** [m asl]	[m]		**T** [m^2 s^{-1}]	**K** [m s^{-1}]	T_{min} [m^2 s^{-1}]	K_{min} [m s^{-1}]	T_{max} [m^2 s^{-1}]	K_{max} [m s^{-1}]
RHE1-1-OPA1 [3]	548.00 518.18	554.32 523.48	-130.95	-136.25	6.32	radial-composite	5×10^{-13}	7×10^{-14}	2×10^{-13}	3×10^{-14}	2×10^{-12}	2×10^{-13}
RHE1-1-OPA2 [3]	612.18 571.68	621.50 579.39	-184.45	-192.16	9.32	radial-composite	3×10^{-13}	3×10^{-14}	1×10^{-13}	1×10^{-14}	2×10^{-12}	2×10^{-13}
RHE1-1-LIA1	707.00 649.29	720.35 660.06	-262.06	-272.83	13.35	radial-composite	8×10^{-12}	6×10^{-13}	4×10^{-12}	3×10^{-13}	1×10^{-11}	8×10^{-13}

Tab. 3-42: Summary of the hydraulic packer testing in borehole RHE1-1: Hydraulic head estimates

[1] Interval length according to m MD.

[2] Based on the results presented by the field test contractor.

[3] Based on results of RHE1-1-OPA1a and RHE1-1-OPA2a, respectively.

Test interval details and associated hydraulic model							**Hydraulic head** [m TVD]			**Hydraulic head** [m asl]			**Formation pressure**		
Test name	**Interval depth**				**Interval length** [1]	**Hydraulic model**	**Best** [2] **h**	**Lowest** [2] **h_{min}**	**Highest** [2] **h_{max}**	**Best** [2] **h**	**Lowest** [2] **h_{min}**	**Highest** [2] **h_{max}**	**Best** [2] **P_S**	**Lowest** [2] **$P_{S\,min}$**	**Highest** [2] **$P_{S\,max}$**
	From [m MD m TVD]	**To** [m MD m TVD]	**From** [m asl]	**To** [m asl]	[m]		[m TVD]	[m TVD]	[m TVD]	[m asl]	[m asl]	[m asl]	[kPa]	[kPa]	[kPa]
RHE1-1-OPA1 [3]	548.00 518.18	554.32 523.48	-130.95	-136.25	6.32	radial-composite	-142	-76	-215	530	463	603	6'506	5'853	7'221
RHE1-1-OPA2 [3]	612.18 571.68	621.50 579.39	-184.45	-192.16	9.32	radial-composite	-178	-40	-268	565	427	655	7'390	6'038	8'275
RHE1-1-LIA1	707.00 649.29	720.35 660.06	-262.06	-272.83	13.35	radial-composite	-147	-142	-149	534	529	536	7'860	7'817	7'881

Tab. 3-43: Summary of the hydraulic packer testing in borehole RHE1-1: Permeability

[1] The calculation is based on the hydraulic conductivity provided by the field test contractor in the corresponding DR and standard conditions (density: 1'000 kg m^{-3}, dynamic viscosity: 1×10^{-3} Pa s). Values are rounded.

[2] Interval length according to m MD.

[3] Based on results of RHE1-1-OPA1a and RHE1-1-OPA2a, respectively.

Test interval details						**Permeability estimates** [1]		
Test name	**Interval depth**				**Interval length** [2]	**Best k**	**Lowest k_{min}**	**Highest k_{max}**
	From [m MD m TVD]	**To** [m MD m TVD]	**From** [m asl]	**To** [m asl]	[m]	[m^2]	[m^2]	[m^2]
RHE1-1-OPA1 [3]	548.00 518.18	554.32 523.48	-130.95	-136.25	6.32	8×10^{-21}	3×10^{-20}	8×10^{-20}
RHE1-1-OPA2 [3]	612.18 571.68	621.50 579.39	-184.45	-192.16	9.32	3×10^{-21}	3×10^{-21}	2×10^{-20}
RHE1-1-LIA1	707.00 649.29	720.35 660.06	-262.06	-272.83	13.35	6×10^{-20}	1×10^{-21}	2×10^{-20}

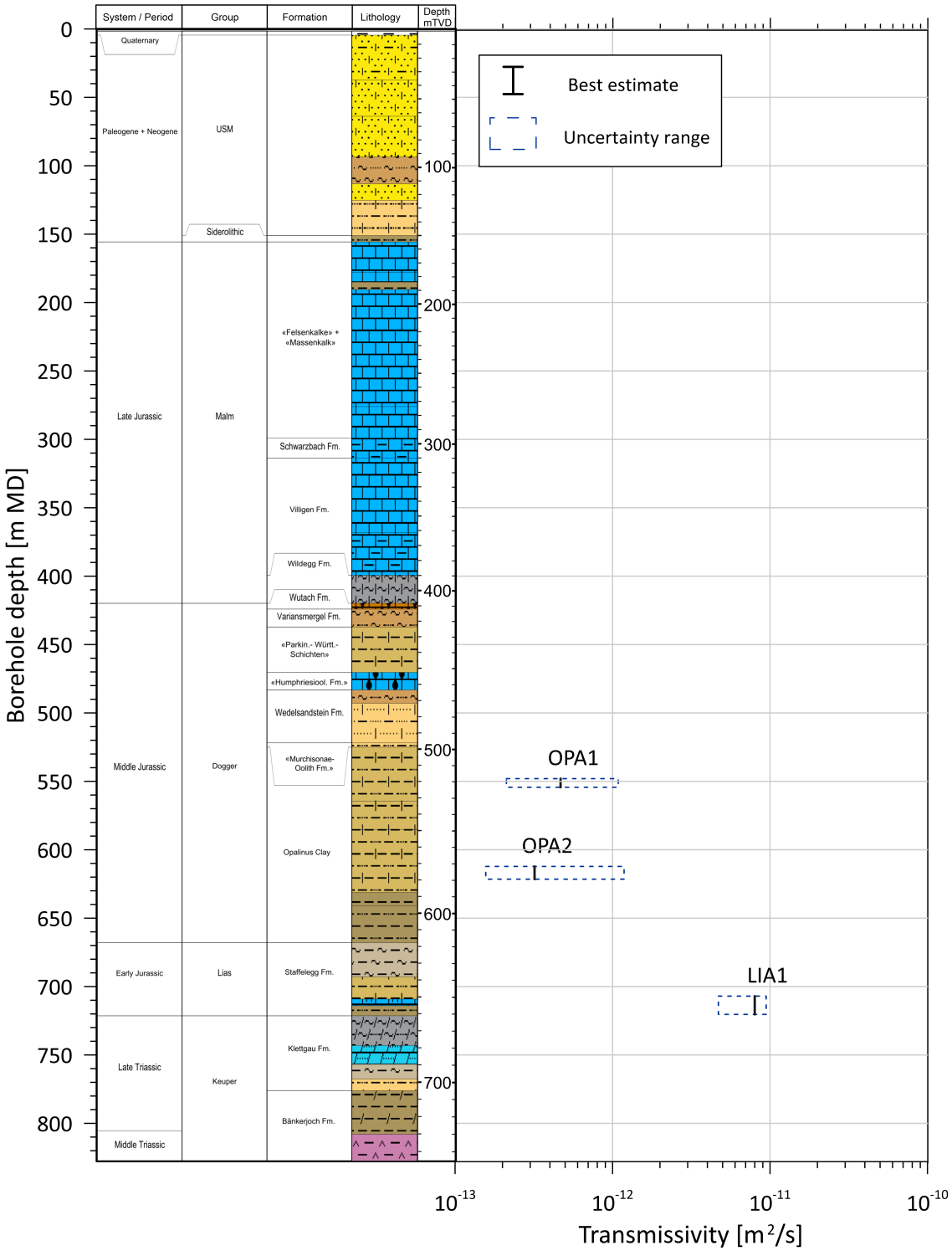

Fig. 3-19: Summary of the hydraulic testing in borehole RHE1-1: Formation transmissivity profile

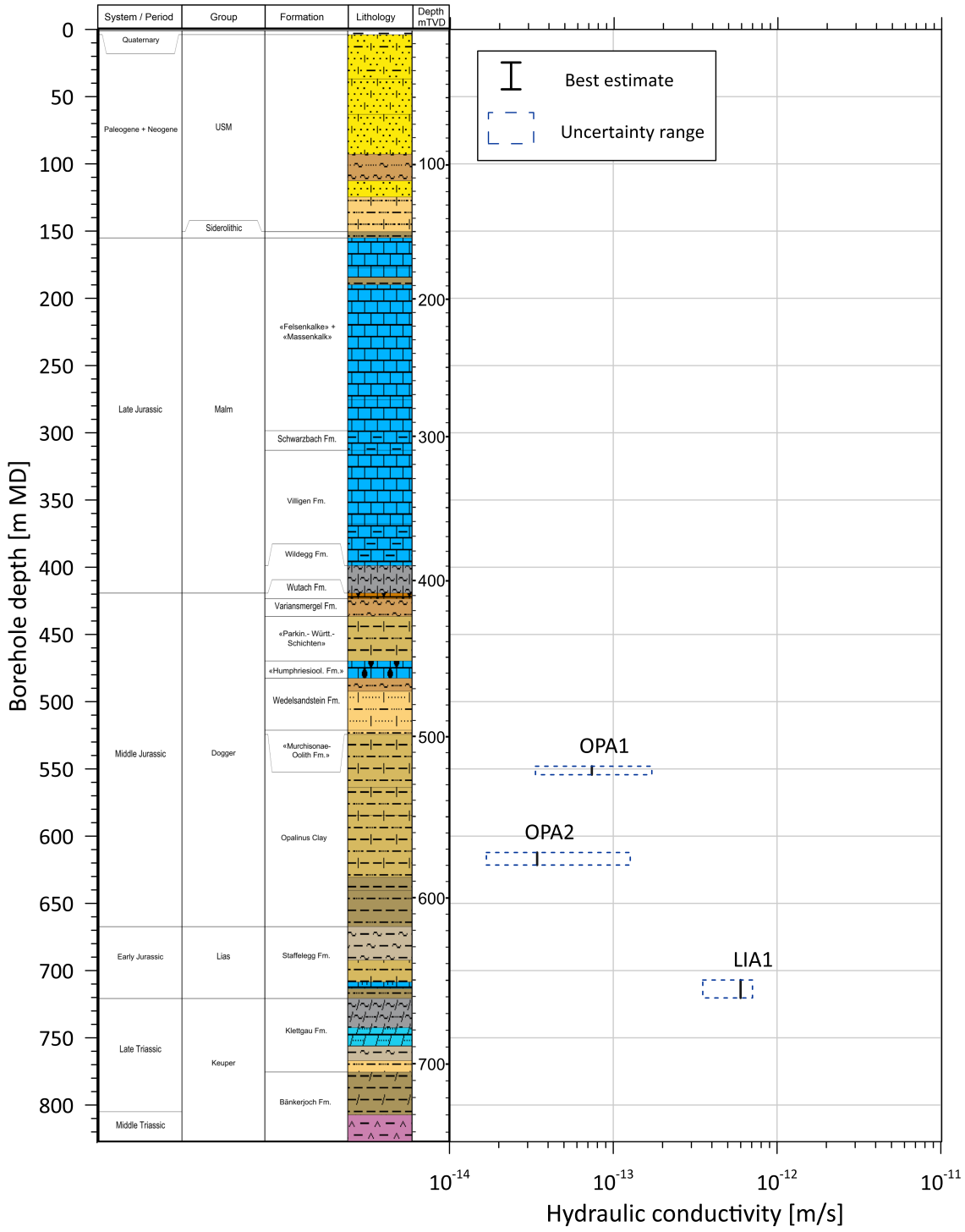

Fig. 3-20: Summary of the hydraulic testing in borehole RHE1-1: Formation hydraulic conductivity profile

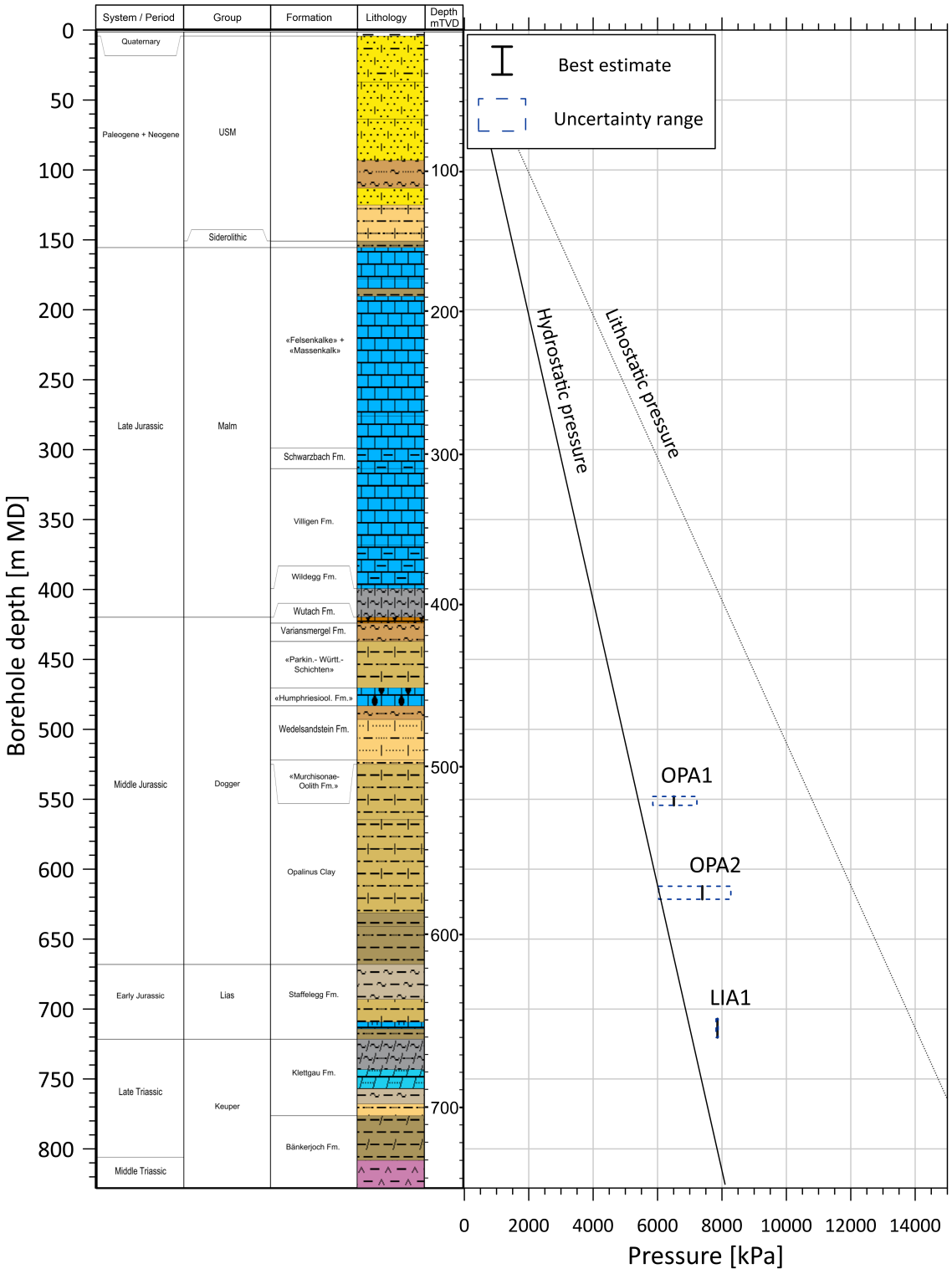

Fig. 3-21: Summary of the hydraulic testing in borehole RHE1-1: Static formation pressure profile

The lithostatic pressure is based on the assumption of a mean density of 2'000 kg m^{-3}.

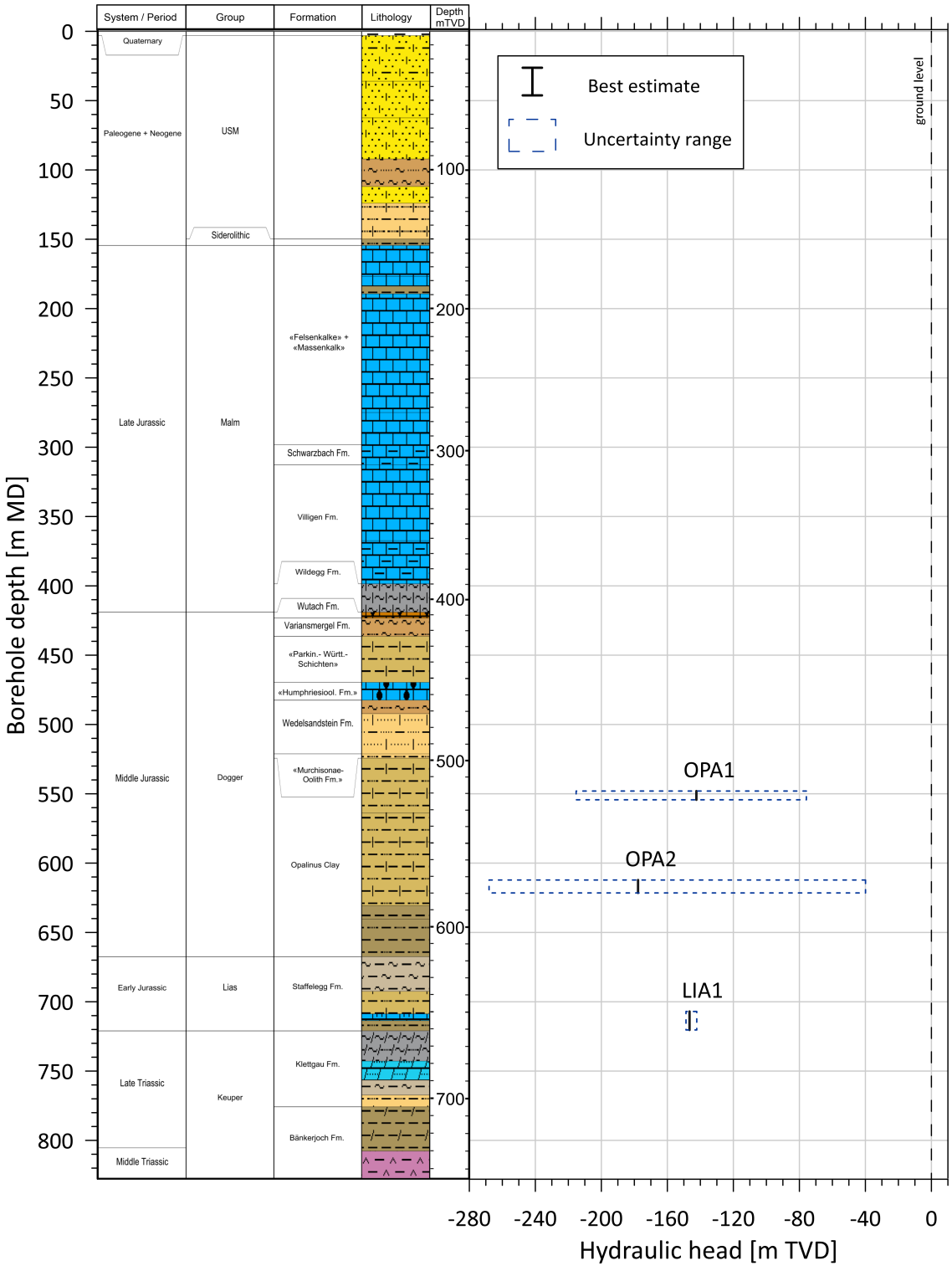

Fig. 3-22: Summary of the hydraulic testing in borehole RHE1-1: Formation hydraulic head profile (m TVD)

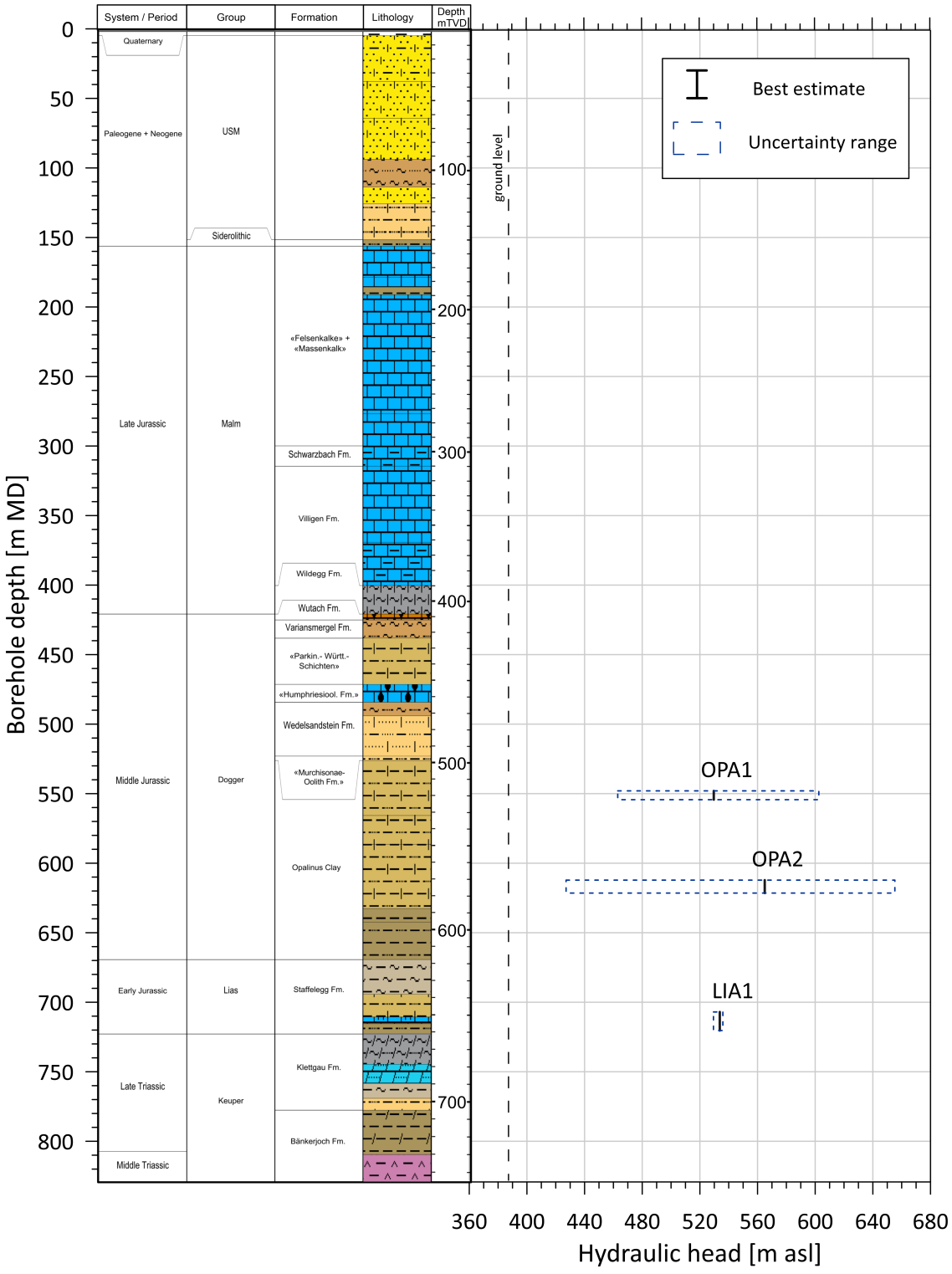

Fig. 3-23: Summary of the hydraulic testing in borehole RHE1-1: Formation hydraulic head profile (m asl)

3.6.1.2 Discussion of data and test results

After drilling and petrophysical borehole logging, the "pristine" / "undisturbed" Opalinus Clay was investigated by tests RHE-OPA1a and RHE1-1-OPA2a. Both were started with an initial compliance and pressure recovery phase followed directly by a slug withdrawal phase based on the experience from previous hydraulic testing in other boreholes in the TBO test campaign. Subsequently, the slug pressure recovery phase was started by closing the shut-in valve. On completion of the tests, a pulse test phase was performed: a pulse injection in RHE1-1-OPA1a and a pulse withdrawal in RHE1-1-OPA2a.

For the two hydraulic tests RHE1-1-OPA1a and RHE1-1-OPA2a which investigated the Opalinus Clay prior to disturbances like the GTPT, fluid exchange or injection tests, the best estimates for the hydraulic conductivity varied by approximately a factor of 2, between 3.4×10^{-14} m s^{-1} for test RHE1-1-OPA2a and 7.4×10^{-14} m s^{-1} for test RHE1-1-OPA1a. The analyses were based on 2-zone radial composite flow models that considered the observed near borehole conditions (skin) as a separate zone. The uncertainty in the estimates of the hydraulic head was generally high for all tests performed in the Opalinus Clay. Like the results for other boreholes in the TBO campaign, the estimates of the hydraulic head from the tests in the Opalinus Clay yielded "apparent" hydraulic heads which are not considered as realistic due to physical processes that cannot be captured by the hydraulic modelling software used, e.g. poroelastic effects. The analysis of RHE1-1-OPA2a is presented in detail in Section 3.5.2.

The test interval of test RHE1-1-LIA1 was located in a cored borehole section of the Staffelegg Formation of the Lias Group including the Frick, Beggingen and Schambelen Members. The analysis (*cf.* Section 3.5.1) used a 2-zone radial composite model, representing a skin in terms of a thin zone close to the borehole. The best estimate derived for the formation hydraulic conductivity was 6.0×10^{-13} m s^{-1}. As with the other tested formations of very low permeability, the high estimated hydraulic pressure is considered not realistic due to physical processes that cannot be captured by the hydraulic modelling software used.

3.6.2 Investigation of the artificially disturbed formation

While test RHE1-1-OPA1a was analysed to determine the hydraulic conductivity and static pore pressure before the GTPT sequence, hydraulic test RHE1-1-OPA1c aimed to characterise the disturbed formation after the performance of the GTPT (test RHE1-1-OPA1b). It was of short duration to comply with drill site safety regulations (i.e. risks associated with borehole stability). Due to its highly complex pressure history and short duration as well as highly uncertain test results from the on-site and quick-look analyses, the analysis was not pursued. The hydraulic test RHE1-1-OPA1c did not allow to determine hydraulic parameters for the formation disturbed by the GTPT. The analysis of the GTPT itself is not included in this report.

Tests RHE1-1-OPA2b to d were especially designed to characterise the behaviour of the formation due to changes in the effective stress field around the borehole. These tests were all analysed using a consistent flow model approach in agreement with the analysis of test RHE1-1-OPA2a (2-zone radial composite flow model that considered the observed near borehole conditions as a separate zone) but with time-varying properties. The analysis of the test RHE1-1-OPA2b was focused on the estimation of the hydraulic formation properties after the fluid exchange in the test interval. The objective of test RHE1-1-OPA2c was to determine the transmissivity behaviour of the Opalinus Clay in relation to increasing interval pressure. The pressure inside the test interval was increased stepwise while measuring varying flow rates until stabilisation. Fig. 3-24 shows the stabilized flow rates for the constant head / constant pressure

phases HI301 to HI309. The numerical model for the analysis of test part RHE1-1-OPA2c allowed for a changing formation hydraulic transmissivity and reproduces the observed pressure and flow rates well. The last part of the hydraulic test, RHE1-1-OPA2d, was started after a long pressure recovery phase following the multi-step constant head / constant pressure test series. It was initiated by a constant head / constant pressure withdrawal phase (HW, Fig. 3-24), followed by a pressure recovery phase and a pulse withdrawal phase in order to study self-sealing properties of the Opalinus Clay.

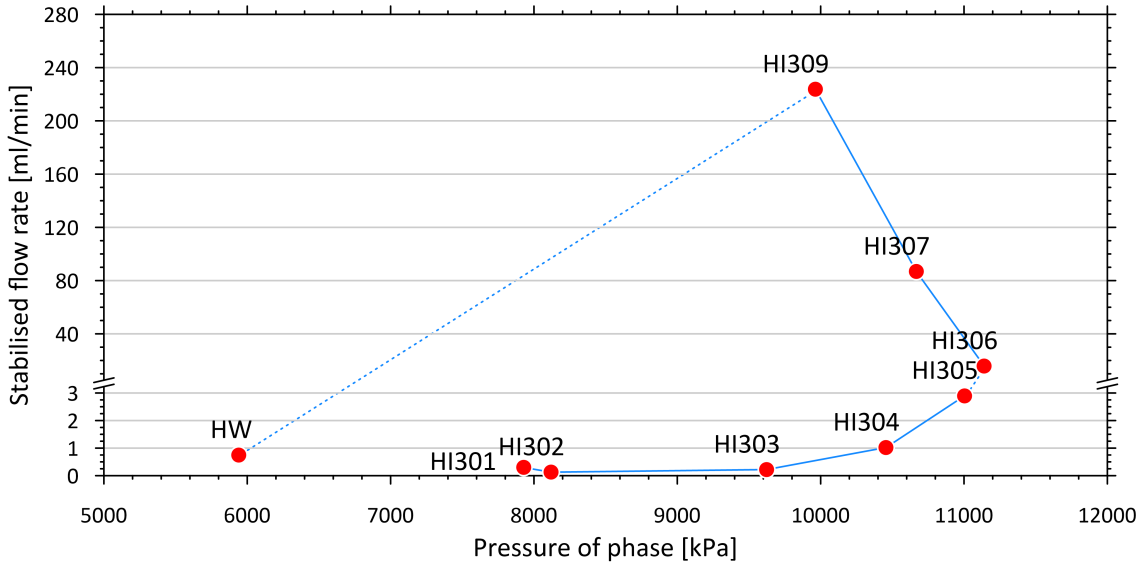

Fig. 3-24: Stabilised flow rates of each phase during RHE1-1-OPA2c (HI301 to 309) and OPA2d (HW)

Compared to the hydraulic parameters estimated from test RHE1-1-OPA2a performed with drilling mud as test interval fluid, the best estimates for hydraulic test RHE1-1-OPA2b (PW3) showed a slightly lower transmissivity value of 9.5×10^{-14} m^2 s^{-1} (ranging between 6×10^{-14} m^2 s^{-1} and 3×10^{-12} m^2 s^{-1}), and a lower value for the hydraulic head of 412 m asl (ranging between 307 m asl and 512 m asl) using synthetic porewater as test interval fluid. The test results show a wider range for hydraulic transmissivity, covering the RHE1-1-OPA2a test results. Regarding the hydraulic head estimates, the uncertainty ranges of tests RHE1-1-OPA2a and b partially overlap, whereas the best head estimates deviate by approximately 155 m. Note that the initial hydraulic formation properties before the constant head / constant pressure (HI) test series (RHE1-1-OPA2c) were determined from PW3 and PW5, at which a short over-pressuring prior to PW5 (HI2, Fig. 3-14) resulted in an increased estimate of the formation hydraulic transmissivity (*cf.* Fig. 3-25).

During test part RHE1-1-OPA2c the pressure in the test interval was increased stepwise to more than 11 MPa (Figs. 3-14 and 3-24). Over the different phases of tests RHE1-1-OPA2b and c, the hydraulic transmissivity of the near borehole (inner) zone of an assumed radius of 0.1 – 0.4 m increases from 2.2×10^{-12} m^2 s^{-1} (RHE1-1-OPA2b, PW3) to 5.7×10^{-9} m^2 s^{-1} (RHE1-1-OPA2c, HI309) and recovers to an estimated value of 4.6×10^{-11} m s^{-1} during the following pressure recovery phase (RHE1-1-OPA2c, MRS) of 21 hours. Fig. 3-25 shows the development of the hydraulic transmissivity for the (outer) formation zone, estimated to increase as a function of the interval pressure from 9.5×10^{-14} m^2 s^{-1} (RHE1-1-OPA2b, PW3) to 5.6×10^{-9} m^2 s^{-1} (RHE1-1-OPA2c, HI309). During the constant head / constant pressure phases HI302 to HI305 the outer

zone is almost not disturbed by the pressure increase in the interval, whereas the inner zone hydraulic transmissivity varies between 9.4×10^{-13} m^2 s^{-1} and 4.6×10^{-11} m^2 s^{-1}. After the shut-in, the formation (outer) hydraulic transmissivity recovers during the pressure recovery phase (RHE1-1-OPA2c, MRS) to an estimated value of 3.2×10^{-12} m^2 s^{-1} (ranging between 9×10^{-13} m^2 s^{-1} and 6×10^{-12} m^2 s^{-1}). During RHE1-1-OPA2d, when the interval pressure was bleed-off during a constant head / constant pressure withdrawal phase (HW) and the following recovery period (HWS) including PW8 (Fig. 3-15), the best estimate of the (outer) formation hydraulic transmissivity varied between 5.3×10^{-12} to 5.4×10^{-11} m^2 s^{-1}, and 4.4×10^{-11} to 1.0×10^{-10} m^2 s^{-1} for the hydraulic transmissivity of a near borehole (inner) zone which extended to a radius of 0.28 m.

The general increase in the estimated values of the outer zone hydraulic transmissivity shows the model-based representation of the opening of fractures as implemented by a 2-zone radial composite flow model. Therefore, the estimated hydraulic transmissivity values should be considered as qualitative values, resulting from analyses which considered specific assumptions (e.g. a fixed radius of the inner zone, and a fixed formation pressure of 6'000 kPa during test RHE1-1-OPA2c). The sharp drop of the estimated values in the pressure recovery phase (MRS) at lower pressures may be interpreted as an indication of self-sealing of the Opalinus Clay. Please take into consideration that the uncertainty ranges are overlapping, and the best estimate of the pressure recovery phase (RHE1-1-OPA2c, MRS) is nearly in the range of an undisturbed formation based on the results of PW3 (RHE1-1-OPA2b). The fact that a renewed increase in pressure (RHE1-1-OPA2d, HWS and PW8) results in higher hydraulic transmissivity estimates may suggest a reactivation of fractures. However, this phenomenon should not be over-interpreted due to the existing uncertainties and the assumptions made in the history of RHE1-1-OPA2d (HW-HWS-PW8). These assumptions determine the pressure distribution around the interval, which can only confirm the assumptions made. The resulting parameter ranges are therefore merely qualitative information.

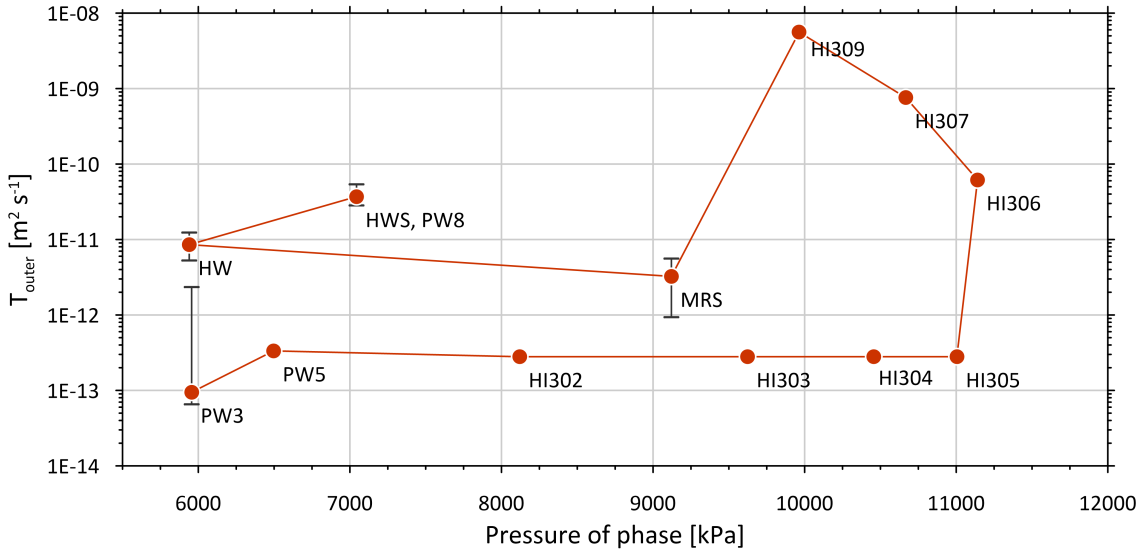

Fig. 3-25: Summary of the development of the (disturbed) outer zone formation hydraulic transmissivity as a function of the interval pressure during hydraulic tests RHE1-1-OPA2b to RHE1-1-OPA2d, including the uncertainty ranges of selected phases

4 Summary

The Rheinau-1-1 (RHE1-1) exploratory borehole is the eighth borehole drilled within the framework of the TBO project.

A total of three sections were tested with hydraulic packer tests in borehole RHE1-1 in August and September 2021. All hydraulic packer tests were performed in cored borehole sections using an HDDP packer system in a double packer configuration (*cf.* Tab. 3-24). The test activities were performed in the following geological formations (*cf.* Dossier III):

- Dogger Group with a focus on the Opalinus Clay (RHE1-1-OPA1 and RHE1-1-OPA2)
- Lias Group with a focus on the Staffelegg Formation with the Frick, Beggingen and Schambelen Members (RHE1-1-LIA1)

Besides the hydraulic tests performed according to the established test strategy (*cf.* Section 3.1) and used to determine the hydraulic parameters of investigated test intervals, the multi-part test RHE1-1-OPA2 (RHE1-1-OPA2b to OPA2d) was designed to characterise the behaviour of encountered structures due to changes in the effective stress field around the borehole in the Opalinus Clay.

All hydraulic tests were supported by on-site field analyses to optimise the test procedures. The pressures and flow rates measured during all tests are illustrated in Figs. 3-10 to 3-16. The main results and best estimates of the hydraulic formation parameters are presented in Tabs. 3-41 to 3-43 and Figs. 3-19 to 3-23. The hydraulic test analyses of RHE1-1-LIA1 and RHE1-1-OPA2a (*cf.* Sections 3.5.1 and 3.5.2) were selected for a detailed description in this report.

Regarding the effect of changes in the effective stress field around the borehole on the hydraulic parameters, tests RHE1-1-OPA2b to OPA2d confirmed a pressure dependency of the formation hydraulic transmissivity for an interval pressure greater approximately 10 to 11 MPa. Note that the radial 2-zone composite model used for the test analysis considers the transition between the near borehole zone and the formation at a distance between 0.1 m and 0.4 m from the centre of the borehole. After the opening of fractures at approximately 11 MPa, continuous injection at interval pressures of about 10 MPa indicates an increase in formation transmissivity by about 4 orders of magnitude compared to the transmissivity of the "pristine" formation. Conversely, the termination of the injection and depletion or bleed-off of the interval pressure below approximately 10 MPa is associated with a reduction (approximately 3 orders of magnitude) in the hydraulic formation transmissivity. Hence a strong sensitivity of the hydraulic properties to changes in effective stresses is observed only when the interval pressure is increased by approximately 3 to 4 MPa above the hydrostatic pressure.

The best estimates and uncertainties for the hydraulic conductivities and transmissivities of the "pristine" formations lie within a reasonable range and are within the expected spectrum of values for the investigated formations (e.g. Nagra 2008, Nagra 2014a and b). The hydraulic conductivities obtained for the "pristine" Opalinus Clay are very low and range over one order of magnitude in total.

The extrapolated hydraulic heads are not within an expected range (Luo et al. 2013). Due to unavoidable short hydraulic test durations compared to the duration of the borehole pressure history, the hydraulic heads appear to be affected by a large overestimation. They are considered as "apparent" hydraulic heads.

General investigations concerning the physical explanation for the overestimation of the hydraulic heads are continuing. The presented analyses consider temperature effects in the test intervals and pressure-induced effects resulting from the high-density drilling mud used after drilling through the interval centre. Nagra has installed long-term pressure monitoring systems in borehole MAR1-1 and other selected boreholes.

5 References

Agarwal, R.G. (1980): A new method to account for producing time effects when drawdown type curves are used to analyze pressure buildup and other test data. Proceedings of the 55th Annual Fall Technical Conference and Exhibition of the Society of Petroleum Engineers. Paper SPE 9289.

Barker, J.A. (1988): A generalized radial flow model for hydraulic tests in fractured rock. Water Resour. Res. 24/10, 1796-1804.

Birkhäuser, P., Roth, P., Meier, B. & Naef, H. (2001): 3D-Seismik: Räumliche Erkundung des mesozoischen Sedimentschichten im Zürcher Weinland. Nagra Technischer Bericht NTB 00-03.

Black, J., Holmes, D. & Brightman, M. (1987): Crosshole investigations – Hydrogeological results and interpretations. Nagra Technical Report NTB 87-37.

Bredehoeft, J.D. & Papadopulos, S.S. (1980): A method for determining the hydraulic properties of tight formations. Water Resour. Res. 16/1, 233-238.

Cooper, H.H., Bredehoeft, J.D. & Papadopulos, S.S. (1967): Response of a finite-diameter well to an instantaneous charge of water. Water Resour. Res. 3/1, 263-269.

Detournay, E. & Cheng, A.H.-D. (1988): Poroelastic response of a borehole in a non-hydrostatic stress field. International Journal of Rock Mechanics and Mining Sciences & Geomechanics Abstracts 25/3, 171-182.

Geofirma Engineering Ltd. & INTERA Inc. (2011): nSIGHTS Version 2.50 User Manual. INTERA Inc., Austin, TX, USA.

Grauls, D. (1999): Overpressures: Causal mechanisms, conventional and hydromechanical approaches. Oil & Gas Science and Technology – Rev. IFP 54, 667-678.

Isler, A., Pasquier, F. & Huber, M. (1984): Geologische Karte der zentralen Nordschweiz 1:100'000. Herausgegeben von der Nagra und der Schweiz. Geol. Komm.

Jacob, C.E. & Lohman, S.W. (1952): Non-steady flow to a well of constant drawdown in an extensive aquifer. Trans. Amer. Geophys. Union, Vol. 33, pp. 559-569.

Jäggi, K. & Vogt, T. (2020): OPA: Sondierbohrung Benken, Langzeitbeobachtung 2019, Dokumentation der Messdaten. Nagra Arbeitsbericht NAB 20-05.

Jäggi, D., Laurich, B., Nussbaum, C., Schuster, K. & Connolly, P. (2017): Tectonic structure of the "Main Fault" in the Opalinus Clay, Mont Terri rock laboratory (Switzerland). Swiss Journal of Geosciences 110, 67-84.

Lisjak, A., Garitte, B., Grasselli, G., Müller, H.R. & Vietor, T. (2015): The excavation of a circular tunnel in a bedded argillaceous rock (Opalinus Clay): Short-term rock mass response and FDEM numerical analysis. Tunnelling and Underground Space Technology 45, 227-248.

Luo, J., Monningkoff, B. & Becker, J.K. (2013): Hydrogeological model Zürich Nordost and Südranden. Nagra Arbeitsbericht NAB 13-24.

Marschall, P., Croisé, J., Schlickenrieder, L., Boisson, J.Y., Vogel, P. & Yamamoto, S. (2003): Synthesis of hydrogeological investigations at the Mont Terri site (Phases 1 – 5). Mont Terri Technical Report TR 01-02. Mont Terri Project, Switzerland.

Nagra (1997): Hydrological investigations at Wellenberg: Hydraulic packer testing in boreholes SB4a/v and SB4a/s. Methods and field results. Nagra Technischer Bericht NTB 95-02.

Nagra (2001): Sondierbohrung Benken – Untersuchungsbericht. Nagra Technischer Bericht NTB 00-01.

Nagra (2008): Vorschlag geologischer Standortgebiet für das SMA- und das HAA-Lager – Geologische Grundlagen. Nagra Technischer Bericht NTB 08-04.

Nagra (2014a): SGT Etappe 2: Vorschlag weiter zu untersuchender geologischer Standortgebiete mit zugehörigen Standortarealen für die Oberflächenanlage. Geologische Grundlagen. Dossier II: Sedimentologische und tektonische Verhältnisse. Nagra Technischer Bericht NTB 14-02.

Nagra (2014b): SGT Etappe 2: Vorschlag weiter zu untersuchender geologischer Standortgebiete mit zugehörigen Standortarealen für die Oberflächenanlage. Geologische Grundlagen. Dossier VI: Barriereneigenschaften der Wirt- und Rahmengesteine. Nagra Technischer Bericht NTB 14-02.

Nagra (2019): Preliminary horizon and structure mapping of the Nagra 3D seismics ZNO-97/16 (Zürich Nordost) in time domain. Nagra Arbeitsbericht NAB 18-36.

Peres, A.M., Onur, M. & Reynolds, A.C. (1989): A new analysis procedure for determining aquifer properties from slug test data. Water Resour. Res. 25/7, 1591-1602.

Pickens, J.F., Grisak, G.E., Avis, J.D., Belanger, D.W. & Thury, M. (1987): Analysis and interpretation of borehole hydraulic tests in deep boreholes: Principles, model development, and application. Water Resour. Res. 23/7, 1341-1375.

Pietsch, J. & Jordan, P. (2014): Digitales Höhenmodell Basis Quartär der Nordschweiz – Version 2013 (SGT E2) und ausgewählte Auswertungen. Nagra Arbeitsbericht NAB 14-02.

Ramey, H.J. & Agarwal, R.G. (1972): Annulus unloading rates as influenced by wellbore storage and skin. Soc. Pet. Engr. J. 12/5, 453.

Roche, V., Childs, C., Madritsch, H. & Camanni, G. (2020): Controls of sedimentary layering and structural inheritance on fault zone structure in three dimensions. A case study from the northern Molasse basin, Switzerland. Journal of the Geological Society 177/3, 493-508.

Appendix A: Abbreviations, nomenclature and definitions

Tab. A-1: Lithostratigraphy abbreviations for test names in RHE1-1

Lithostratigraphy	**Abbreviation**
Opalinus Clay (Dogger)	OPA
Lias Group	LIA

Tab. A-2: Test name definitions for hydraulic packer testing

[1] Based on the preliminary information

Abbreviation	**Example**
Borehole abbreviation – lithostratigraphy abbreviation[1] + number of test	RHE1-1-LIA1: First test interval in the Lias Group in borehole RHE1-1

Tab. A-3: Test event abbreviations for hydraulic packer testing

Test phase	**Abbreviation**
Compliance phase	COM
Packer deflation phase	DEF
Partial depressurisation of the top packer to degas the test interval	DEGA
Fluid displacement in the test interval	DISP
Constant head injection test (constant pressure difference)	HI
Pressure recovery after constant head injection test (shut-in)	HIS
Withdrawal test applying constant differential head	HW
Pressure recovery after constant head withdrawal test (shut-in)	HWS
Packer inflation phase	INF
Pressure recovery after multi-rate test (shut-in)	MRS
Pulse injection test	PI
Initial pressure recovery 'static pressure recovery' (SIT closed)	PSR
Pulse withdrawal test	PW
Slug withdrawal test (flow phase)	SW
Slug withdrawal test – pressure recovery with closed SIT (shut-in)	SWS
Constant rate injection test	RI
Constant rate withdrawal/pumping test	RW
Pressure recovery after constant rate withdrawal test (shut-in)	RWS

Tab. A-4: Parameter definitions

Abbreviation / symbol	**Description**	**Unit**
c_{tz}	Test zone compressibility	Pa^{-1}
C_i	Concentration (salinity) of one inflow i	$g\ l^{-1}$
EC_i	Electrical conductivity of one inflow i	$\mu S\ cm^{-1}$
g	Acceleration due to gravity (9.81)	$m\ s^{-2}$
h_s	Static hydraulic head (freshwater head) $h_s = z_{ref} - z_{int} + \left[\frac{P_f + \rho_{int}\ g\ (z_{int} - z_2) - P_{atm} - P_{offset}}{\rho_w\ g}\right]$	m asl
k	Intrinsic permeability	m^2
K	Hydraulic conductivity	$m\ s^{-1}$
K_{in}	Inner-zone hydraulic conductivity	$m\ s^{-1}$
K_{out}	Outer-zone hydraulic conductivity	$m\ s^{-1}$
K_s	Hydraulic conductivity of skin zone	$m\ s^{-1}$
n	Fractional flow dimension, e.g. Barker (1988)	-
P	Pressure (at QSSP-P2 level, if not otherwise specified)	Pa, kPa
P1	Pressure below bottom packer / interval P1 (downhole probe)	Pa, kPa
P2	Pressure in test interval (downhole probe)	Pa, kPa
P2*	(Absolute) pressure in test interval (memory gauge)	Pa, kPa
P3	Pressure in annulus (above top packer, downhole probe)	Pa, kPa
P4	Pressure in test tubing above SIT (downhole probe)	Pa, kPa
P_{atm}	Atmospheric pressure	Pa, kPa
P_f	Static formation pressure (fitting parameter, at QSSP-P2 level, respectively P2* level)	Pa, kPa
P_{int}	Pressure at centre of test interval	Pa, kPa
P_{offset}	Offset of a pressure probe at atmospheric pressure	Pa, kPa
P_S	Static formation pressure (at centre of test interval if not specified otherwise)	Pa, kPa
ΔP_{packer}	Interval packer pressure changes	bar
q	Flow rate	$m^3\ s^{-1}$
q_i	Flow rate of one inflow i	$m^3\ s^{-1}$
Q, Q_{tot}	Cumulative flow volume	m^3
r_d	Radius of discontinuity	m
r_s	Radius of the skin zone extension	m
$r_{w\ int}$	Borehole radius of the test interval	mm
ρ_{int}	Density of interval fluid	$kg\ m^{-3}$

Tab. A-4: conti.

Abbreviation / symbol	**Description**	**Unit**
ρ_w	Density of formation water (fluid)	kg m^{-3}
S	Storage coefficient	-
s	Skin factor	-
S_s	Specific storage	m^{-1}
$S_{s\ in}$	Inner-zone specific storage	m^{-1}
$S_{s\ out}$	Outer-zone specific storage	m^{-1}
S_{ss}	Specific storage of skin zone	m^{-1}
t_s	Thickness of the skin zone extension	m
T	Transmissivity	$m^2\ s^{-1}$
T_i	Transmissivity of one inflow i	$m^2\ s^{-1}$
t, dt	Time, elapsed time	s
T_{int}, T1, T2, T3, T4, T2*	Temperature in test interval, temperature downhole probe (sensors 1, 2, 3 or 4 associated with specific transducer; sensor T2* associated with memory gauge)	°C
ΔV_{int}	Interval volume changes	mL
z_2	Depth of pressure sensor of test interval P2	m MD
z_{int}	Depth of interval centre	m MD
z_{ref}	Reference point elevation	m asl

Tab. A-5: Non-parameter abbreviations

Abbreviation	**Description**	**Unit**
ΔP	Change in pressure	Pa, kPa
ΔV	Change in volume	m^3
1D	One dimensional	
2D	Two dimensional	
3D	Three dimensional	
AG	Aktiengesellschaft (company limited by shares "Ltd.")	
API	American Petroleum Institute	
BHPH	Borehole pressure history	
BOP	Blow out preventer	
RHE1-1	Rheinau-1 drill site, borehole 1	
cps	Counts per second	
CU	Copper	

Tab. A-5: conti.

Abbreviation	**Description**	**Unit**
DA	Detailed analysis	
DAS	Data acquisition system	
DR	Detailed report	
EU	External upset coupling	
EUE	External upset end	
FM	Flow model	
FS	Full scale	
GmbH	Gesellschaft mit beschränkter Haftung (company with limited liability)	
GTPT	Gas threshold pressure test	
HDDP	Heavy-duty double packer system	
HLW	High level waste	
HTT	Hydraulic test tool	
IARF	Infinite acting radial flow region	
ID	Inner diameter	
IPI	Inflatable Packers International, Perth, Australia	
IT	Information technology	
L/ILW	Low and intermediate level waste	
ln	Litre normal	ln
MAR1-1	Marthalen-1 drill site, borehole 1	
MD	Measured depth	m
MHF	Micro-hydraulic fracturing	
NBR	Nitrile butadiene rubber	
NDSA	Naphthalene disulfonate acid	
NL	Siting region Nördlich Lägern	
OD	Outer diameter	
PA1	Bottom packer of the hydraulic line of the HDDP	
PA2	Top packer of the hydraulic line of the HDDP	
PCP	Progressive cavity pump	
POOH	Pull out of hole	
PPG	Piston pulse generator	
PRV	Pressure release valve	
QC	Quality control	
QLA	Quick look analysis	

Tab. A-5: conti.

Abbreviation	**Description**	**Unit**
QLR	Quick look report	
QSSP	Quadruple sub-surface probe	
Rd	Reading	
RIH	Run in hole	
SIT	Shut-in tool	
SSE	Sum of squared errors	
TBO	Tiefbohrung(en) (German for deep borehole(s))	
TVD	True vertical depth	m
WS	Water sample	
WT	Water table	
WTW	Wissenschaftlich-technische Werkstätten GmbH	
ZH	Zürich	
ZNO	Siting region Zürich Nordost	

Appendix B: Analysis plots of the hydraulic packer tests RHE1-1-LIA1 and RHE1-1-OPA2a

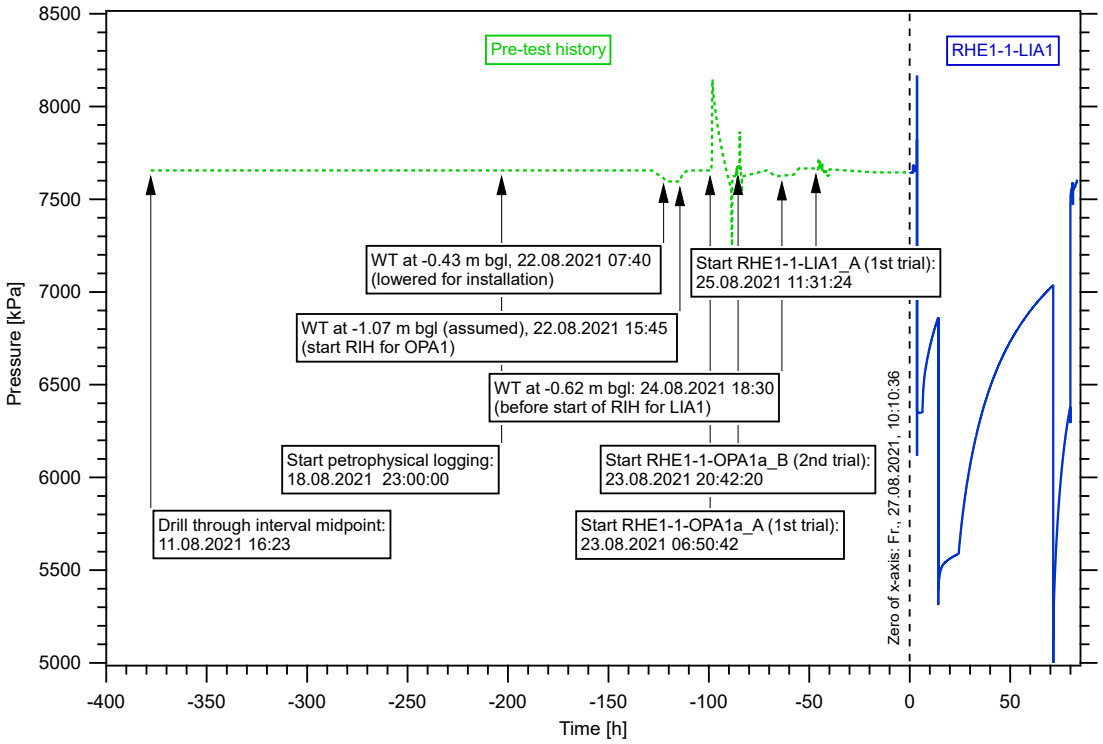

Fig. B-1: Hydraulic test RHE1-1-LIA1: Entire record of the borehole pressure history used in the analysis

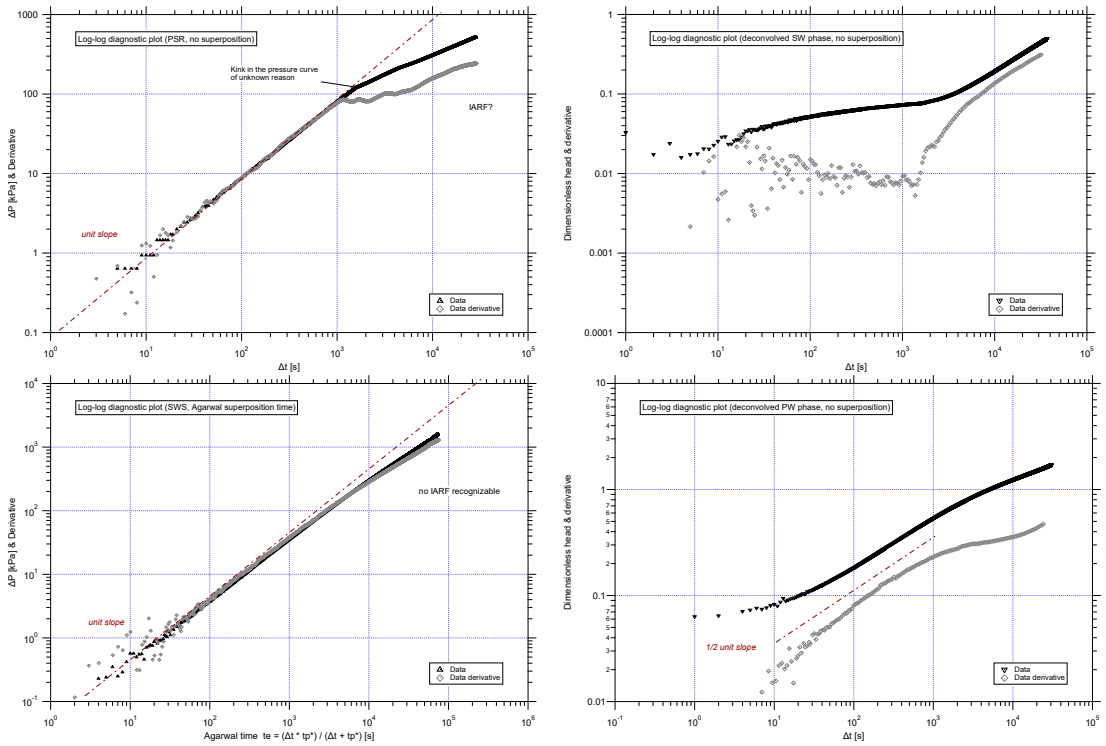

Fig. B-2: Hydraulic test RHE1-1-LIA1: Log-log plots of PSR phase (no superposition, top left graph), SW phase (de-convoluted, top right graph), SWS phase (Agarwal time, bottom left graph) and PW phase (de-convoluted, bottom right graph)

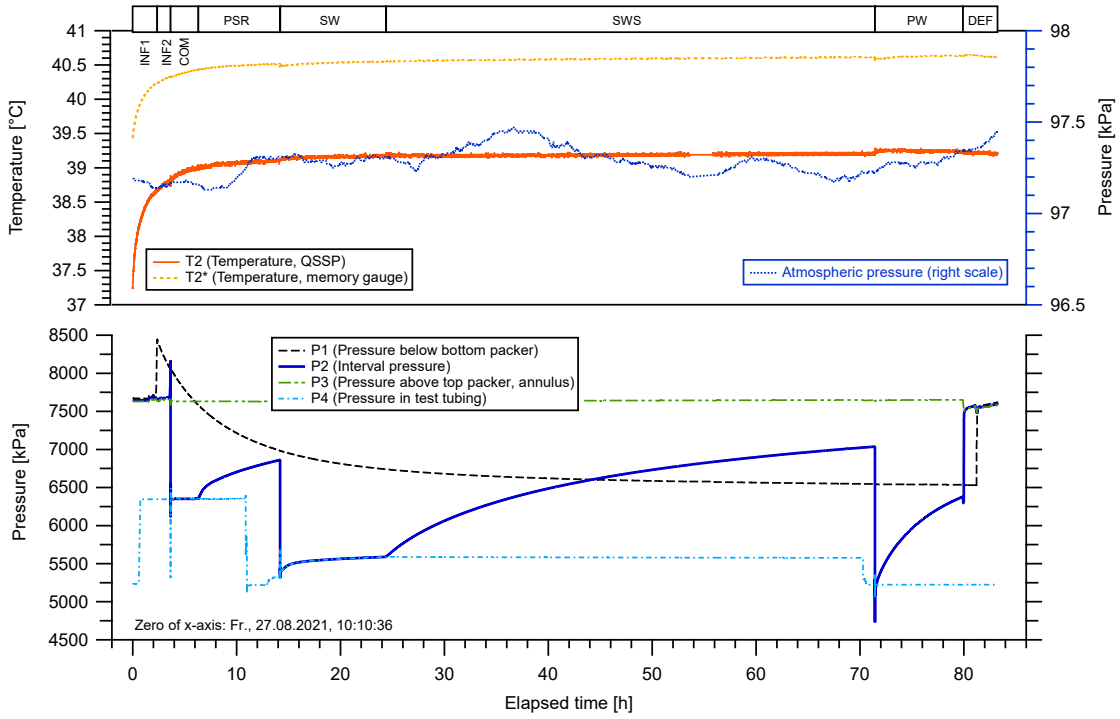

Fig. B-3: Hydraulic test RHE1-1-LIA1: Interval temperature ($T2^*$ memory gauge sensor), atmospheric pressure and downhole pressures of QSSP sensors (P1, P2, P3, P4) as well as temperature measurement at the QSSP (T2 sensor)

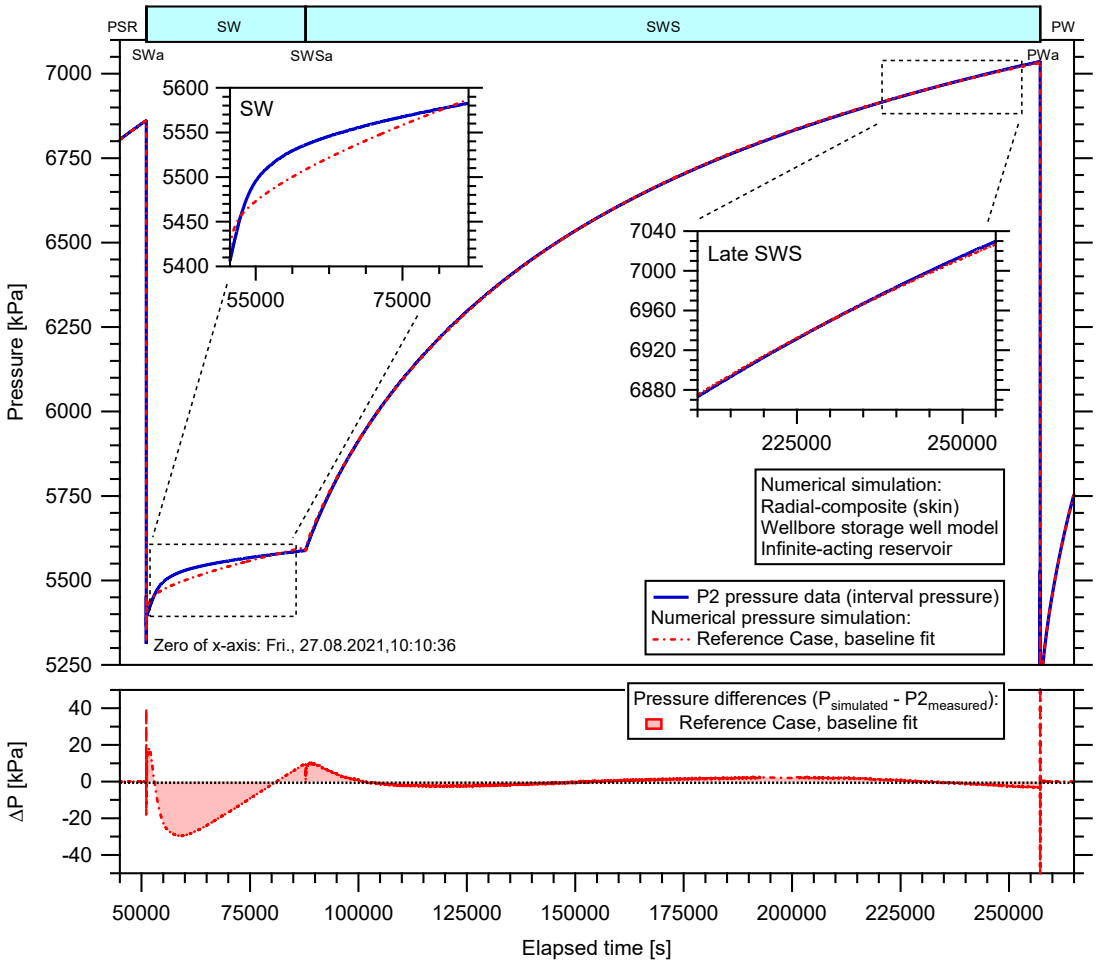

Fig. B-4: Hydraulic test RHE1-1-LIA1: Cartesian pressure graph with the simulation result using the parameters resulting from a parameter optimisation using a radial-composite model (top: SW-SWS sequence with zoom on SW and late SWS phase; bottom: pressure residual plot)

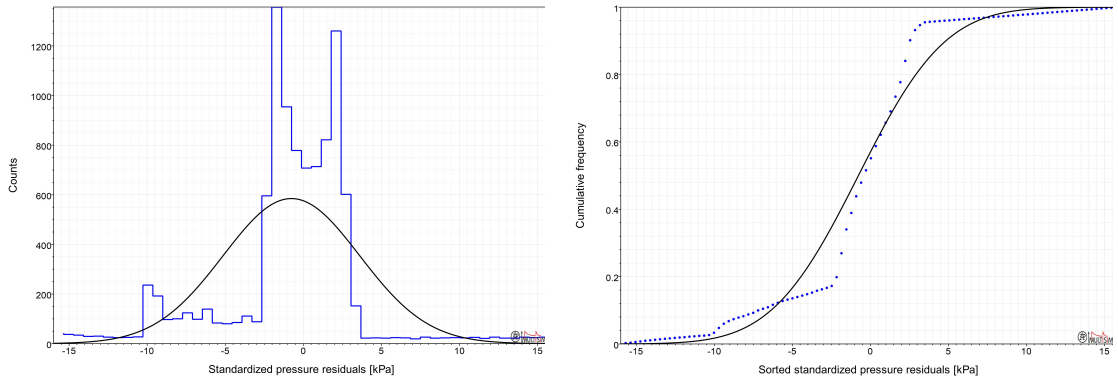

Fig. B-5: Hydraulic test RHE1-1-LIA1: Probability distribution function plot (left) and cumulative distribution function plot (right) of the simulation based on the optimised parameter set for the SW-SWS sequence

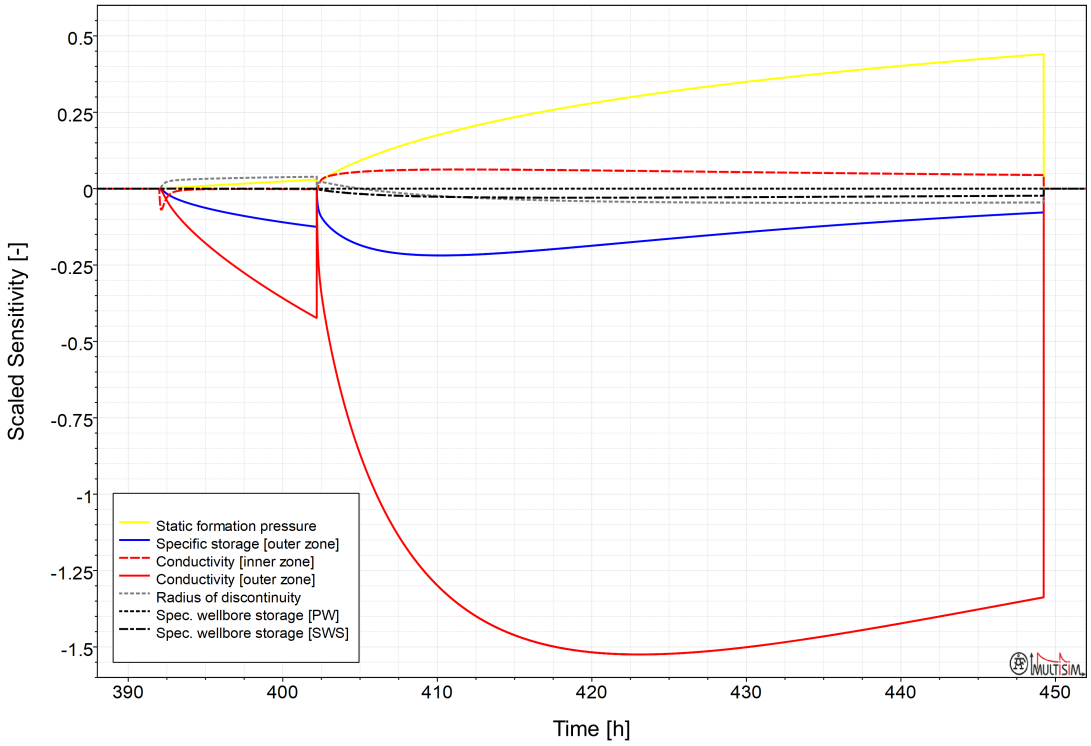

Fig. B-6: Hydraulic test RHE1-1-LIA1: Sensitivities of the optimised parameters for the initial simulation

Time denotes hours since start of borehole pressure history.

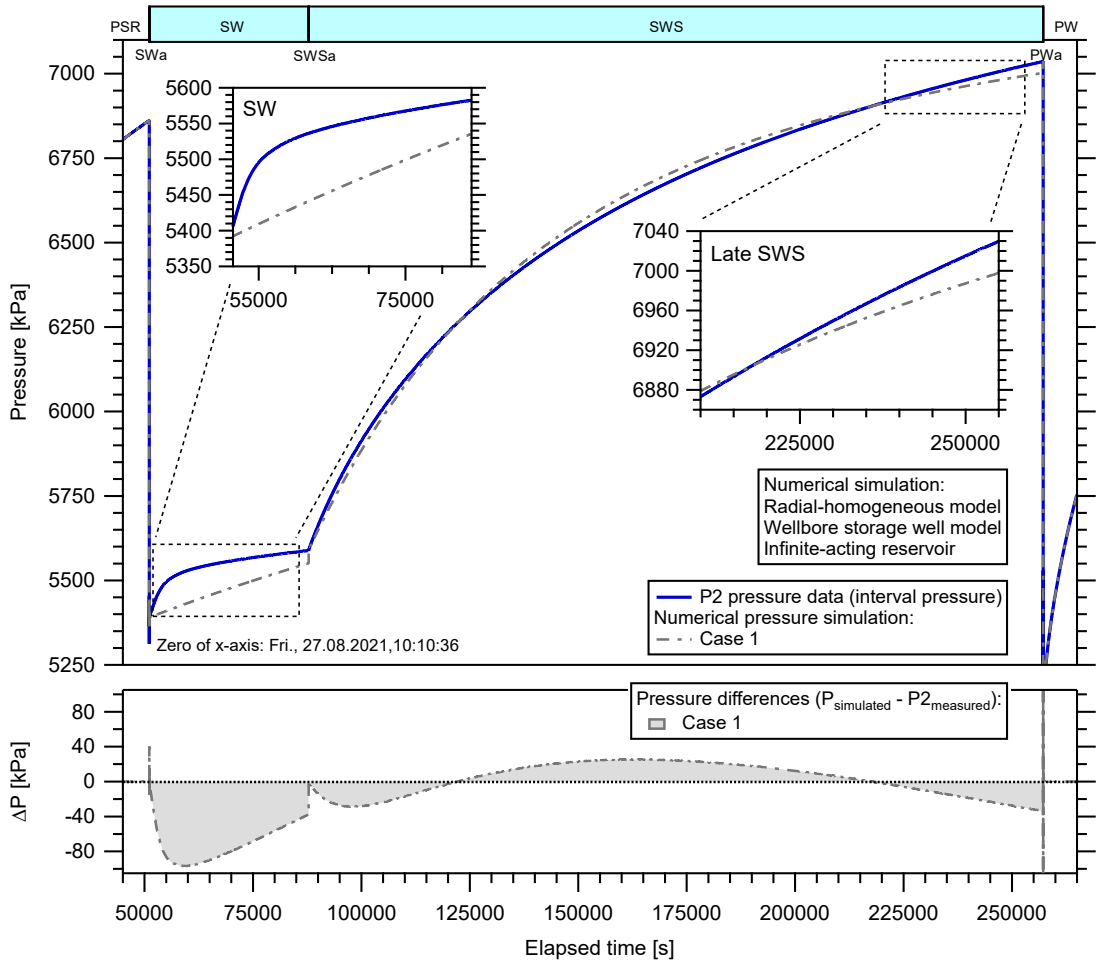

Fig. B-7: Hydraulic test RHE1-1-LIA1: Cartesian pressure graph with simulation result using the parameters resulting from a parameter optimisation using a radial-homogeneous model (top: SW-SWS sequence with zoom on SW and late SWS phase; bottom: pressure residual plot)

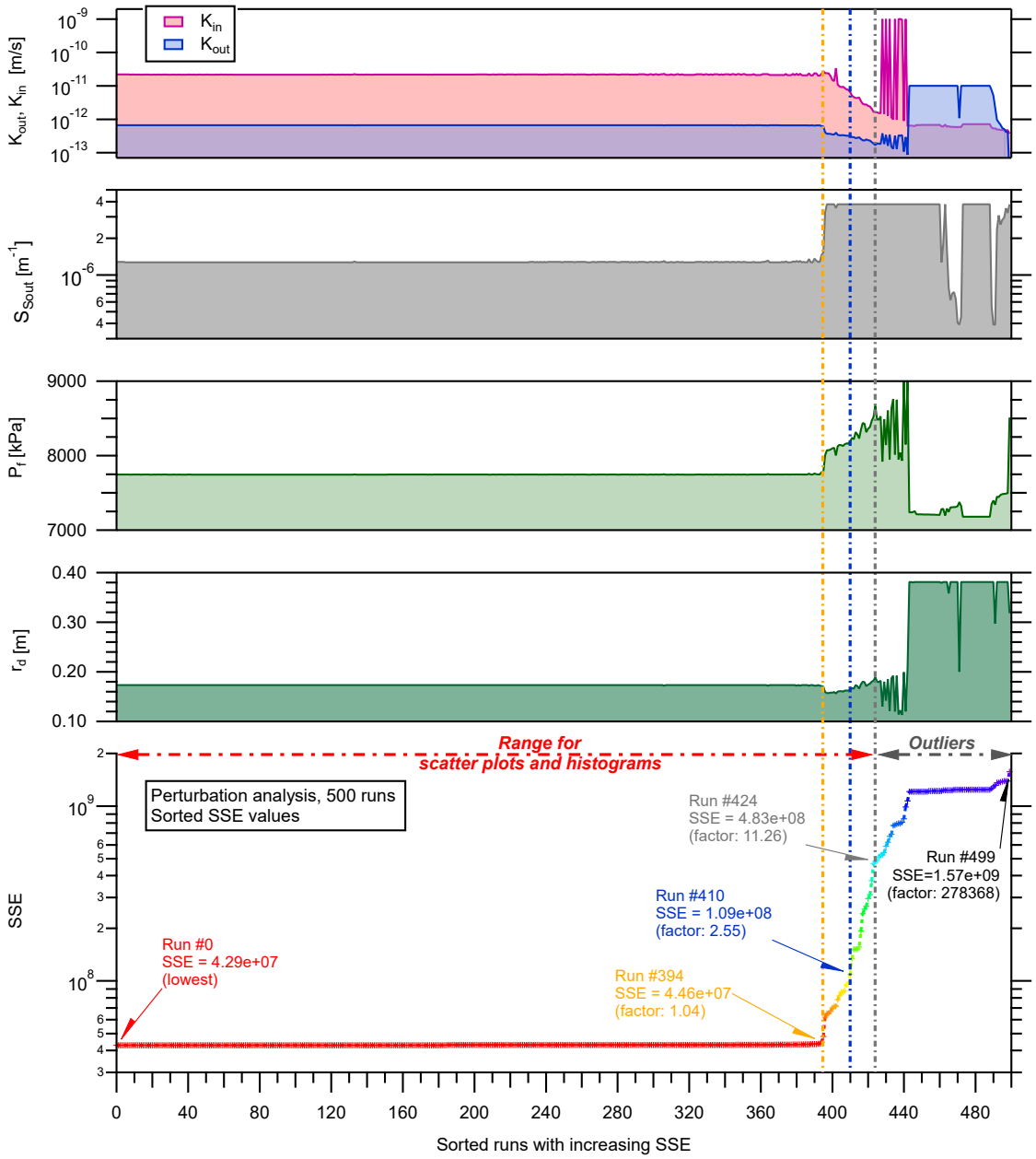

Fig. B-8: Hydraulic test RHE1-1-LIA1: Optimised parameters plotted against sorted SSE values of all perturbation runs and, in the lowest chart section, SSE value against the increasing run number

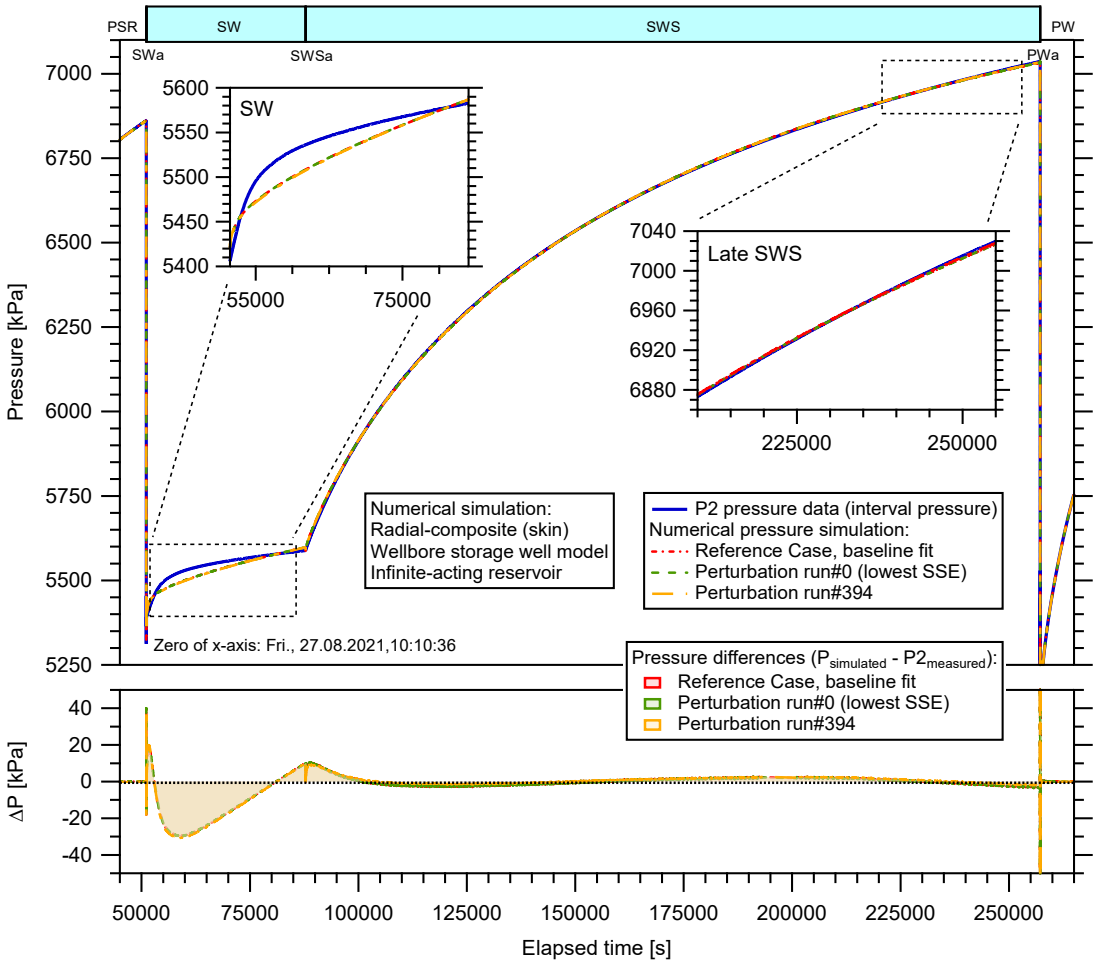

Fig. B-9: Hydraulic test RHE1-1-LIA1: Cartesian pressure graph with simulations resulting from the use of the perturbation parameter sets associated with the lowest SSE (run #0) and the upper limit of the uncertainty range (run #394) as well as the initial simulation (top: SW-SWS sequence with zoom on SW and late SWS phase; bottom: pressure residual plot)

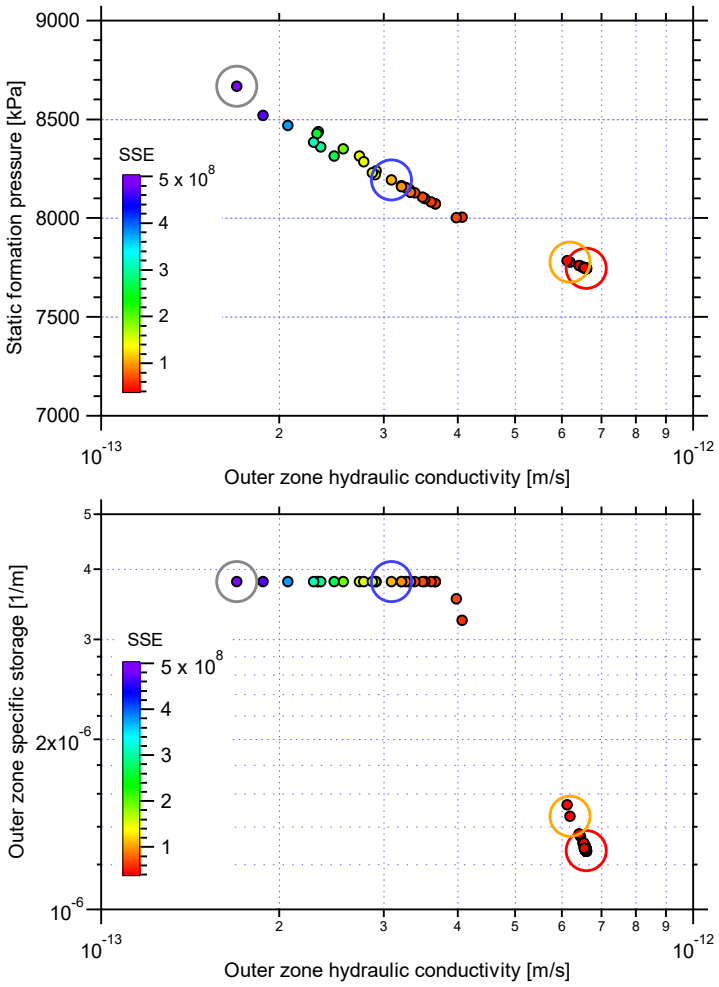

Fig. B-10: Hydraulic test RHE1-1-LIA1: Scatter plots of the perturbation parameter sets and associated SSE values of the optimised parameters showing P_f versus K_{out} (top figure) and S_{Sout} versus K_{out} (bottom figure)

Shown are the first 425 runs, sorted by their SSE value. The red circle indicates the parameter values associated with the lowest SSE value. The orange circle marks the parameter values of run #394 (limit of used parameter set to evaluate the uncertainty range), the blue circle run #410 and the grey circle run #424.

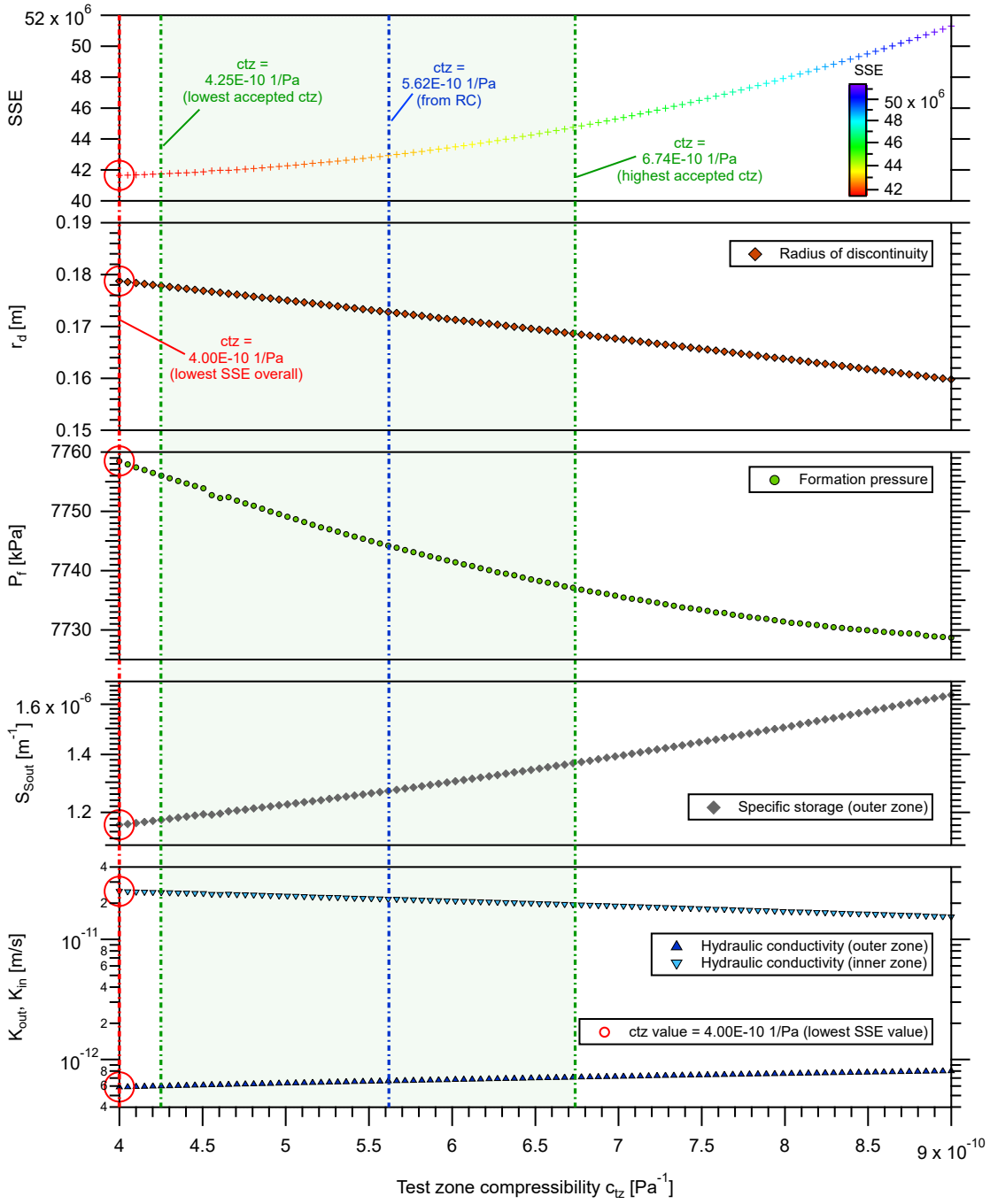

Fig. B-11: Hydraulic test RHE1-1-LIA1: Parameter sets of the sampling analysis of the test zone compressibility (c_{tz})

The SSE value is given for each set (top curve in graph). The blue dashed line indicates the c_{tz} value used in the initial simulation (Reference case, RC), the red dashed line and red circles mark the parameters associated with the lowest SSE, the green dashed lines mark the parameters associated with the uncertainty range, and the green rectangle indicates the uncertainty range.

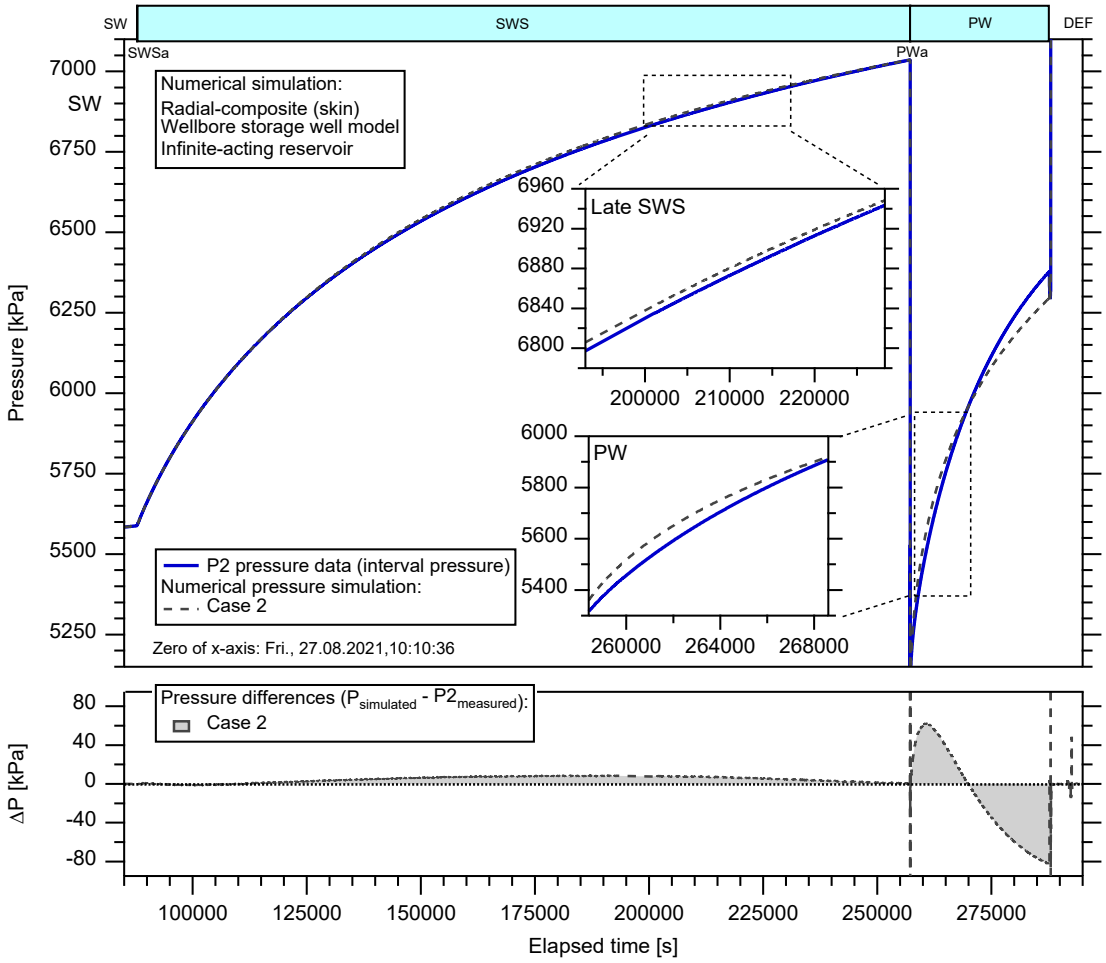

Fig. B-12: Hydraulic test RHE1-1-LIA1: Cartesian pressure graph with simulation result using the parameters resulting from a parameter optimisation on the SWS-PW sequence with a radial-composite model (top: SW-SWS sequence with zoom on late SWS phase and early time PW; bottom: pressure residual plot)

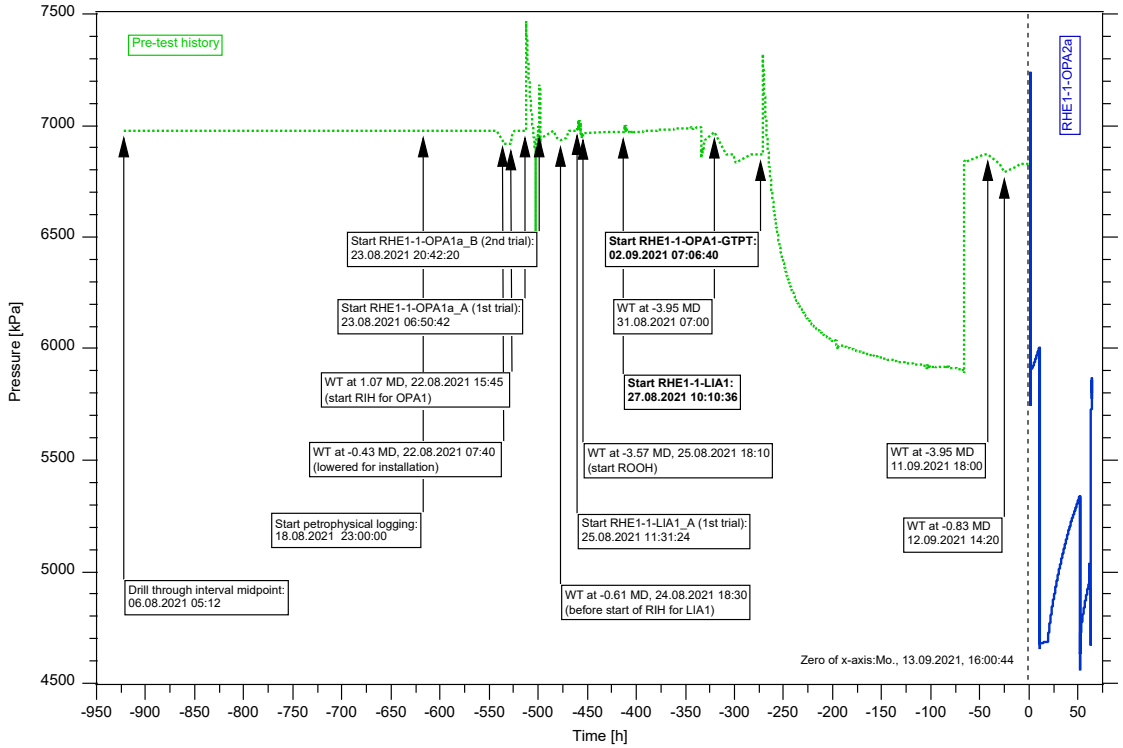

Fig. B-13: Hydraulic test RHE1-1-OPA2a: Entire record of the borehole pressure history used in the analysis

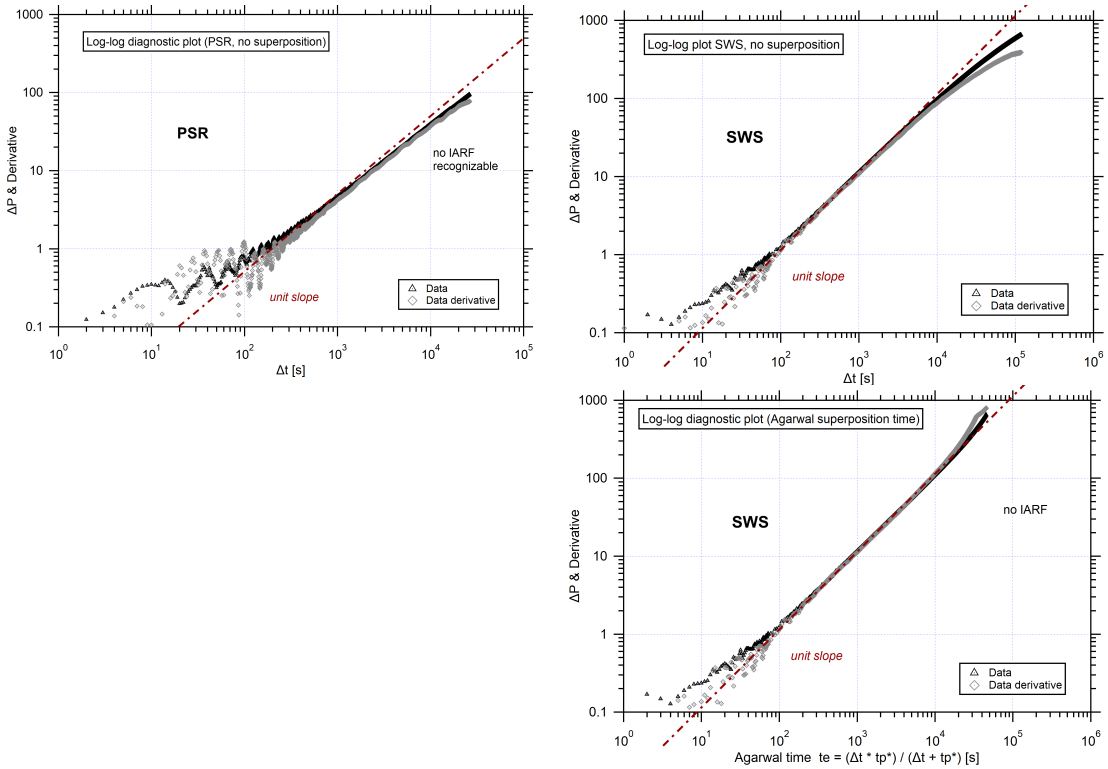

Fig. B-14: Hydraulic test RHE1-1-OPA2a: Log-log plots of PSR phase (no superposition, top left graph), the SWS phase (without superposition, top right graph) and the same SWS phase with Agarwal time (bottom right graph)

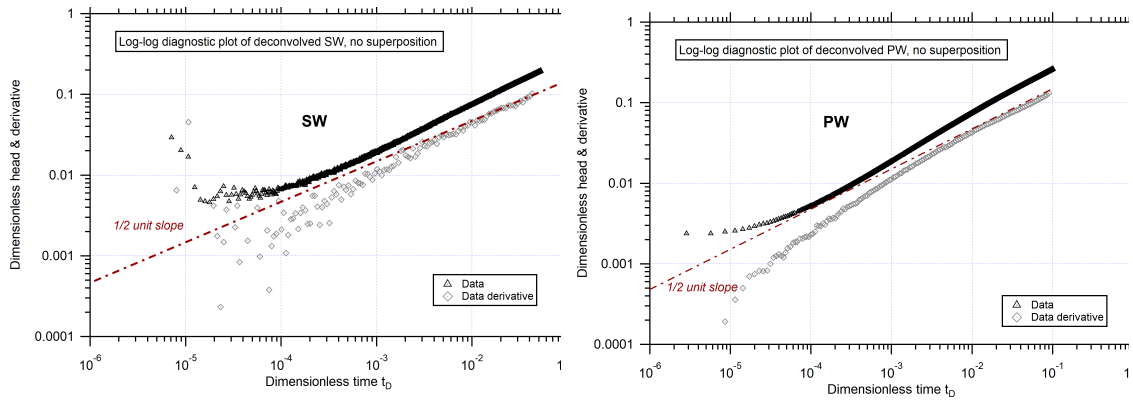

Fig. B-15: Hydraulic test RHE1-1-OPA2a: Deconvolved slug flow phase (SW, left graph) and deconvolved pulse phase (PW, right graph)

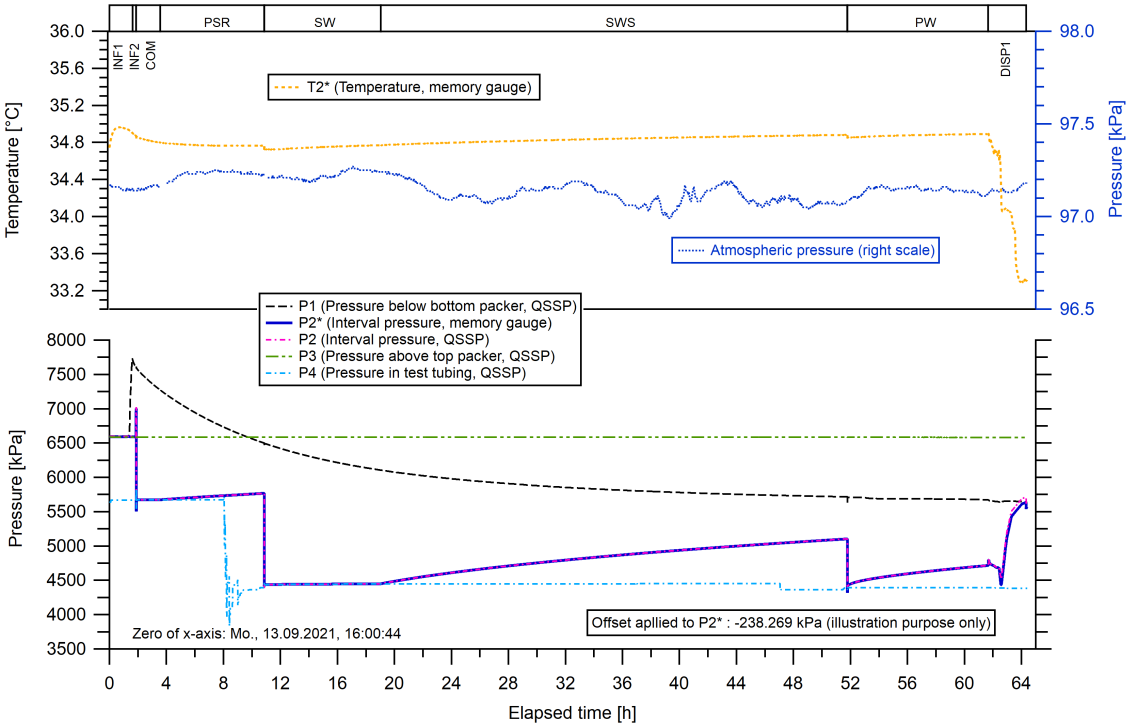

Fig. B-16: Hydraulic test RHE1-1-OPA2a: Interval temperature (T2* memory gauge sensor), downhole pressures of QSSP sensors (P1, P2, P3, P4), atmospheric pressure and pressure of memory gauge (P2* sensor shown with an offset to ease comparison with P2)

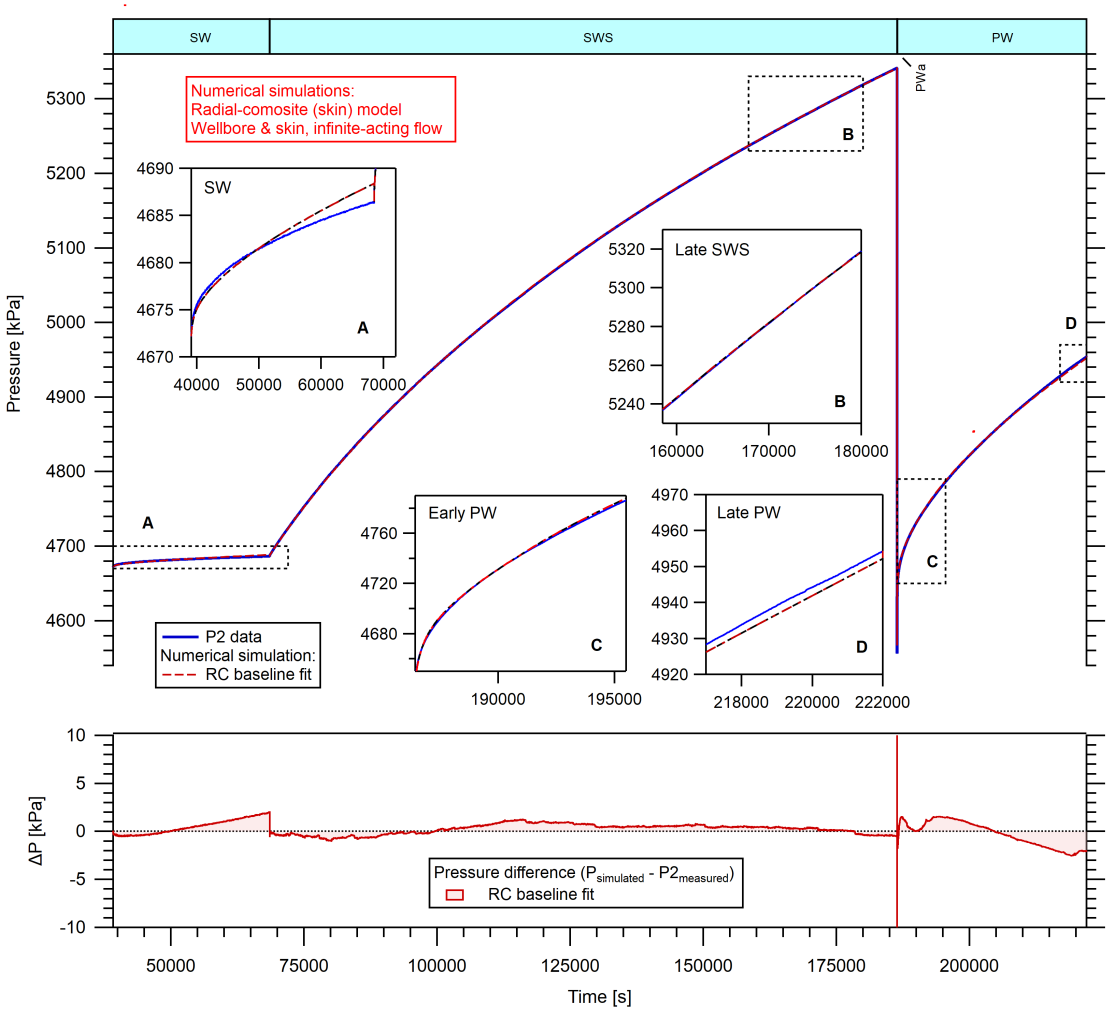

Fig. B-17: Hydraulic test RHE1-1-OPA2a: Cartesian pressure graph showing the numerical simulation based on the resulting parameter set of a parameter optimisation for the pressure sequence SW-SWS-PW, called reference case (RC) (top: SW-SWS-PW sequence with zoom on different sections; bottom: pressure residual plot)

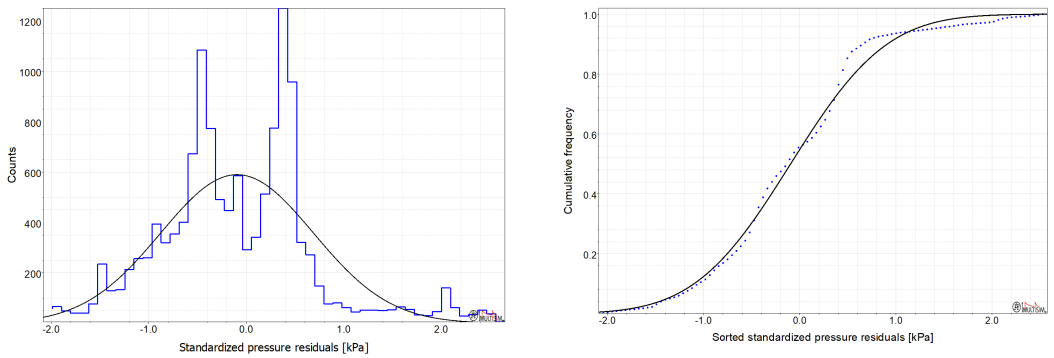

Fig. B-18: Hydraulic test RHE1-1-OPA2a: Probability distribution function plot (left) and cumulative distribution function plot (right) of the simulation based on the optimised parameter set for the SW-SWS-PW sequence

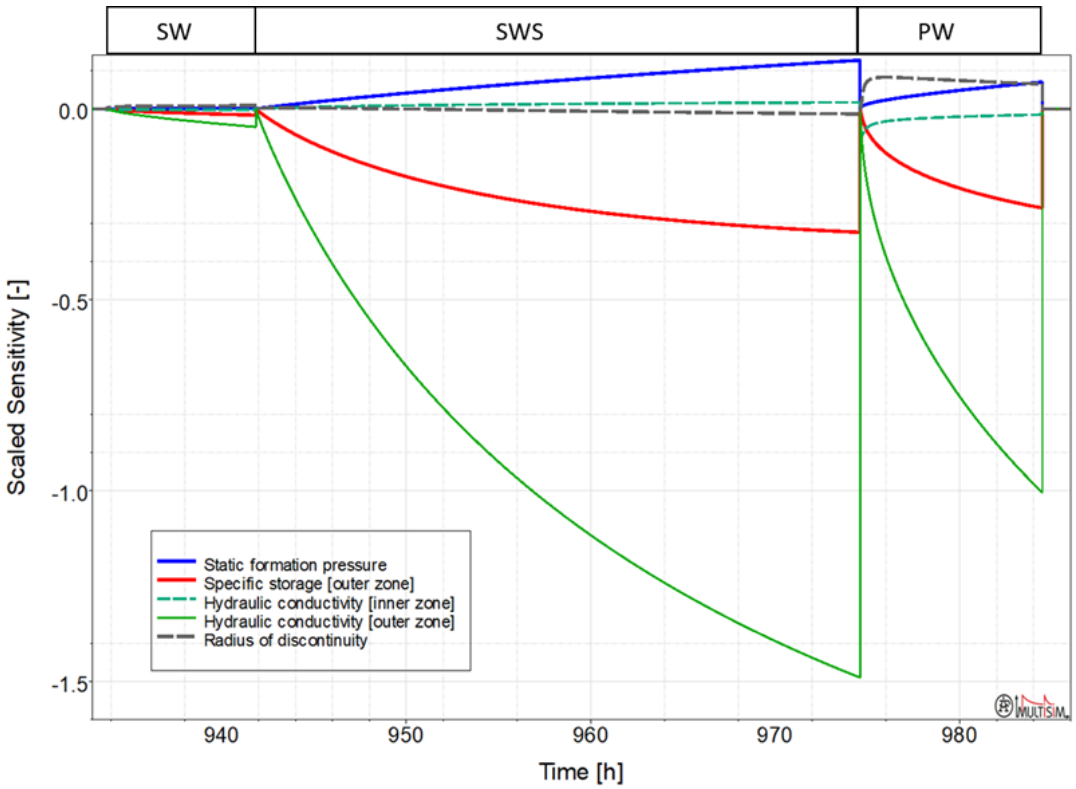

Fig. B-19: Hydraulic test RHE1-1-OPA2a: Sensitivities of the optimised parameters for the initial simulation

Time denotes hours since start of borehole pressure history.

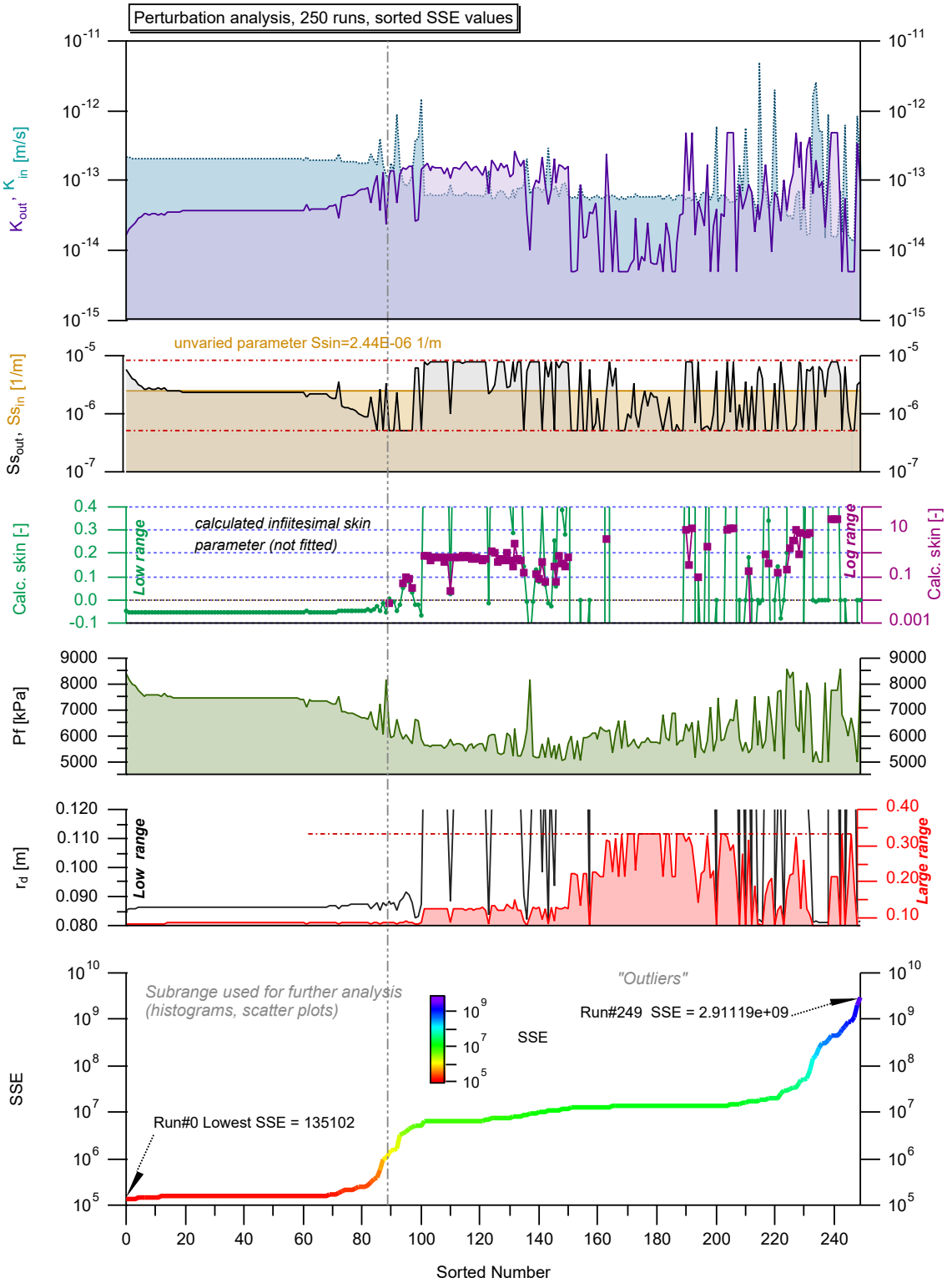

Fig. B-20: Hydraulic test RHE1-1-OPA2a: Optimised parameters plotted against sorted SSE values of all perturbation runs and, in the lowest chart section, SSE value against the increasing run number

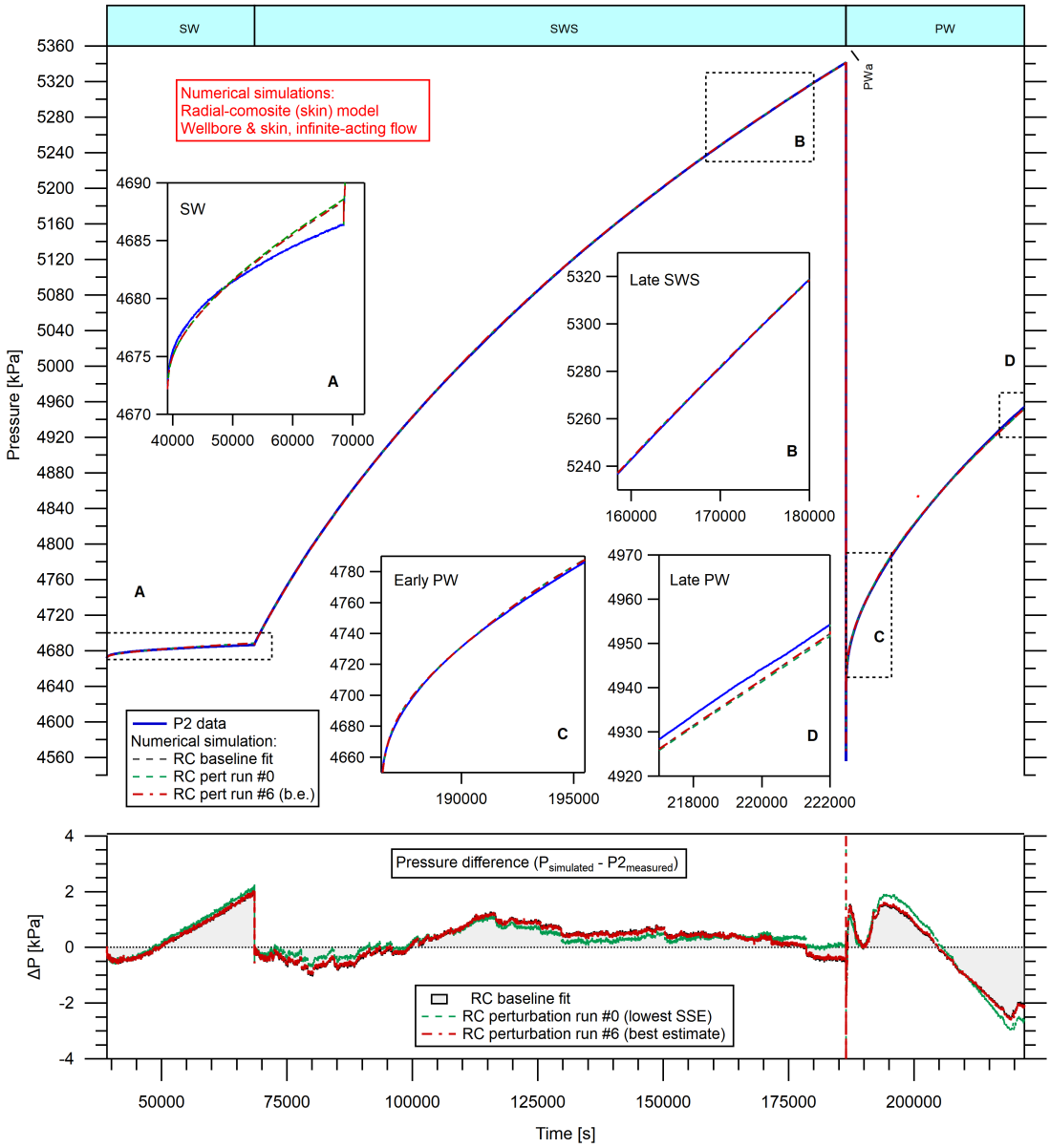

Fig. B-21: Hydraulic test RHE1-1-OPA2a: Comparison of the simulation based on the initial parameter set (reference case – RC) with the simulations associated with the parameter set of the lowest-SSE during the perturbation (run #0) and with the simulation run #06 (best estimate) derived from the perturbation analysis (top: SW-SWS-PW sequence with zoom on different sections; bottom: pressure residual plot)

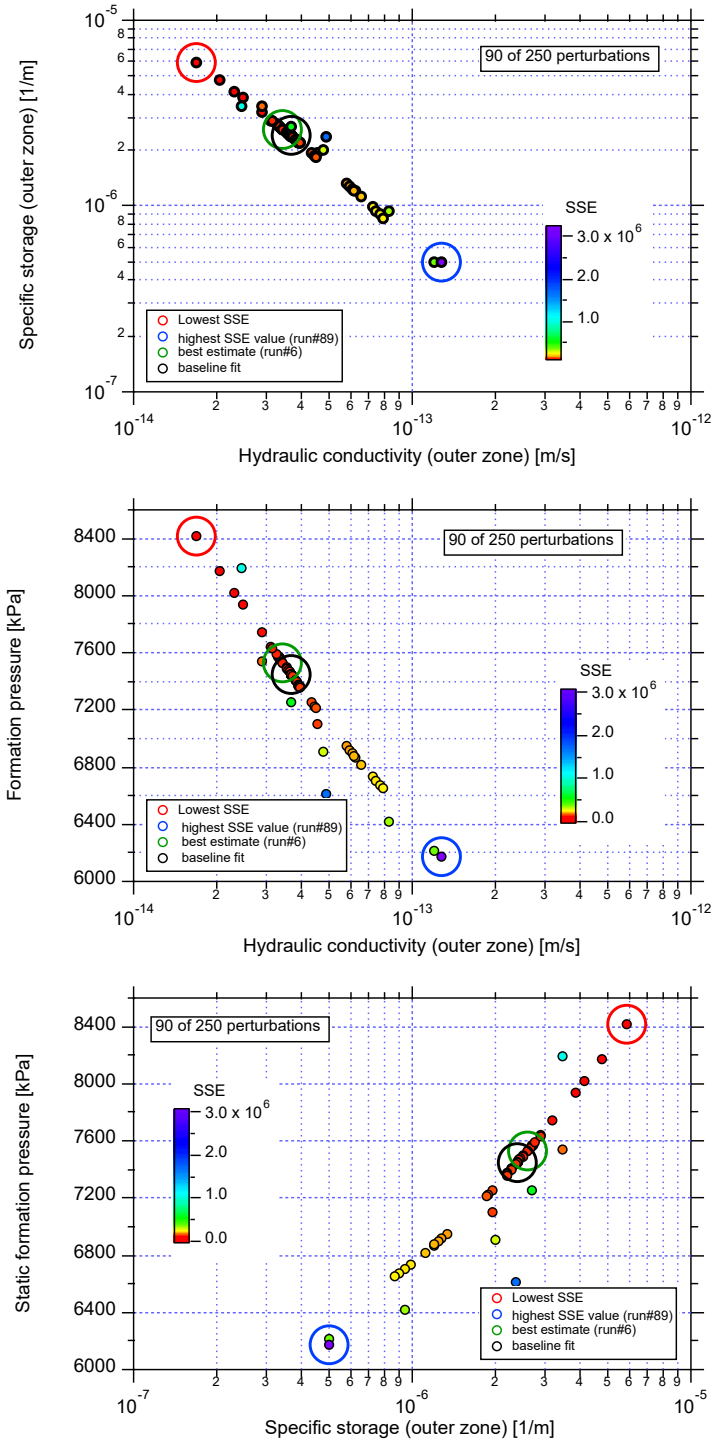

Fig. B-22: Hydraulic test RHE1-1-OPA2a: Scatter plots of formation parameters associated with their SSE values from perturbation analysis showing S_S versus K (top), P_f versus K (center) and P_f versus S_S (bottom figure)

The large circle markers in each graph indicate: minimum SSE run (red), maximum SSE run (blue), best estimate run (green) and initial parameter set (black).

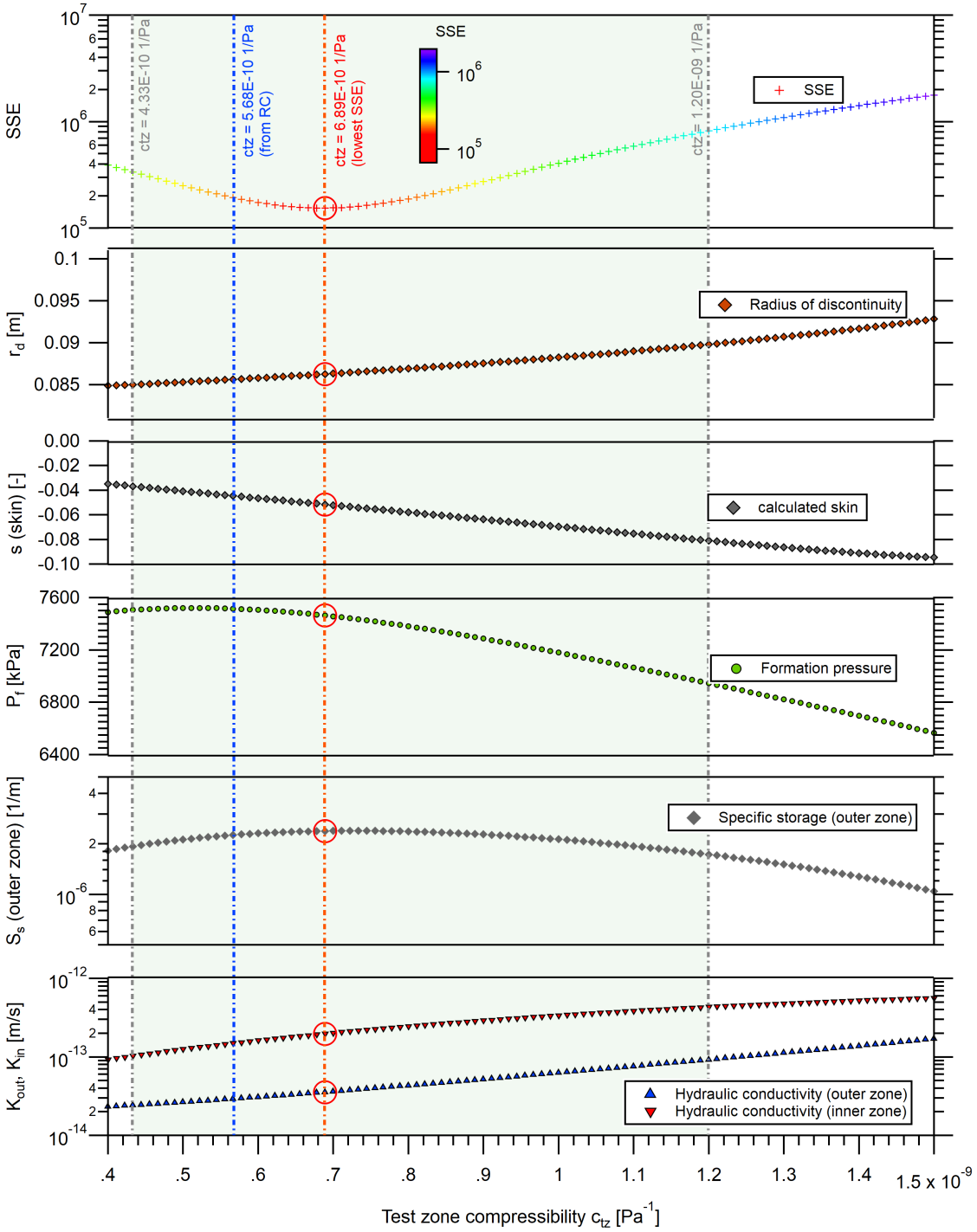

Fig. B-23: Hydraulic test RHE1-1-OPA2a: Sampling analysis of the test zone compressibility (c_{tz})

The SSE value is given for each simulation (top curve in graph). The blue dashed line indicates the c_{tz} value used in the initial parameter set, the red dotted line indicates the parameters associated with the lowest SSE. The green rectangle indicates the estimated uncertainty range. Note that the skin (s) is a calculated parameter and not a fitted parameter.